Investigation of Blast Load Characteristics On Lung Injury

by

Tyson Josey

A thesis
presented to the University of Waterloo
in fulfillment of the
thesis requirement for the degree of
Master of Applied Science
in
Mechanical Engineering

Waterloo, Ontario, Canada, 2010

Author's Declaration

I hereby declare that I am the sole author of this thesis. This is a true copy of the thesis, including any required final revisions, as accepted by my examiners.

I understand that my thesis may be made electronically available to the public.

Abstract

In many parts of the world, civilians and peacekeepers are exposed to potentially serious injury from blasts and explosions. Providing insight into the trauma thresholds for blast injury is necessary for the development of blast protection equipment and identification and subsequent treatment of blast injury. [Phillips, 1988] Blast injury can be categorized as primary, secondary, tertiary, quaternary and quinernary, corresponding to different aspects of the blast loading and injury mechanisms. Primary blast injury occurring in the lungs is of importance, since lung injury results in one of the highest rate of blast mortality.

Much of the existing blast injury data was obtained from animal testing with sheep and subsequently extrapolated to humans using scaling techniques. More recently, mathematical, experimental and numerical models have been developed and employed to investigate blast injury. In this study, a detailed finite element model of a sheep thorax and human thorax (developed at the University of Waterloo) was used to predict primary blast lung injury based on a range of blast loading conditions. The models were developed based on available anatomical data and material properties to model the organs and tissues, and were evaluated using the LS-Dyna explicit finite element code. The models were previously validated for the prediction of lung PBI using Friedlander-type blast waves. All results were compared to existing literature to further verify and validate the numerical models as wells as to provide insight on the effect of loading conditions on blast injury. The blast loading input for these simulations used idealized blast waves, based on a blast physics approach. Blast loads were verified using the Chinook CFD software.

The effects of idealized blast waves on predicted lung injury were investigated to determine the importance of peak pressure, blast wave duration and impulse. The duration and peak pressures for the waves were selected based on the Bowen and UVa curves, and included a right angle triangular shape and a square wave to allow for the different parameters to be considered. These results were compared to the Bowen and revised Bowen injury models. The results show that the peak overpressure is dominant in predicting injury for blast loads with long durations (>8 ms). The impulse was dominant in predicting injury for blast loads with short durations (<1 ms). For blasts loads with intermediate durations (1 ms < 8 ms) both the shape of the blast load wave and peak overpressure play a role in primary blast lung injury.

The effect of orientation of the body position on primary blast lung injury was investigated. Simulations were performed using the sheep and human numerical models along with a model of a commonly used experimental device, the Blast Test Device (BTD) cylinder. These models were oriented in different positions by rotating the body relative to the blast flow. Injury results for the BTD were calculated using the Injury 8.1 injury prediction software. The BTD simulations served several purposes; it was used as a reference for the human and sheep simulations and its effectiveness as a tool to predict body orientation was evaluated. In general, all of the models predicted appropriate and similar levels of injury for the body in its default orientation, and these predictions were comparable to the accepted injury levels for this insult. For other orientations the BTD was not able to predict the appropriate blast injury. This highlighted the importance of proper placement and orientation of the BTD when used in simulations or physical experiments. The overall injury (based on the results from the right and left lung) predicted by the sheep and human thorax was similar for all orientations. However, very different results were obtained when the predicted injury for the right and left lungs was compared. The differences between the sheep and the human were examined and the differences in injury between the right and left lung is a result of the differences in anatomy between the two species.

This study has evaluated the importance of blast wave parameters in predicting primary blast injury, an important consideration for the improvement of blast protection, and the effect of body orientation on primary blast injury, an important consideration for experimental testing and a starting point for the evaluation of complex blast loading. Future work will focus on the evaluation of injury in complex blast environments.

Acknowledgements

I'd like to sincerely thank my supervisor, Dr. Duane Cronin for granting me the opportunity to expand my knowledge.

At Martec Limited I would like to thank Dave Whitehouse, for his encouragement and support in this study. I would like to extend my appreciation to Aris Markis at Med-Eng and to Kevin Williams at DRDC Valcartier for their role in this program.

Finally I would like to thank Chris Salisbury for all of his guidance and technical support. Thanks for keeping me connected while I was working away from the University.

Dedication

This thesis is dedicated to my wife, Michele, for supporting me throughout this journey.

Table of Contents

List of Figures

List of Tables

List of Equations

Chapter 1
Introduction

1.1 Background

The need to be able to understand the mechanism of blast lung injury along with having an appropriate and reliable tool to predict the injury is of great importance. Currently there are a number of ongoing wars and conflicts in which peacekeepers and civilians may be exposed to blasts. To reduce the severity of human injury from these explosions research is being carried out in the realm of blast protection. Blast protection encompasses the protection and mitigation from blasts and explosions in respect to buildings, vehicles and personnel.

Primary blast injury to humans is caused by the pressure wave generated by an explosion or blast. The high pressure wave delivers injury by impacting the body and transferring its energy into the body and organs. Air filled organs such as the lungs and gastro-intestinal tract are the most susceptible to primary blast injury. [Weiler-Ravell, 1975] The eardrums are also very susceptible and have the lowest injury threshold. This study deals with primary blast injury of the lungs. Depending on the size of the explosion and the location of the individual with respect to the explosion, serious or fatal injuries may occur.

To further complicate injury prediction the blast wave will behave differently in enclosed spaces than in an open free-field area. Estimating injury in the free field has been studied and correlations have been made which relate injury to charge size and distance. Injury estimate curves have been produced and are a result from early animal testing and from accounts of troops on the battlefield. These empirical correlations are however not valid for explosions in enclosed spaces or in any situation where a complex blast wave is generated. In many situations a complex blast wave is produced, such as in urban warfare situations

where there is fighting in close quarters. [Nelson. 2006] The geometry of these situations leads itself to producing complex blast waves when an explosive source is detonated.

The research presented uses numerical models developed at the University of Waterloo along with commercially available Computation Fluid Dynamics (CFD) and Finite Element Analysis (FEA) computer codes to estimate primary blast lung injury to a human subjected to explosions. These codes have been validated with data from physical experiments.

1.2 Motivation

Due to the rise of violence and threat of global terror, blast injury is a becoming a common threat with the increased number of explosions being carried out against people. [Belanger, 2005; Mayo 2006b] A fundamental understanding of trauma thresholds for simple and complex-type blasts is essential for the development of improved blast protection systems. [Hayda, 2004; Kessler, 2004] This is particularly true for primary blast injury (PBI) of the lung, as it results in the most common fatal PBI. Blast lung injury is diagnosed in 45% of the fatalities from explosions. [Almogy, 2006] Existing personnel vulnerability test data is based on animal models, which predominantly consider free field or simply shaped blast waves. Several models have been developed and correlated to this data. However, the basic elements of a blast wave that lead to PBI are not well understood. This is of particular importance since many blast injuries occur within structures or enclosed areas, leading to very complex loading on the human body.

In order to predict blast injury to the human there are currently only a limited number of options available. Four widely used options currently available to predict injury are:

i. Accounts of recorded injury in literature from blast exposure
ii. Injury prediction curves based on animal tests and free-field blast parameterizations
iii. Predictions based on experimental pressure readings from a cylinder, used to simulated the human thorax (Blast Test Device)
iv. Coarse numerical models used to model the thorax

Along with having a limited amount of options used to predict injury, many of these options are only valid for free-field scenarios or scenarios where an individual is next to a reflecting surface. When predicting injury in enclosed spaces, where complex blast waves arise, several techniques used to predict injury, are not valid and therefore should not be used. The early work in the blast injury field was performed by subjecting animals to blast waves and then extrapolating their injuries to humans. This work focused on free-field type blasts and the results from these studies are still being used by scientists and engineers today; as there are limited options for predicting blast injury in enclosed spaces. Only recently has an effort been made in predicting blast injury in enclosed spaces. As the blast waves that are produced are complex and dependant on the geometry of the environment and reflecting surfaces it is not possible to apply the curves from free-field experiments in these situations. The current method of predicting injury for complex blast environments involves placing a cylinder inside the flow-field and measuring the pressure at four locations along the cylinder. This cylinder is known as a Blast Test Device (BTD) and is frequently used in experimental trials. The gauges are placed at a height of half that of the cylinder, used to represent the mid-sternum area of the thorax. The cylinder is used to represent the human thorax. The recorded pressure values are then processed and correlated to injury. These cylinder models are crude measuring techniques and are not representative of the tissue and internal organs of the thorax. The cross section of the cylinder (a circle) is not representative of the human thorax. There has also been attempts to numerically model the human thorax in order to predict injury, however many of the numerical finite element models used to predict injury have been very coarse and unable to capture the required wave mechanics of the tissues. The goal of this project is to use a high resolution model of the human thorax to predict blast injury.

Without the use of numerical modeling to model the blast waves and pressures produced from an explosive charge, physical experiments would need to be conducted. A trial series, which may involve a large number of explosive experiments, can take a great amount of effort and time to complete. It is therefore worthwhile to pursue computer based, numerical modeling options. Using a numerical modeling approach can dramatically reduce the effort and expense to replicate a particular experiment. Utilizing computer simulations allows the flexibility of performing a specific experimental without the need to physically build and construct the scenario. Parametric studies can also be performed to understand trends and the sensitivity of the model to input conditions.

1.3 Research Objective and Goals

The main goal of the research was to investigate primary blast injury to the lungs under different blast conditions, orientations and to compare the experimental blast injury on sheep to humans.

In order to have confidence in the model and ensure that it is able to properly estimate injury from complex blast waves in enclosed spaces basic tests were first performed. The results from these basic tests ensure that the model is behaving similarly to that noted in the literature. Although in the current literature most of the existing models and experiments have been used with overly simplified models and test apparatus, these will serve as a foundation for the work in this study.

After establishing a baseline and ensuring the model is producing appropriate results the goal was to investigate the key parameters that cause primary blast injury to the lung. A study using simplified waveforms and comparing the shape, peak pressure and duration of the blast wave was performed with the intent on identifying factors that play a significant role in predicting primary blast lung injury. The numerical results were also investigated to determine the how the pressures inside the lungs are generated; being able to slice through the torso and view the stress distribution inside the torso was only possible by using a numerical model.

Many of the existing blast injury data have been derived from animal experiments. Most of these tests involved performing experiments in which sheep were subjected to simple and complex blast waves. The University of Waterloo has developed a numerical model of a sheep thorax that was used for comparison between the predicted injury of a sheep and human thorax, using these numerical models.

Examining the results from the human and thorax models indicated how the differences between the geometries and location to the blast wave could affect injury. This study led to a follow-on study with the goal being to determine the role of body-orientation (to a blast wave) has on injury. For this study a number of simulations were performed in which the body was rotated about its axis and subjected to the same blast wave. This study indicated that the severity of injury caused by a blast wave is also a function of the orientation the person is to the wave. There is also the possibility of severely damaging one lung and only having minimal damage to the other.

The following six chapters present the work that was performed in this study. Chapter 2 presents the background information on blast and blast lung injury along with the relevant historical data used to evaluate blast lung injury. The latest and most commonly used tools to investigate blast lung injury are also presented. Chapter 3 provides an overview of the numerical modeling approach used to estimate blast lung injury. Chapter 4 presents the results of a study performed to identify some of the dominant and key parameters used to predict blast lung injury. Chapter 5 examines the effect of body orientation on primary blast lung injury. Chapter 6 shows the results from a study comparing blast lung injury from sheep and human torso, and discusses the relevance of using a sheep as a human surrogate for blast experiments. Chapter 7 provides the overall conclusions and recommendations from the results of this study.

Chapter 2
Literature Review

The main goal of this study was to investigate the numerical human thorax developed at the University of Waterloo in response to blast loading. The model has been developed and improved to predict primary blast lung injury [Greer, 2006]. In order to evaluate the model and resultant predicted injury, a thorough understanding of the injury associated with blasts is required. The blast loadings that are of interest for this study area a direct result of explosives and detonations of charges. Blast loading can range from a simple blast wave to a complex environment consisting of a number of reflections and coalescing of blast waves. Although a number of injuries can occur from explosives, of most importance for this study is the primary blast lung injury. An overview of blast loading is presented followed by a summary of the blast injury types and injury mechanisms. A review of the current experimental and numerical blast injury models is also presented. As predicting blast injury resulting from complex blast waves is a difficult problem, there are currently only a few models that are able to predict injury from complex blasts. Models related to simple blast waves were studied and compared with the University of Waterloo numerical model to ensure that the model was able to both predict injury from simple and complex blast waves.

2.1 Blast Loading

Abrupt shock loading can occur from a number of different phenomenons, however the method that is of interest to this project is the resultant blast loading from explosions. The flow field generated from a blast wave is complicated, however the most widely used parameters to characterize a blast are the pressure and time variables. In order to accurately model a blast wave the pressure versus time profile of the wave must be known. This project focuses on explosions in air. The methods used to model explosions in air may not directly apply to explosions in other mediums, such as underwater explosions.

2.1.1 Explosive Charges

Explosives are categorized as either high-order explosives (HE) or low-order explosives (LE). The difference between the two classifications is in the type of explosive wave produced. In HE explosions a supersonic, shock wave is generated and sustained as the detonation wave travels through the medium. LE explosives produce a subsonic explosion and do not produce an over-pressurization wave. [CDC, 2006] For LE explosives the energy in the charge is released much slower as compared to HE and the explosive is burned through a process known as deflagration. In HE explosives the charge combusts near instantaneously (typical detonation velocity is approximately 6900m/s for TNT explosive [Cooper 1996c]), releasing the energy almost instantaneously. HE explosives are generally more stable than LE explosives. Examples of LE explosives are black powder, gunpowder and rocket propellants. Examples of HE explosives include nitroglycerine, ammonium nitrate, trinitrotoluene, C4, RDX and ANFO. [Mayo 2006a] Conventional explosive contain compounds of hydrogen, oxygen, nitrogen and carbon. The explosive material may be in the form of a liquid, gas or solid and are classified as either primary or secondary explosives. [Baker, 1973]

Explosive are generally held in a casing of metal or other hard compounds. When detonated high pressures are produced and the casing is unable to contain the high temperature and high pressure gases. When the casing is compromised the gases are allowed to escape. As the casing is disrupted, this results in a number of fragments moving at high speeds being released in the vicinity of the blast. These fast moving fragments can be fatal or provide serious injury if they impact a human subject. [Hunter, 1941] This study does not deal with injury obtained from fragments and penetration. For the purposes of this study the casing and fragmentation portions of the explosive will not be considered. The composition

of the explosive source will also be ignored, however the loading case used to predict injury will be based on actual charges and actual compositions.

When an explosive is detonated it generates a high pressure wave that advances outwards, interacting with everything in its path. [Kinney, 1962] The initial solid explosive undergoes a combustion process transforming the solid into a high pressure gaseous state. In the case of a solid explosive, initially the molecules of oxygen are bonded to the combustible material. When the charge is initially detonated, a blast wave (from a booster charge or blasting cap) travels through the explosive and breaks the bonds between the oxygen and combustible material. Once the bond is broken the oxygen ignites with the combustible material. This process produces a substantial increase in pressure and a pressure build up inside the explosive, which is released into the surroundings. [Meyers, 1994]

The magnitude of force of the blast wave is related to the composition of explosive charge, the size of the charge and the distance from the center of initiation. [Katz, 1988] Figure 1 shows a schematic of the pressure pulse generated from a charge. When the charge is initiated a high pressure is generated which expands outwards, compressing the air near the wave front. Following the high pressure phase, the high pressure gas rushes away from the location of initiation, the original location of detonation decompresses as the blast wave travels farther away. This leads to a volume of below atmospheric pressure, known as the negative phase. [Stuhmiller, 1991]

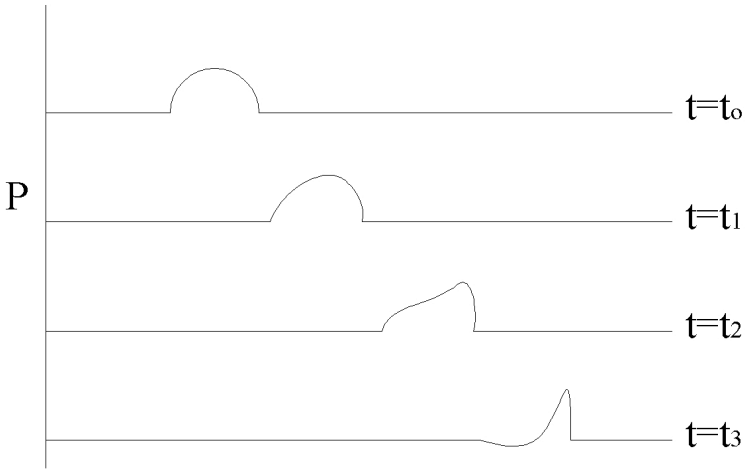

Figure 1: "Shocking up" of pressure pulse [Cronin, 2004]

2.1.2 Simple Blast Waves

In order to study the injury caused by explosions in air it is necessary to simplify and understand the blast loading wave. When charges are initiated the blast wave moves radially outwards into the undisturbed air. In areas where there are other objects close to the blast source the blast wave will eventually interact with objects, creating a complex wave field including reflections and attenuations. To understand the fundamentals of blast waves it is necessary to consider an idealistic blast wave in free-field conditions (i.e. no interactions with the ground, bodies or other objects). The approach is to examine an idealistic blast wave in air before it has contacted other surfaces or objects.

The blast resulting from the detonation of an explosive charge is shown in Figure 2. The image clearly shows the blast front; a slight discontinuity is observed as light passes through

the blast front. The blast front, the leading edge of the blast wave has a denser air, which allows the pressure wave to travel faster than it would through ambient pressure air.

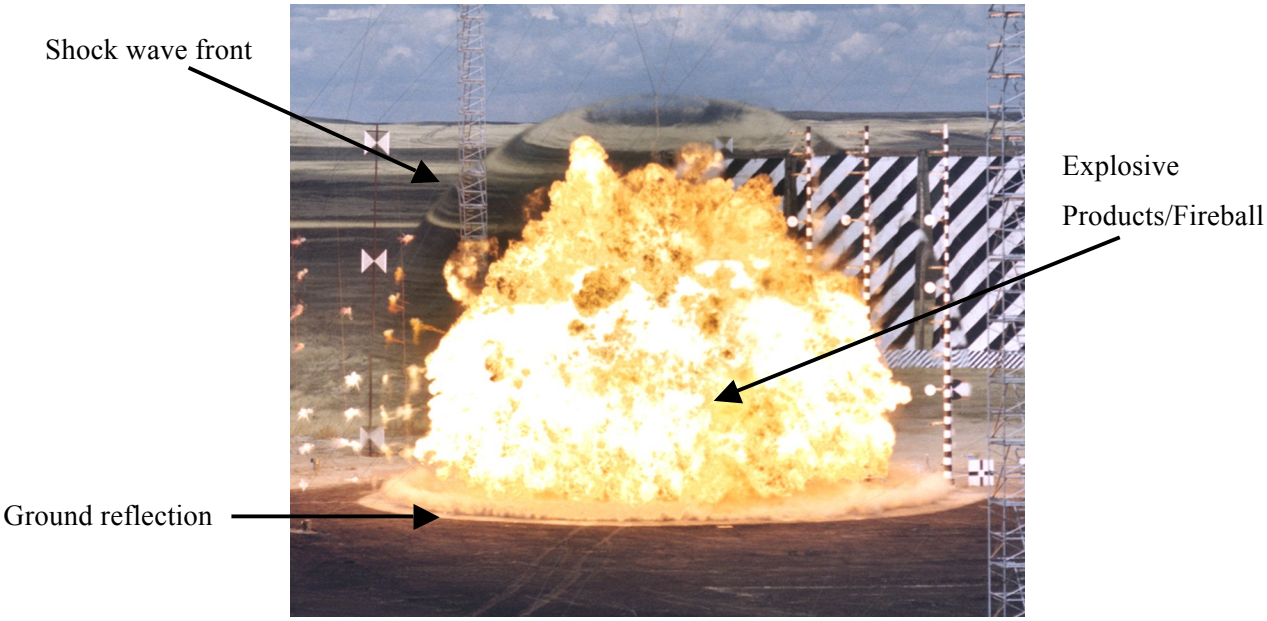

Figure 2: Blast wave generated from an explosive charge

A simple or ideal blast is an idealistic representation of a blast wave in air. This type of wave is assumed to be formed by a spherical charge, resulting in a spherical expansion wave. The expansion of the blast wave is also assumed to have occurred in a homogenous atmospheric environment. The idealistic blast wave is therefore spherically symmetric and the characteristics of the expanding wave are only related to time and the distance from the center of the explosive source.

The blast field experienced at a point, a given distance from the explosive source center, can be represented by Figure 3. The characteristics of the idealized pressure wave are

composed of an instantaneous rise in pressure to a fixed point ($P_s^+ + p_o$) at a given time (t_a); known as the time of arrival. This is followed by a decay in pressure to ambient (p_o) that occurs over a given time ($ta+T^+$). The duration for which it takes the instantaneous pressure rise to return to ambient is known as the positive phase. When the pressure reaches ambient, it then further decays below ambient and creates a partial vacuum reaching an ultimate low pressure ($p_o - P^-_s$), until the pressure rises back to ambient. The time it takes for the pressure to go from below ambient back to ambient ($ta+T^++T^-$) is known as the negative phase.

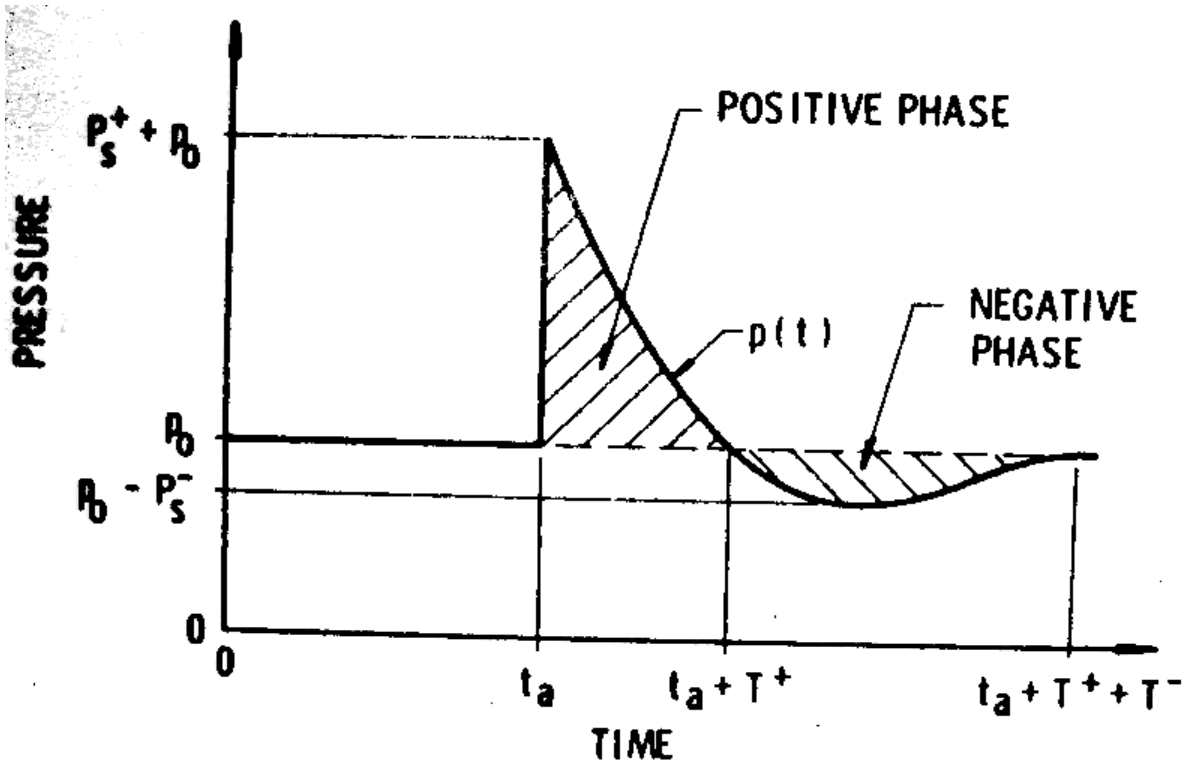

Figure 3: Ideal Blast Wave [Baker, 1973]

In order to numerically model this idealistic blast wave a number of mathematical equations have been presented. The positive phase portion of the blast wave has been studied and examined much more than the negative phase. A number of equations have been put forth, ranging from overly simplified versions to complex equations. The most widely

accepted version of this is known as the modified Friedlander equation and is represented by Equation 1. In this equation time is measured from the time of arrival of the blast wave . [Baker, 1973]

$$p(t) = p_o + P_s^+\left(1 - \frac{t}{T^+}\right)e^{\frac{-bt}{T^+}}$$

where:

p_o is the ambient pressure

P_s^+ is the peak overpressure

T^+ is the positive phase duration

b is the rate of decay factor of the falling pressure

Equation 1: Modified Friedlander equation

Although the positive phase portion of the blast wave has been studied and numerous equations have been developed for this portion there has been very little interest in the negative phase portion. The negative phase portion is perceived to be minimal as compared to those of the positive phase. The most widely accepted equation for the negative phase was presented by Brode and is shown in Equation 2. [Baker, 1973] In this equation time is measured from the start of the negative phase duration.

$$p(t) = p_o - P_s^- \left(\frac{1}{T^-}\right)\left(1 - \frac{t}{T^-}\right)e^{\frac{-4t}{T^-}}$$

where:

p_o is the ambient pressure

P_s^- is the lowest pressure

T^- is the negative phase duration

Equation 2: Blast wave negative phase

2.1.3 Complex Blast Waves

As an explosive charge is detonated the high pressure wave travels outwards from the center of initiation. The high pressure, high speed wave makes contact with everything in its path. The contact between the wave and objects in its path will result in reflections, rarefactions and attenuations of the blast wave. [Katz, 1998] The resulting flow field of the blast therefore is not accurately represented by the Friedlander idealized blast wave when interaction with objects occurs. The exact waveform cannot be determined empirically as it depends on the geometry of the objects in the environment. In order to determine the wave field in a complex environment, a numerical simulation or an experimental simulation is required to obtain the pressure at desired locations.

Complex blast waves are important to study, as most often they are the type of waves that are seen in actual scenarios, such as detonations in confined spaces. For example, complex waves can be generated by the reflection of blast waves off of the geometry of a vehicle interior. [Pizov, 1999] On a battlefield, soldiers residing in foxholes dug into the ground can be affected by complex blast waves. As a blast is detonated near the hole the incident wave is able to propagate into the foxhole and reflect of its surfaces, causing an assortment of reflected waves. [Stuhmiller, 1991] Blasts occurring in streets or in buildings will also

produce complex blast waves as the wave reflects off of the buildings, walls and objects in the vicinity. [Frykberg, 1988]

A charge placed above a flat reflecting surface, such as the ground will produce a complex blast wave. The distance the charge is placed above the ground is known as the height of burst (HOB). A diagram of this example is shown in Figure 4.

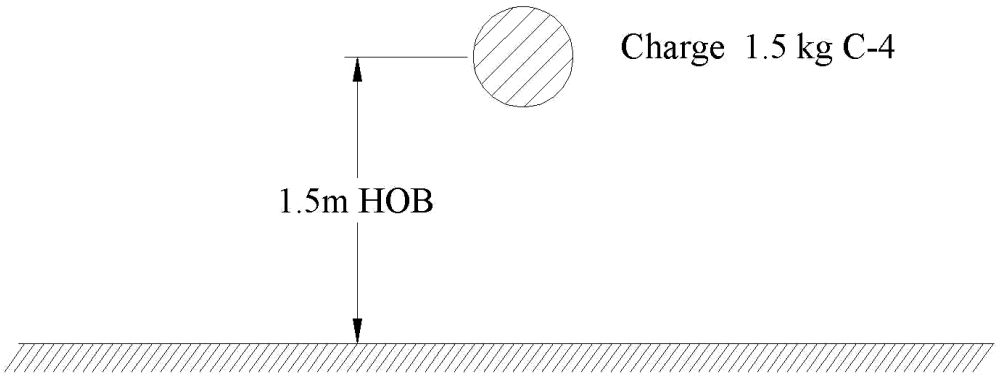

Figure 4: Bare spherical charge above ground [Cronin, 2004]

In this scenario the explosive is initiated and the blast wave radiates outwards. When the blast wave travels a distance equivalent to the height of burst it makes contact with the ground. As the ground is infinitely rigid the wave reflects off of the ground and travels back into the initial blast wave, as is shown in Figure 2. Using a pressure gauge it is possible to measure the interaction between the waves. In this example if a gauge is located directly above the center of the charge, the resulting pressure versus time plot will indicate the initial primary blast wave, followed by the presence of a secondary pressure peak, which represents the reflected blast wave from the ground. The formation of these waves is shown in Figure 5. A characteristic of complex blast wave is the presence of stepped waves, indicating rise

and drops in pressure, due to reflections and rarefactions. This is in contrast to the idealized wave, which only includes one peak pressure waveform. The pressure history of the complex waveform shows the initial incident waveform that would be visible in the free field, followed by the waveforms from the reflecting surfaces. In this example there is only one reflecting surface, however where more reflecting surfaces are present the resulting waveform will depend on the geometry of the reflecting surfaces. The change in geometry will both affect the magnitude and timing of the blast waves.

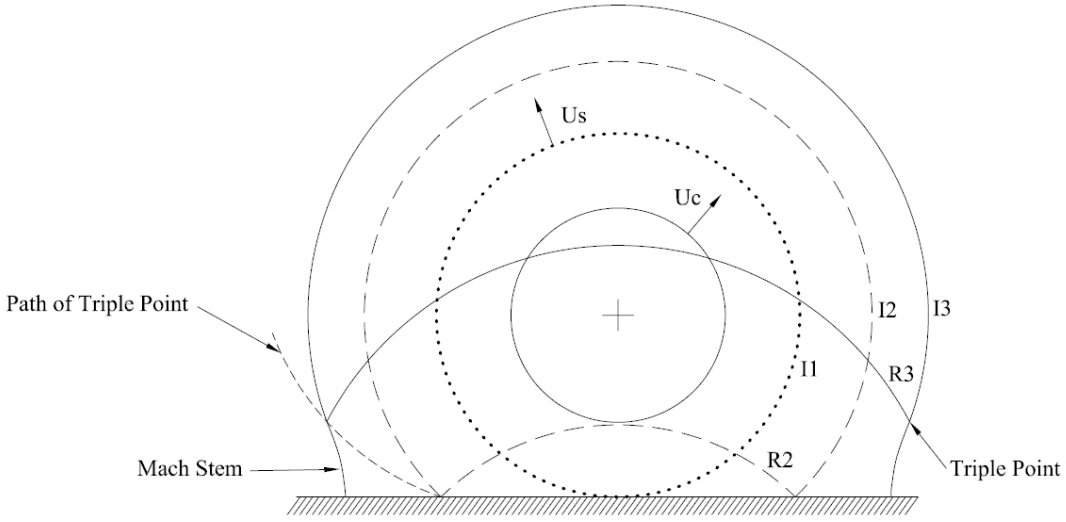

Figure 5: Complex blast wave formed from ground interaction [Cronin, 2004]

Blast waves can be reflected off a variety of surfaces, including walls, floors and ceilings. As the blast wave impacts the surface the reflected waves strength is related to the angle of contact with the surface; low angles produced lower strength reflection pressures whereas perpendicular angles produce very high reflected pressures. The strongest reflected wave results when the high pressure wave impacts perpendicular to the surface. At this point the blast wave is further compressed on impact and a reflecting wave begins to travel towards the incident wave. The region where this occurs is known as the reflected region. It contains a

very high pressurized zone as compared to a region where no reflection has occurred. The shock wave in this single reflected region can end up being 2 to 20 times greater than the incident shock. [Wightman, 2001] Stronger and more complicated shocks are produced in enclosed spaces or when the shock makes contact with multiple reflecting surfaces. In enclosed spaces the blast wave may undergo repeated reflections from the interior walls and any objects in the space. Complex blast waves in an enclosure have three characteristics:

i. The incident blast wave
ii. A number of reflected waves
iii. The static pressurization of the enclosure.

A complex blast wave in an enclosure will lead to a longer pressure-time history as compared to a blast in the free field. The longer pressure time histories enable the gases to heat and expand, filling the enclosure and then eventually venting through any openings. [Stuhmiller, 1991] One of the simplest scenarios that produces complex blast waves is the detonation of an explosive in an enclosed room. Even with the simple geometry and a charge placed in the center of the room the resulting blast waves are complex and require CFD simulations to predict the blast flow field. [Stuhmiller, 1997]

Figure 6 displays a plot of three pressure signatures. In Figure 6a, an idealized Friedlander curve is shown. Figure 6b shows the pressure time history record from an actual gauge in an experimental trial. This results show the similarly to the Friedlander curve, as can be seen by the near instantaneous rise in pressure, the decay to ambient and the negative duration phase. Noise and other artifacts are clearly visible as the plot is not smooth. These slight variations in the plot can be due to vibrations or the effect of placing a physical gauge in the flow field. Figure 6c shows a plot from an actual complex blast wave. This plot consists of an initial pressure and decay wave followed by a number of secondary peaks and decays. The

secondary waves are a result of the interactions between the initial wave and its surroundings. Reflections, rarefactions, coalescing and attenuation of waves all play factors in the pressure signature of the complex wave; the signature shown is from a blast wave inside a military bunker.

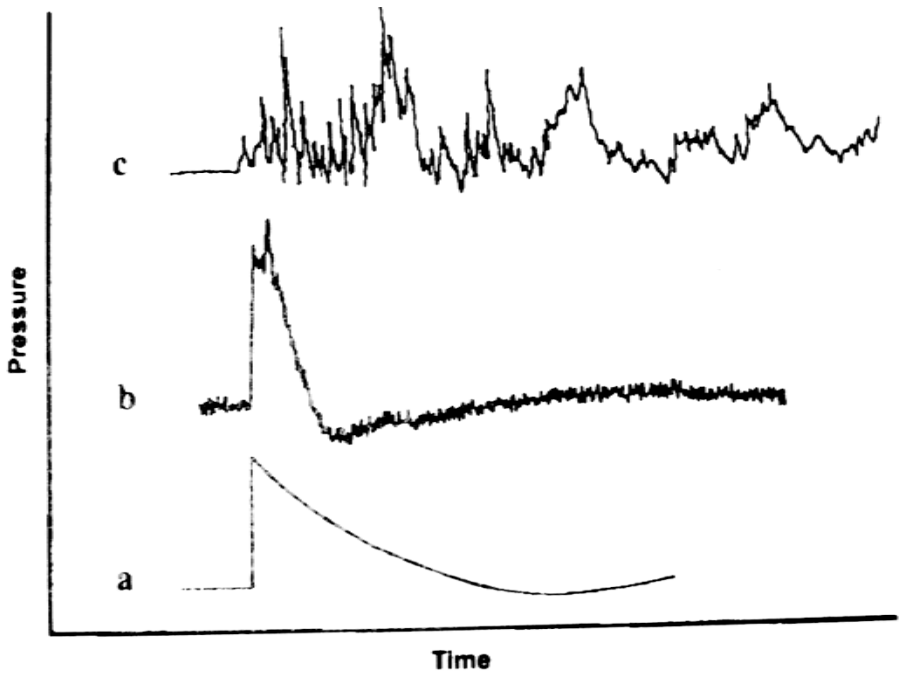

Figure 6: Blast wave comparisons: (a) idealized blast wave (b) Actual blast wave recorded via a pressure transducer (c) Complex blast wave [Mayorga, 1997]

Enclosed spaces allow the generation of complex blast waves. The reflection of waves from walls, ceilings and floors in enclosed environments enables the development of complex waves with long durations. In terms of blast injury, this allows for a greater transfer of energy to the body. This greater transfer of energy as compared to an idealized blast wave leads to increased bodily injury. [Chaloner, 2005]

2.2 Thorax

2.2.1 Anatomy

Primary blast lung injury is of particular interest as it is the leading cause of death for victims of primary blast injury. [Damon, 1968] In order to understand the trauma and the injury mechanisms responsible for this type of injury it is important to understand the anatomy and function of the thorax. Figure 7 shows a schematic of the respiratory system of a human.

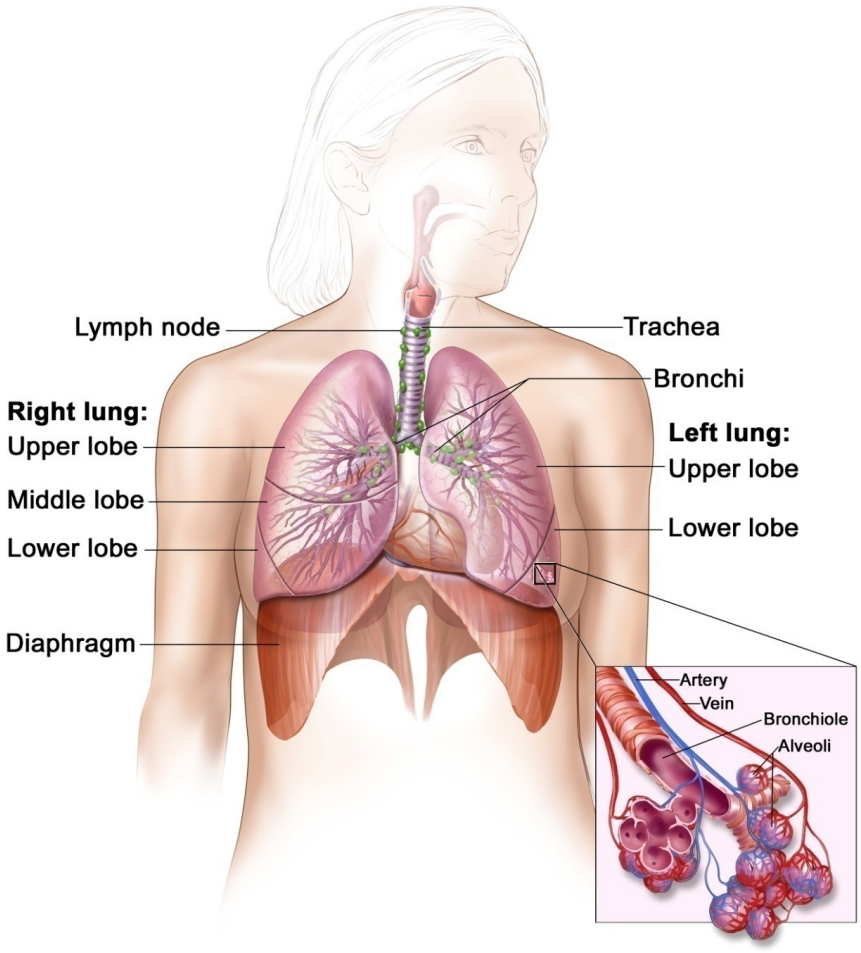

Figure 7: The respiratory system [CIJ, 2009]

The thorax consists of the thoracic cage, which protects the internal organs, including heart, lungs and mediastinum. The thoracic cavity is supported by the ribs that are attached to the sternum and cerebral column. The ribs are not rigidly connected to these points and are able to move slightly, to allow for expansion and compression of the chest cavity, as is observed in breathing. In between the bones of the ribs there is intercostal tissue and muscle. The thoracic cavity, among other things is responsible for protecting the lungs, heart and other organs; the heart is located slightly left of center in the chest cavity.

2.2.2 Lungs

The lungs are responsible for exchanging oxygen and carbon dioxide between the blood and inhaled air. The lungs are separated from the chest wall by the pleura, a thin membrane. The visceral pleura immediately surrounds the lungs and the parietal pleura lines the thoracic cavity. The lungs are not rigidly attached to the chest wall but are suspended in a fluid, known as pleural fluid.

Air enters through the mouth and into the trachea and is divided into the right and left lungs, by means of the bronchial tubes. The lungs consist of lobes; the right lung is made up of three lobes and the left lung contains two lobes. The lobes are similar to a balloon with a sponge like tissue; air enters and exits the lobes by a further division of the bronchial tube. The smallest subdivision of the bronchial tubes is referred to as bronchioles. At the end of the bronchioles lies the alveoli, or tiny air sacs. The alveoli are embedded with capillaries, where the exchange of oxygen and carbon dioxide takes place.

The ability to breathe is a function of a pressure differential in the thoracic cavity. The diaphragm, which is located below the lungs, is a wall of muscle separating the chest cavity

from abdominal cavity. To drawn in air the diaphragm moves downwards toward the abdomen, resulting in a pressure reduction in the thoracic cavity, allowing air to be drawn in and fill the lungs. Moving the diaphragm upwards allows for the exhalation of air from the lungs. The difference in pressure between the alveolar pressure and the pleural pressure is known as the transpulmonary pressure. A positive transpulmonary pressure is required to keep the lungs inflated. The pulmonary surfactant is a substance that reduces the surface tension in the alveoli, allowing the lung to easily be inflated and protecting them from collapse.

2.3 Primary Blast Injury

2.3.1 Overview

Blast was first documented as potential cause of injury and fatality in the American Civil War. [Mitchell, 1864] During the Second World War a classification system of blast injuries was created by Zuckerman. Injuries were classified as primary, secondary, tertiary, quaternary and quinary. Severity of injury related to the magnitude of the explosion and the site of its occurrence. [Mayo, 2006b] Pressure waves are also related to size of explosive charge and inversely related to its distance at a given site from the explosion source. [Katz, 1988] Figure 8 shows the expected injury based on the distance an individual is from a high-order explosive detonation.

Location	*Close Proximity*	⇨	⇨	⇨	⇨	⇨	⇨	*Distant*
Total body disruption								
Burns and inhalation injuries								
Toxic Inhalations								
Traumatic Amputations								
PBI of the lung and bowel								
Tertiary blast injuries								
PBI of the ear								
Secondary Blast Injuries								

Figure 8: Expected injuries to unprotected victims at relative distances from a HE detonation in free-field air [Bellamy, 1991]

2.3.2 Primary Blast Injury

The mechanism of primary blast injury is a result of the blast wave pressure exerting a force on the area of the human body. The force exerted on the body is transmitted to the internal structures by the movement of the tissue. [Phillips, 1986] With regards to blast waves in air, the pressures generated from the explosive being detonated causes pressure disturbances, which travel through the air. [Mayo, 2006a]

The high pressures generated by a blast wave impact the body and cause primary blast injury. For free-field blasts the potential injury severity generated by the blast wave decreases exponentially as the distance from the charge source increases. This corresponds to the forces of the blast wave being reduced as the wave travels outwards. [Mayo, 2006b]

For the same explosive charge, the rate and severity of injury generally increased when the explosive is detonated in an enclosed space. The overpressure generated from a blast in an enclosed space is amplified and much larger than a free field blast. This amplification in pressures is a direct cause of the increased injury observed. [Katz, 1989] In contrast to blasts in free field, blast injury in enclosed spaces is not directly correlated to the distance from the explosive source. As there are standing waves, reflections from objects and walls, the distance from the charge source is only one part of the injury encountered in enclosed spaces. [Mayo, 2006a] A blast wave that may only cause minimal primary injury in a free field can cause severe injury or can be lethal if the person is standing near a reflective surface. [Phillips, 1986]

Primary blast injury, also called barotraumas, mainly affects the air filled organs. [Argyros, 1997] As air is much more compressible than water, the air filled organs are more susceptible to blast injury. The most susceptible areas of the body are the middle ear, lungs and digestive tract. The tympanic membranes, followed by the lungs are most commonly injured by blast waves. [Mayo, 2006a] Injury can occur from the effects of overpressure or underpressure. [DePalma, 2005] Along with the air filled organs, air-fluid interfaces are sites of injury. It has been reported that organs are damaged by dynamic pressure changes. At air-fluid interfaces the injury occurs as a result of the interaction between high-frequency stress wave and a lower frequency shear wave. [Cooper, 1991, Guy, 1998a]

The actual injury mechanism is not fully known, however there are three main theories used in defining the mechanism of primary blast injury as a result of the high pressures. These are spalling, implosion and inertial effects.

The spalling mechanism refers to the interface disrupting between two media with different densities. The disruption occurs when a compression wave in the denser medium reflects at the boundary between the two materials. The disruption at the interface causes the material to be damaged and injured. [Phillips, 1986]

The implosion mechanism is the compression of a gas bubble in a liquid medium caused by a shock wave travelling through the medium. This can lead to the pressure in the gas bubble rising above that of the shock pressure. As the shock passes across the fluid and over the gas bubble, the bubble can collapse and re-expand explosively and cause local damage to the structure. [Phillips, 1986]

The inertia effects injury mechanism causes damage where two adjacent objects are imparted with the same or similar forces. When the densities of the adjacent objects differ, the lighter object will be accelerated more than the other. This increased acceleration will cause tears and greater stress at the interface between these two materials. Blast experiments on animals have shown that inertia effects are the most likely mechanism for primary blast injury. There is no direct evidence to support spallation and implosions in regards to biological blast injury. [Phillips, 1986; Ho, 2002]

It is believed, based on experimental data that the blast wave does not enter the body through the pharynx, but the wave energy enters the body by transmission through the thoracic wall, when the incident wave contacts the body. The energy is transmitted as stress and shear waves. [Cooper, 1996a] These waves are able to injury the body in different manners. The shear waves consist of waves of long duration and low velocity. [Mellor, 1992] These waves are responsible for the large displacement and distortions of tissues and

organs. [Cooper, 1996b] Injury results from these waves when the distortion causes the wave to overcome its elasticity and results in tears and contusion injuries. Stress waves are high frequency, low amplitude waves and travel near or faster than the speed of sound in the tissues. Injury most likely occurs where these waves are reflected or change their speed. Injury occurs at these locations through spalling and organs such as the lung are especially susceptible to this injury as the density changes very often as there are a several air/fluid interfaces. [Guy, 1998a]

2.3.3 Patterns of Primary Blast Injury

Primary blast injury is unique to the detonation and blast waves generated from explosions. Primary blast injury mainly affects the air containing organs and the air-fluid interfaces of the individual exposed to the blast wave. The energy waves transferred to the body are reflected at these air-fluid interfaces and result in tearing and disruptive forces, causing injury. [Katz, 1988] The dynamic pressure differences at these tissue interfaces lead to injury. [DePalma, 2005] Air containing organs are more susceptible to injury as compared to water containing organs since air is easily compressible and water is not. [Mayo, 2006a] The most susceptible organs are the ears, the lungs and the gastrointestinal track, with injury to the middle ear being the most common form of injury. Lung injury is the second most common injury from blast waves and is the most fatal. [Mayo, 2006b]

An X-ray is shown in Figure 9, which shows the injury sustained to the lungs immediately after the blast. The results from this x-ray can be compared against the results shown in the adjacent x-ray; this x-ray shows the healing of the lung and the reduction of fluid inside the lungs. In this scenario the blast lung injury was not fatal.

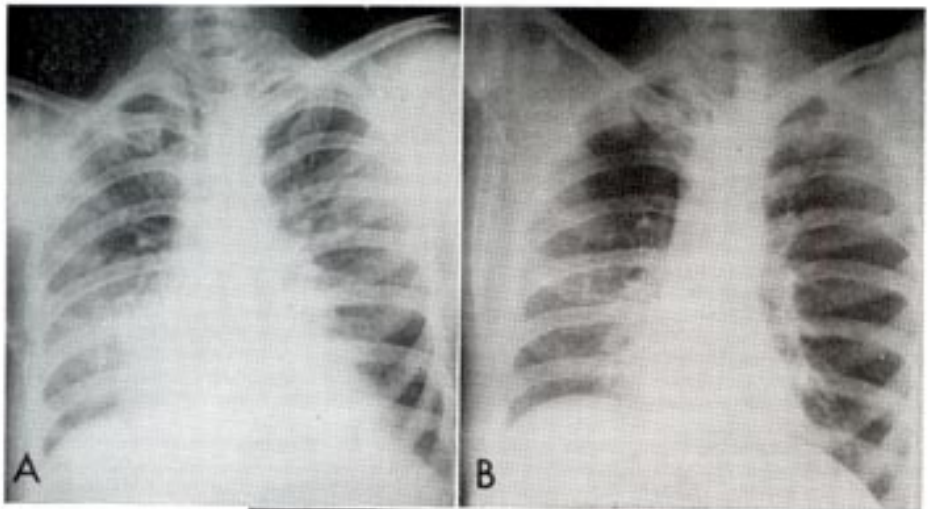

A.) Blast lung injury after 24hours. Injury is shown in X-ray as white infiltrates and haze
B.) Blast lung injury after months of healing

Figure 9: Blast lung injury, injury and healing [Ahnfeldt, 1965]

A recurring injury as a result of an explosion is the perforations in the eardrums. [Katz, 1988] The tympanic membrane is most frequently injured by primary blast. This organ requires some of the lowest pressures to be ruptured. The tympanic membrane is therefore a marker and represents a quick means for identifying primary blast injury. If there is no rupture of the tympanic membrane then it is unlikely that there is significant primary blast injury to the other air containing organs. [DePalma, 2005] Perforations of eardrums are indicators of primary blast injury. [Hunter, 1941] This however is not straightforward and in some cases there may be injury to the lungs when there has been no damage to the tympanic membrane. [DePalma, 2005] If protective equipment is worn (i.e. a protective helmet) there may be no damage to the eardrums, but the patient may suffer from primary blast lung injury.

The gastrointestinal tract is susceptible to primary blast injury, especially the gas containing sections, however injuries are less common as compared to ear or lung primary blast injury. The colon is the most often injured portion of the tract as it contains the most amount of air. [Adler, 1988] The small intestine may also be injured, however it is less common. Primary blast injury to the gastrointestinal tract can result in perforations, very small or large hemorrhages and a restriction in blood supply. Figure 10 shows the hemorrhaging developed in the small intestine of a monkey, subject to an explosion and receiving primary blast injury.

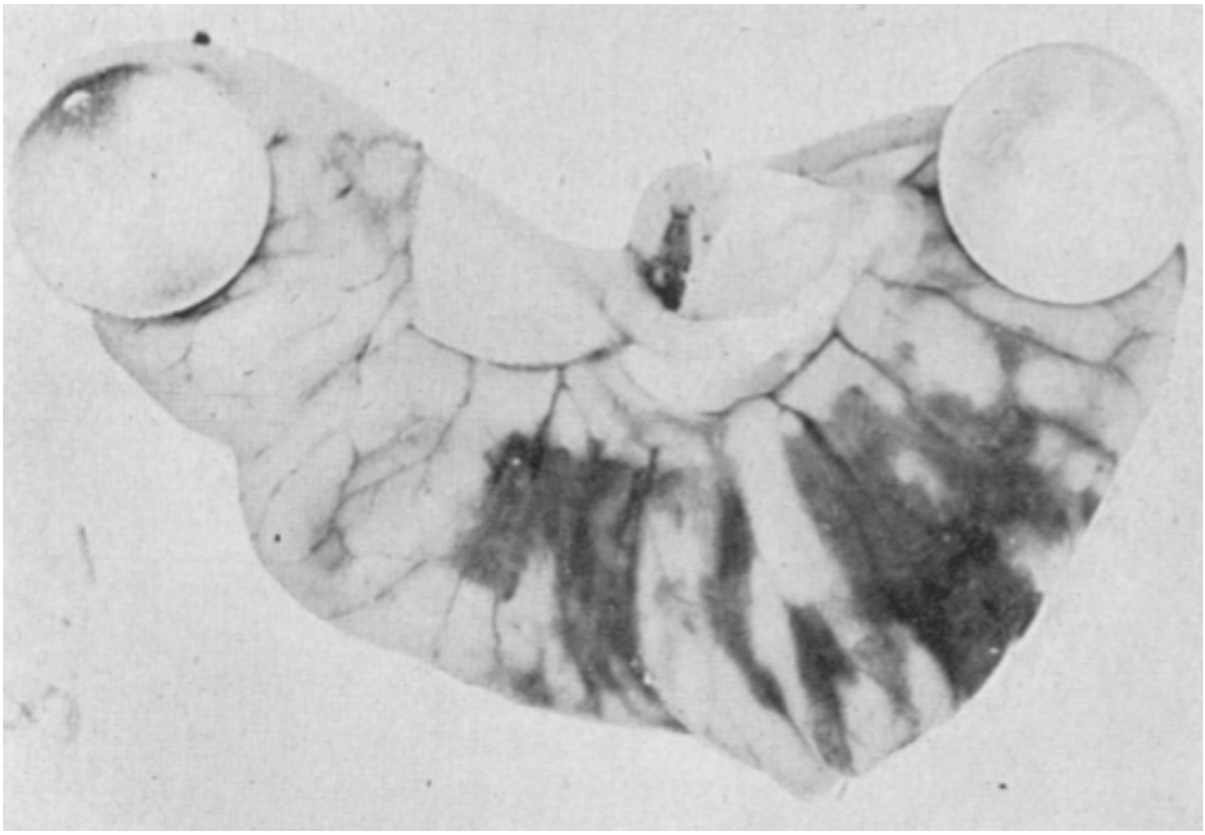

Figure 10: Hemorrhage in the small intestine of a monkey subject to a blast wave [Hunter, 1941]

Injury to the lungs is the cause of the greatest morbidity and mortality in regards to blast injury. [Phillips, 1986] Primary blast lung injury results in alveolar wall damage leading to intra-alveolar hemorrhages and interstitial hemorrhages. An accumulation of fluid beneath the skin, known as edema is also encountered. Figure 11 shows the tears of the alveolar wall as a result of blast lung injury. In severe cases there may be tearing of the alveolar wall and ruptures in the visceral pleura. These injuries lead to collapsing of the lung, pneumothorax and an accumulation of blood in the pleural cavity, hemothorax. Ruptures and tears to the alveoli and pleura can lead to air embolisms as air may enter the circulation system. [Katz, 1988] Air embolism, massive pulmonary contusion and hemorrhage account for the majority of immediate and early deaths from primary blast injury. [Guy, 1998b] The results from animal studies suggest that primary blast injury can result in minimal or no signs of external trauma or injury. [Elsayed, 1997; Hunter 1941; Irwin, 1998] The subject may however be injured severely internally with internal contusions and hemorrhages. External inspections of individual may only show some minor contusions and slight bleeding. The most prominent and lethal lesions occur in the lungs. From post mortem analysis the lesions in the lungs often follow the lines and contours of the ribs. [Hunter, 1941] Figure 12 shows the effect of primary blast injury on the abdominal wall. The visible injury includes skin abrasions, hemorrhaging, and contusions.

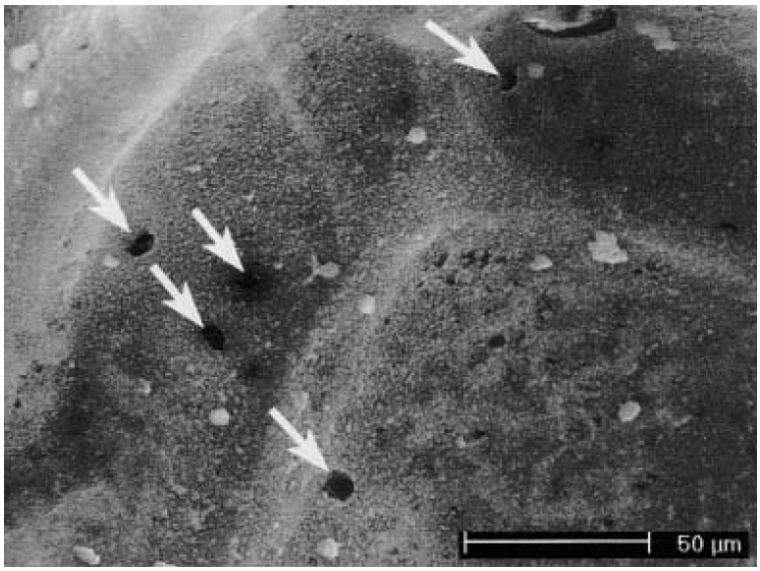

Figure 11: Electron microscope image showing perforations (arrows) of the alveolar wall as a results of blast lung injury [Tsokos, 2003]

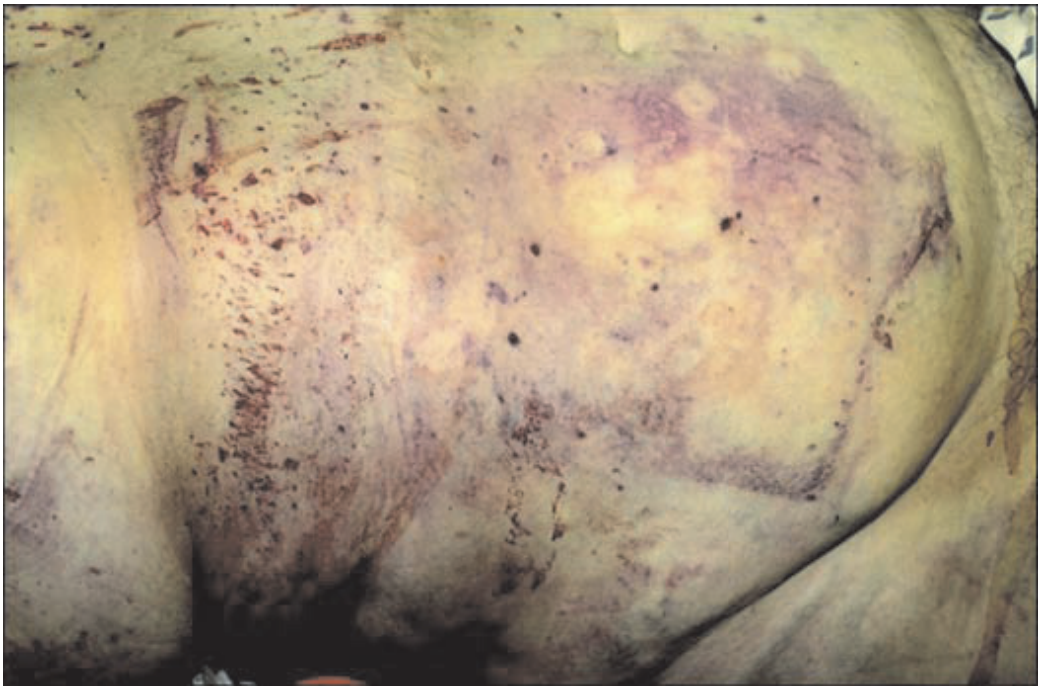

Figure 12: Effect of blast on abdominal wall [Mayo, 2006a]

2.4 Primary Blast Lung Injury

2.4.1 Overview

Blast lung injury is a form of primary blast injury caused directly by the blast wave from an explosion. Blast lung injury is one of the main causes of severe injury and death in subjects exposed to a blast wave. [Cernak, 1999] The severity of blast lung injury is related to the size and type of explosive used, the duration of the blast wave and the magnitude of the pressure wave and the distance the subject is from the explosive source. For enclosed blast scenarios the injury severity is also increased as a direct result of the complex blast waves. [Dorn, 1999] Blast lung injury is used to broadly capture the injuries associated with explosions including pulmonary contusions, hemorrhages and edema with alveolar and vascular injury. [Sasser, 2006]

2.4.2 Theories on Injury Mechanisms

The mechanisms of blast lung injury have been studied and theorized for several years, dating back to the Second World War. There were three main theories in this time used to explain the mechanism of primary blast lung injury and the pulmonary hemorrhages observed in soldiers.

The third and most widely accepted theory stated that the pulmonary hemorrhages are caused by the impact of the pressure wave on the chest wall. This theory has also been correlated with experiments performed on animals, performed in the similar time period. [Hunter, 1941] This theory is still widely accepted however the exact mechanism for injury

has been improved and expanded on the premise that the impact from the blast wave causes injury.

The mechanism of blast lung injury is complex and has been related to the waves that propagate through the body from the energy transfer from the impact of the blast wave. High velocity waves cause pressure differentials at the interface of tissues with different densities. These pressure differentials result in the tissue damage and injury. [Sasser, 2006]

The blast wave does not enter the thorax, it however it transfers energy to the body as the wave impacts the thorax. Injury occurs between the dynamic interactions between the pressure wave, the chest wall, the lung tissue and pulmonary vasculature. The dynamics of the thorax, thorax structure and velocity of the chest wall movement all appear to contribute to the severity of blast lung injury. [Axelsson, 1994; Sasser, 2006; Viano 1989]

One theory of primary blast lung injury is that it occurs due to the propagation of stress waves through the thoracic tissues into the lung. [Stuhmiller, 1996; D'yachenko, 2005] This theory is widely accepted and has been researched. [Guy, 1998a] As the blast wave is transmitted to the body stress waves and shear wave arise in the body and travel to the viscera. These waves are generated by the contact and impact of the blat wave on the torso. The viscera, refers to the organs in the thorax. Shear waves and stress waves injure the viscera in different ways. The shear waves produce large distortions in the tissues and injury results as the viscera is stretched beyond its elasticity and where there is a collision between the viscera and more resistant structures, such as the ribs. Shear waves result in tears, contusions and contra-coup injury. Stress waves cause injury at locations where energy is deposited, such as the locations where the waves reflect or change their speed. This occurs

primarily at locations where there is a change in tissue densities, and at air-water interfaces. The lungs are especially susceptible to this form of injury as there are many air-fluid interfaces in this organ.

2.4.3 Symptoms

Surveying casualties with primary blast lung injury are usually present with a variety of respiratory issues. This may include one or more of the following: difficulty breathing, chest discomfort, cough and hemoptysis. Often patients with blast lung injury will have other injuries incurred from the blast so it may be difficult for an examiner to know the direct problems encountered with blast lung injury. [Sasser, 2006] Acute respiratory distress syndrome (ARDS), is a serious condition that may be present. This condition arises from injury to the lungs and causes inflammation and negatively effects respiration. A reduced heart rate immediately following the blast was observed in animals and noted from reports involving human casualties. Their heart rate recovered to pre-blast values after approximately 60 seconds. In reports from WWI it was observed that individuals had lower blood pressure that may last several hours to several days after being exposed to a blast wave. [Guy, 1998a]

The result of the blast wave on the chest causing blast lung injury results in tearing, hemorrhages, edema and the potentials for air embolisms and barotrauma. [Sasser, 2006] Pressure differentials across the alveolar/air interfaces caused during blast loading lead to the rupture and tearing of the alveolar septa and capillary walls. [Mayo, 2006a] The ability for the waves to be reflected inside the viscera leads to greater injury potential. The reflection of stress waves also correlates and explains the injuries occurred in areas with stress concentrations. The stress waves also explain the injury that may be observed at locations distant from the point of impact. [Guy, 1998a]

Blast lung injury typically results in pulmonary contusions and hemorrhages. [Cohn, 1997] The pulmonary hemorrhages observed can be divided into three types: pleural or subpleural, multifocal or diffuse parenchymal and hemorrhages surrounding airways and vascular structures. Pleural or subpleural hemorrhages are usually observer in both lungs however the injury is usually more severe on the side facing the blast source. These hemorrhages occur in areas of high stress concentration, on the posterior of the lung surface and where the right and left lungs make contact. Damage is also usually visible by markings, which correspond to the intercostal tissue space. Figure 13 shows the markings clearly visible on the lungs of a rabbit resulting from blast lung injury, the areas of injury are coincident with the intercostal tissue.

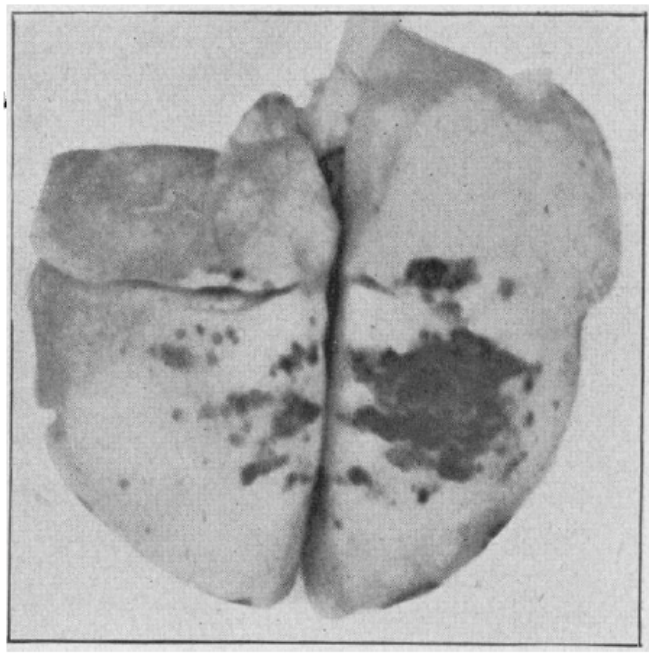

Figure 13: Lungs of a rabbit exposed to blast showing areas of hemorrhage behind the intercostal tissue [Hunter, 1941]

Multifocal or diffuse parenchymal hemorrhages are a result of the stress concentration from the lungs being distorted by the blast wave, resulting in the rupture of the alveolar walls. As these walls are ruptured the spaces are filled with blood and the bronchioles rapidly become filled with blood. Hemorrhages surrounding the airways result in blood vessels being ruptured and filling with blood, giving the appearance of ring hemorrhages. Edema typically occurs in blast lung casualties, resulting in an accumulation of fluid beneath the skin and in the lungs. [Irwin, 1998]

As the viscera is damaged by the high stresses produced in the body from the blast wave, pneumothorax and/or hemothorax are often encountered. Pneumothorax is the accumulation of air in the chest cavity and hemothorax refers to blood in the chest cavity. These conditions make respiration difficult and in some cases not possible. These conditions will reduce the intrathoracic pressure leading to the collapse of the lungs.

Injury to the lung has been the organ studied the most in regards to injury from blast overpressure. It is postulated that blasts can cause air emboli, which originate in the lung and travel to other organs in the body causing sudden death. In situations were air emboli are not produced, severe lung contusions may be just as lethal. [Mayorga, 1997]

In post mortem examinations, the lungs of animals were weighed and it was noted that those with blast lung injury had an increase in lung weight. The increase in lung weight is due to the edema and hemorrhage. The increase lung weight correlated directly with the blast peak pressure and mortality in animal studies. [Sasser, 2006] Figure 14 shows large hemorrhage areas in the lungs of a monkey exposed to blast waves.

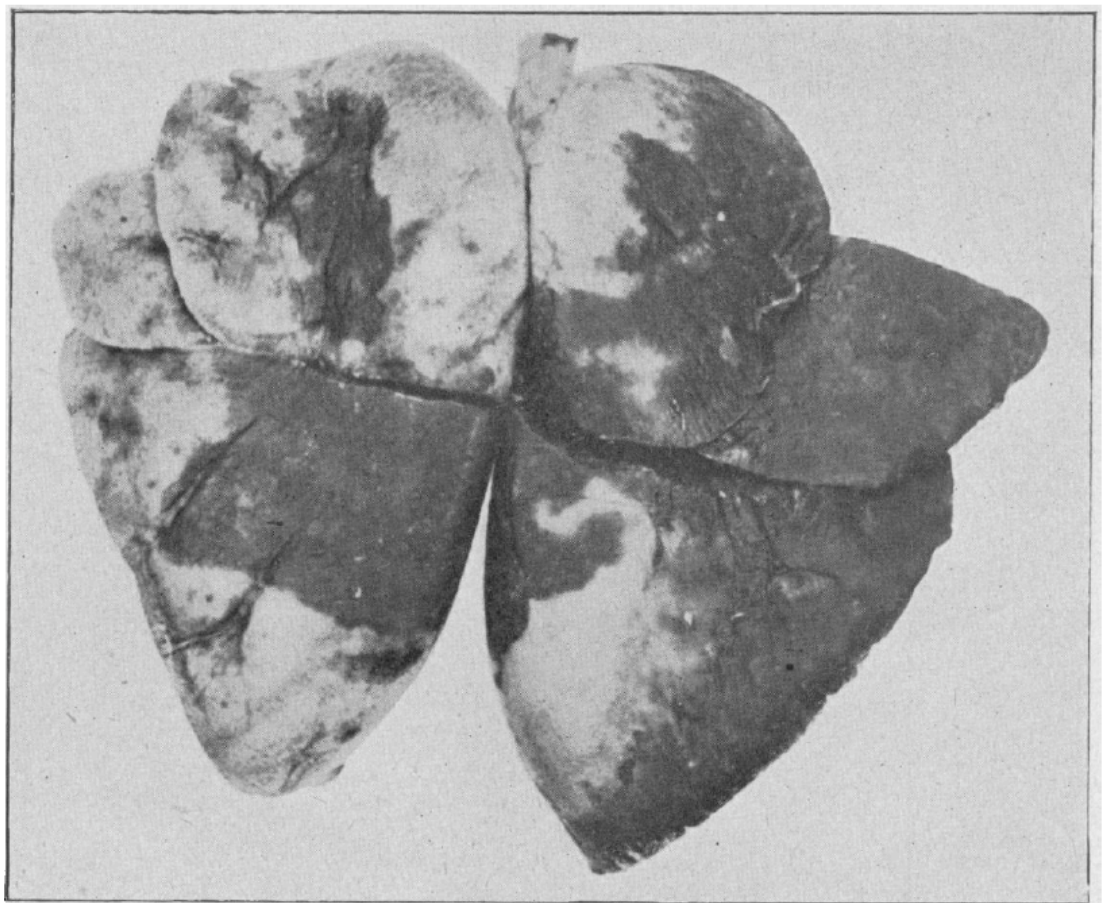

Figure 14: Lungs of a monkey showing areas of hemorrhage from blast lung injury [Hunter, 1941]

Lung infiltrates is a term that is used to describe the appearance of any abnormal substance that has accumulated in the lungs. In surviving casualties who have been exposed to a blast it is possible to diagnose blast lung injury by examining the x-rays of the patients chest. Lungs usually appear very dark on an x-ray because they contain mostly air, which allows the rays to pass through very easily. If the lungs start accumulating fluid, for example, fewer of the x-rays will make it through to the film and those areas appear whiter. The white areas are called infiltrates. Infiltrates can represent many things including pneumonia and other infections, tuberculosis, pulmonary edema, and hemorrhage, just to name a few; however for blast lung

injury the infiltrates generally represent the accumulation of fluid and blood accumulation or contusions. Figure 15 shows the x-ray of a patient with primary blast lung injury, showing the presences of patchy infiltrates.

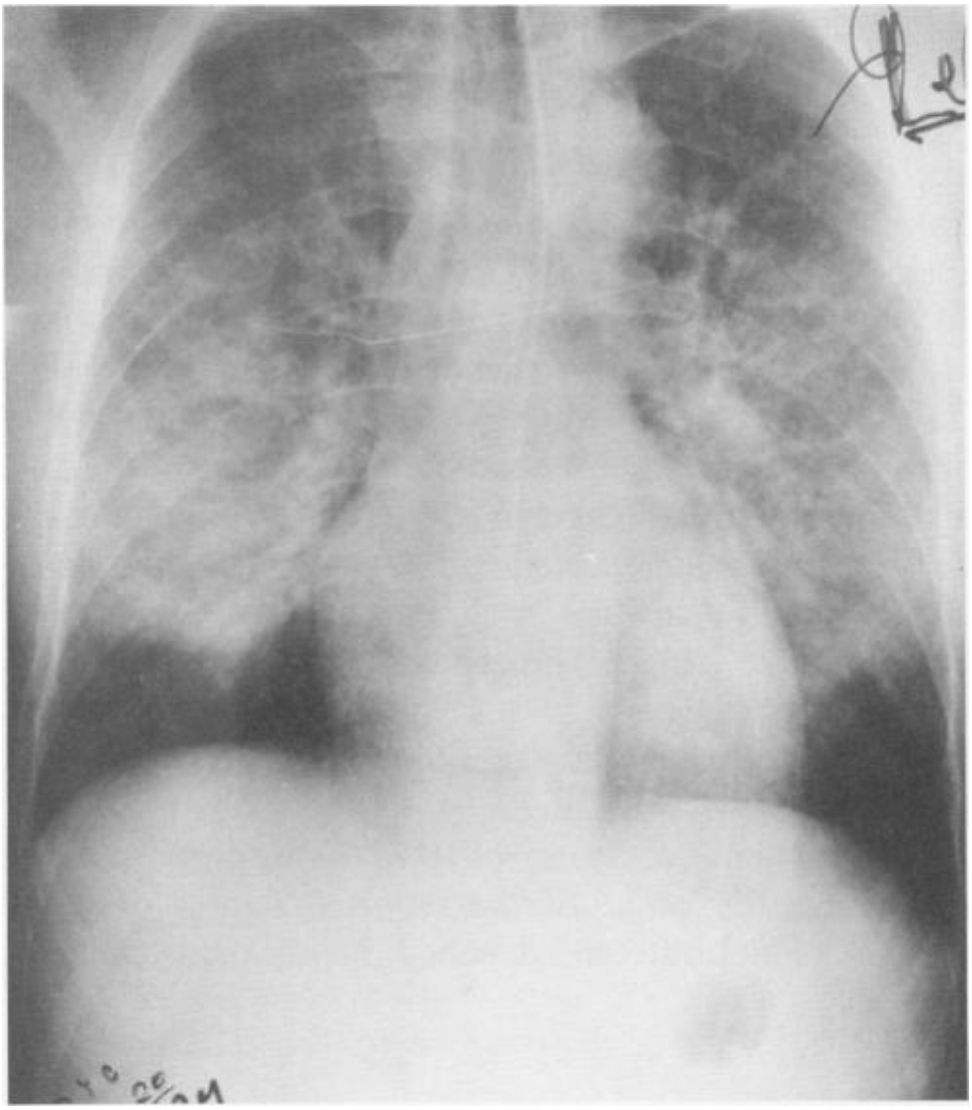

Figure 15: X-ray of patient with primary blast lung injury (6 hours after exposure) Bilateral patchy infiltrates are visible. [Katz, 1988]

It has been observed that the risk of primary blast lung injury increases when the body is subjected to complex blast waves. In Israel the result of two open air explosions resulted in an 8% mortality rate (15 of 204 casualties died). These results are much lower as compared to the aftermath of two explosions in the enclosed space of a bus, which resulted in a 49% mortality rate (46 of 93 casualties died). The increase in deaths was believed to be a result of the complex blast waves that are generated inside an enclosed space. Also the number of casualties with primary blast lung injury was much greater for the individuals on the bus. Overall for a similar explosive charge the degree of severity of injury is increased if the charge is detonated in an enclosed space as compared to an open-air environment. [Chaloner, 2005]

2.5 Other blast Injury

2.5.1 Secondary Blast Injury

The mechanism of secondary blast injury is the collision of fragments with the body. [Chaloner, 2005] The addition of fragments in explosive charges increases the risk of human injury, as there is the possibility of these fragments penetrating the body. Fragments, balls, bolts nails, chase encasing are the leading cause of injury in terrorists bombings. [Mayo, 2006] Fragments can be soil or environmental debris as well.

2.5.2 Tertiary Blast Injury

The mechanism of tertiary blast is the strong blast winds that result from the explosive detonation violently displacing and throwing the body and other objects. [Chaloner, 2005]

Tertiary blast injury may also occur by the blast wave collapsing a building or other objects and causing these objects to impact or fall on the body. [Mayo, 2006b]

Tertiary blast injury is a direct result of the blast wave displacing the subject. The force at which the subject impacts an object or is thrown correlates to the injury sustained. In severe cases, the strength of the blast wind may lead to limb amputations. Other injuries noted include fractures, brain injuries, crushing injuries, and injury from falling objects such as buildings and debris and blunt trauma. [Mayo, 2006b]

2.5.3 Quaternary Blast Injury

Quaternary blast injury is a result of heat, fires, and radiation causing injury. The exposure to the high temperature resulting from an explosion damages tissue and causes injury. [Chaloner, 2005] Certain chemicals such as powdered aluminum can be added to the explosive charge in order to increase the burn time, increasing the risk of quaternary injury. [Mayo, 2006b]

Quaternary injuries are responsible for burns to the subject. As a result of the explosions the thermal effects along with the possibility of nearby objects combusting can inflict injury. Although fires are rare as the explosion consumes the nearby oxygen, the subject may be burnt by a result of the exposure to thermal radiation. Burns to the external skin and burns to the airway passages of the individual may occur as the high temperature is breathed in through the lungs. [Guzzi, 1996]

2.5.4 Quinary Blast Injury

The mechanism of quinary blast injury is the effect of toxic chemicals. These chemicals can be an inherent result of the explosive or may be purposely added to the explosive charge to cause toxic injury effects. [Mayo, 2006a] Quinary blast injury is encountered due to the toxic effects in certain explosions and bombs. Quinary injury results in the individual becoming ill by absorbing or inhaling toxic chemicals. The type of chemical absorbed will determine injury; there have been cases reported where an individual suffered no external injury but was gravely ill because of the chemicals absorbed. [Mayo, 2006a]

2.6 Current Injury Prediction Methods

Several decades of blast injury research have led to the development of a number of injury prediction tools to predict a human's response to blast injury. These tools range from simplified mathematical equations to complex physical apparatus that are instrumented for experimental trials. The tools and prediction methods are generally only applicable to specific blast scenarios and many are not adequate for predicting injury from complex blast waves. The first blast injury prediction tools were based on animal studies leading to tolerance curves based on pressure and duration. [Bowen, 1968] Further prediction methods were developed by simulating the thorax as a mechanical system. [Stuhmiller, 1988] Recently a number of experimental test devices have been developed which claim to be able to predict blast lung injury. These devices work by measuring pressure in a blast flow field and then post processing the recorded data. [Axelsson, 1996] Finite element models are also capable of predicting injury and have the advantage of being able to model the blast flow and human thorax numerically. [Greer, 2006]

2.6.1 Bowen Curves

In order to estimate humans' tolerance to blast injury a number of studies into the effects of blast waves were carried out in the early 1950s and into the late 1960s. As it is not possible to perform severe and potentially lethal experiments on humans, the tests were conducted on animals. Bowen performed tests on thirteen mammalian species to cover blast effects on a wide range of body masses. The bodies were subjected to several different blast waves to further broaden the study. A research program at the Lovelace Foundation involved the biological effects of blast waves in air. A large number of experimental tests were carried out, in which the animals were subjected to a blast wave, when their bodies were near a reflecting surface.

The data from 2097 animals was compiled and used in Bowens study in order to estimate the survivability of a human subjected to a free field blast wave. Most of the data used in the study was available and was taken from experiments in which the animal was located near a flat rigid, reflecting surface. The tests were performed by placing the animal on the ground and detonating the charge above the animal. This method eliminated the ground reflection from the charge and simplified the experimental setup, as the animal did not have to be suspended in the air. The downside of this was that the animal was placed against a rigid surface that would produce blast wave reflections that could influence the data. Bowen states that the biological response was found not to be significantly influenced by the presence of the reflecting surface. [Bowen, 1968] However, it has been shown that the presence of a reflecting surface does have an effect on blast injury. [Katz, 1989] The purpose of Bowens study was to compile and unify the existing data and through analysis techniques predict the survivability of humans in regards to blast waves. The ultimate goal was to predict the survivability percentage of a mammal based on four variables:

i. The maximum reflected overpressure
ii. The duration of the wave

iii. The body mass of the mammal

iv. The species tolerance index (based on the size and weight of the animal)

Knowing the mass of humans and their species tolerance index, it was deemed possible to relate injury to blast overpressure and duration.

In Bowen's study the mortality data used for all of the test cases is valid for a 24 hour period, following the detonation and contact of the body with the blast wave. The majority of the data was derived from animals subjected to a reflected blast wave. Data was also compiled from animals subjected to the blast from shock tubes, however very little free-field test data was used. The high explosive, short duration data was compiled mainly from the animal test in which the animals were subjected to reflecting waves. The shock tube experiments provided data relating to waves with long durations.

The majority of the experimental data was obtained with a charge placed above the animal. The animal was restrained and placed on a concrete pad and the charge placed above the animal. A minimal amount of restraints were used as to not interfere with the data. Depending on the size of the animal, tape, string or a harness was used as restraints. The animal was restrained in a prone position. The only exception being the tests in which some sheep were used. In some of the sheep experiments the animals were suspended upright and a charge placed at chest level in front or behind them.

For the shock tube data, the mammal was placed near the end of the shock tube. Pressures and duration were measured with pressure transducers near the end plate of the shock tube.

The mammals were oriented so that left side of the body was against the end plate of the tube. The only exception to this was when test were done with monkeys; for these experiments the monkey was facing the blast tube. Bowen states that the difference in orientation and its effects was not known.

As it was difficult to accurately measure the pressures and durations with the existing data acquisition equipment of that time, Bowen relied on existing published data on the duration and pressures produced by the detonation of Pentolite. This data was then scaled to equivalent TNT values. Based on a relation that the mammalian response to air blast is dependent on positive phase overpressure impulse for blasts with short durations and on overpressure for blasts with long durations, an equation relating these was derived. This equation is shown in Equation 3. For long durations the factor aT^{-b} approaches zero.

$$P = P^{*}\left(1 + aT^{-b}\right)$$

where:

P is maximum overpressure

T is positive phase duration

P^{*}, a, b are experimentally evaluated constants

Equation 3: Relationship between maximum overpressure and positive phase duration [Bowen, 1968]

In order to scale the results from the animal tests to those of a human a relationship resulting from a study relating the blast duration, ambient pressure and the mass of the mammal were used. Equation 4 was used to scale all of the durations into durations applicable to a 70kg mammal at an ambient pressure of 14.7psi.

$$T = t_t\left(\frac{70}{m}\right)^{\frac{1}{3}}\left(\frac{p_0}{14.7}\right)^{\frac{1}{2}}$$

where:

t_t is the experimental duration

m is the mass of the mammal (kg)

p_0 is the ambient pressure (psi)

T is the scaled duration

Equation 4: Duration scaling equation for ambient pressure of 14.7psi and a 70kg man [Bowen, 1968]

The reported pressure in each of the experiments required a common base line so an equation was used in order to scale the peak overpressure of the blast wave. The equation is shown in Equation 5 and relates the experimental overpressure observed at a given ambient condition to that obtained with an ambient pressure of 14.7psi. The pressures in the equation are recorded as reflected pressures as the reflected pressure was that recorded in the majority of the experimental tests involving the mammals.

$$P = P_R\left(\frac{14.7}{p_0}\right)$$

where:

p_0 is the ambient pressure obtained during the experiment (psi)

P_R is the reflected pressure observed at p_0

P is the scaled reflected pressure

Equation 5: Reflected pressure scaling equation [Bowen, 1968]

By scaling the data to a consistent reference frame and performing a statistical and a parallel-probit analysis Bowen produced survivability curves for HE blasts and long duration, square wave type blasts for each of the animals tested. In all 13 species of animals were used: mouse, hamster, rat, guinea pig, rabbit, cat, monkey, dog, goat, sheep, pig, donkey and steer. Based on the findings the species were separated into two groups; a high tolerance group and a low tolerance group were formed. The two groups were formed based on the species size and weight and their tolerance to blast; large animals were categorized in the high tolerance group and small animals were categorized in the low tolerance group. Humans were placed in the high tolerance group and there probability of survival was estimated based on the findings from the animal results. A summary of the findings is shown in Figure 16 along with the number of animals used to obtain the correlation.

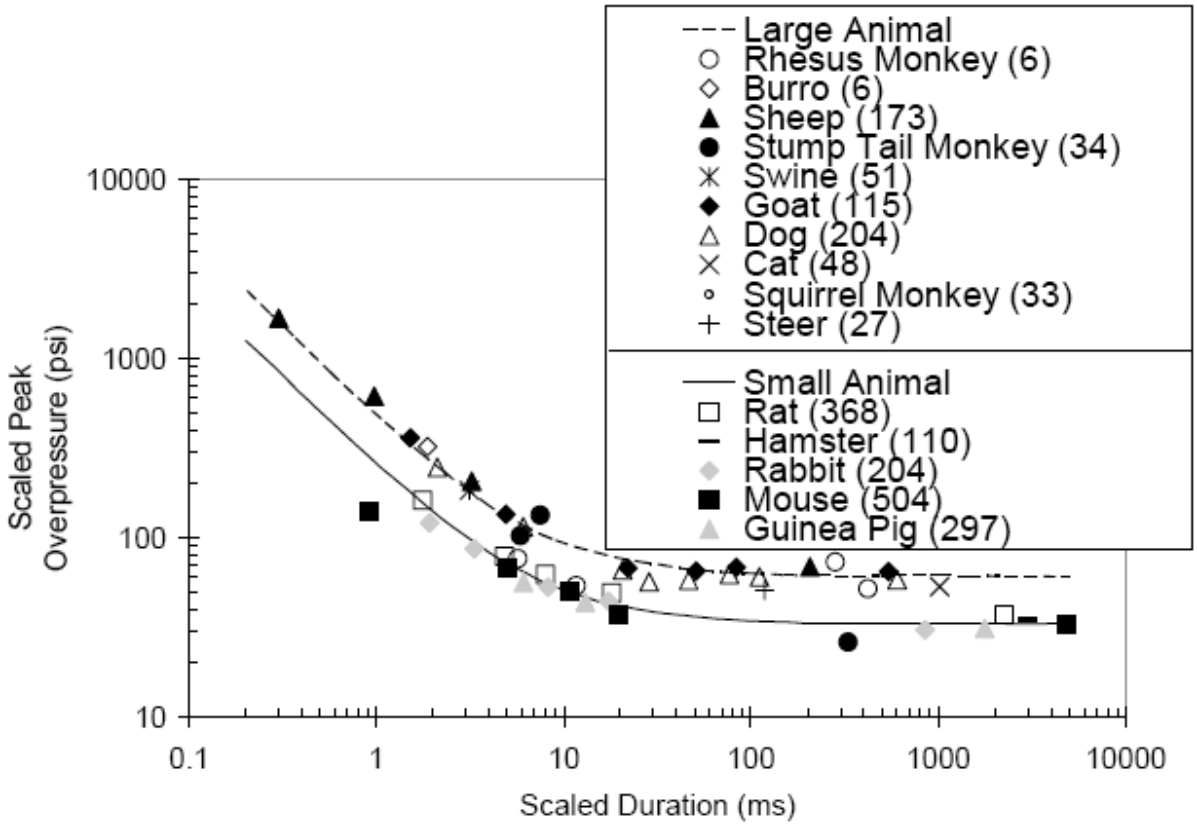

Figure 16: Bowen survivability curves for high and low tolerance animals [Bass, 2006]

Bowen derived three curves used to predict the lethality from overpressure and duration caused by a blast wave in air. The three curves derived depend on the body's orientation to the blast wave and the orientation; the orientation scenarios are shown in Figure 17 and consist of the following:

a. Long axis of the body parallel to the blast winds with the subject facing any direction
b. Long axis of the body perpendicular to the blast winds with the subject facing any direction

c. Thorax near a reflecting surface which is perpendicular to the blast winds with the subject facing any direction

Figure 17 shows the corresponding peak overpressure conditions used in the three, body orientation cases. Depending on the body orientation to the blast wave the pressure used to predict the injury will be different. The original data used to generate the Bowen curves was based on reflected overpressure and the curves have been calculated based on simplifications to produce probabilities based on a blast wave impacting a person who is not near a reflecting surface. For a body parallel to the blast wave the overpressure used to predict injury is simply the incident overpressure of the wave itself; it is assumed that the body does not cause a significant disturbance in the flow. However when the long axis of the body is perpendicular to the blast wave the overpressure used is a sum of the incident overpressure and the dynamic pressure, caused by the effect of the disturbance that the body has in the flow field. For a body near a reflecting wall, the reflected pressure is the normal reflected pressure at this rigid surface. [Godfrey, 1994]

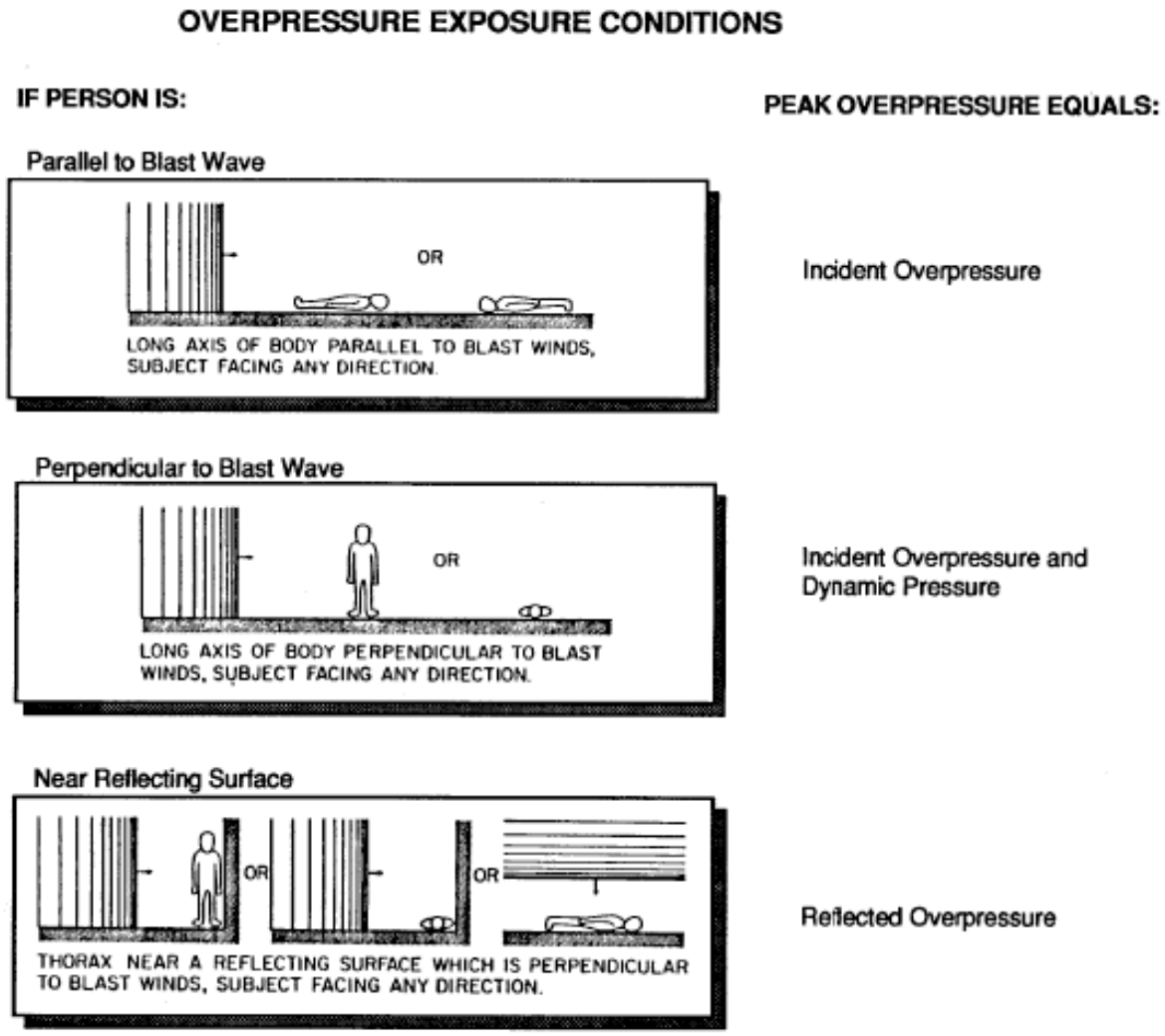

Figure 17: Overpressure exposure conditions [Godfrey, 1994]

Bowen predicted survivability curves for a 70kg man; these curves are applicable for an ambient pressure of 14.7psi. If the mass of the human and/or ambient pressure is different from these values, then scaling laws should be used in order to obtain the correct values for the required mass and ambient pressure. Curves for each of the 3 body orientations are shown in Figure 18, Figure 19 and Figure 20. These curves related the body orientation, the maximum incident overpressure of the wave and the positive phase duration of the blast to

probability of survivability. It is important to note that when comparing Figure 19 and Figure 20 it is clearly illustrated that when the person is near a reflecting surface the probability for survivability is greatly reduced as compared to the same blast in the free field. The reflected pressure from the blast wave has the result of increasing the injury on a person.

Along with curves for probability of survival of 1, 10, 50, 90 and 99 percent, Bowen produced a curve for threshold lung damage. The experimental data enabled the creation of the LD50 curves and the other curves were interpolated. According to Bowen, threshold lung damage is assumed to occur at one-fifth the 50 percent survival overpressure. [Bowen, 1968] Lung damage threshold refers to 'pin head' damage to the lungs having no physiological effects. [NATO, 2007]

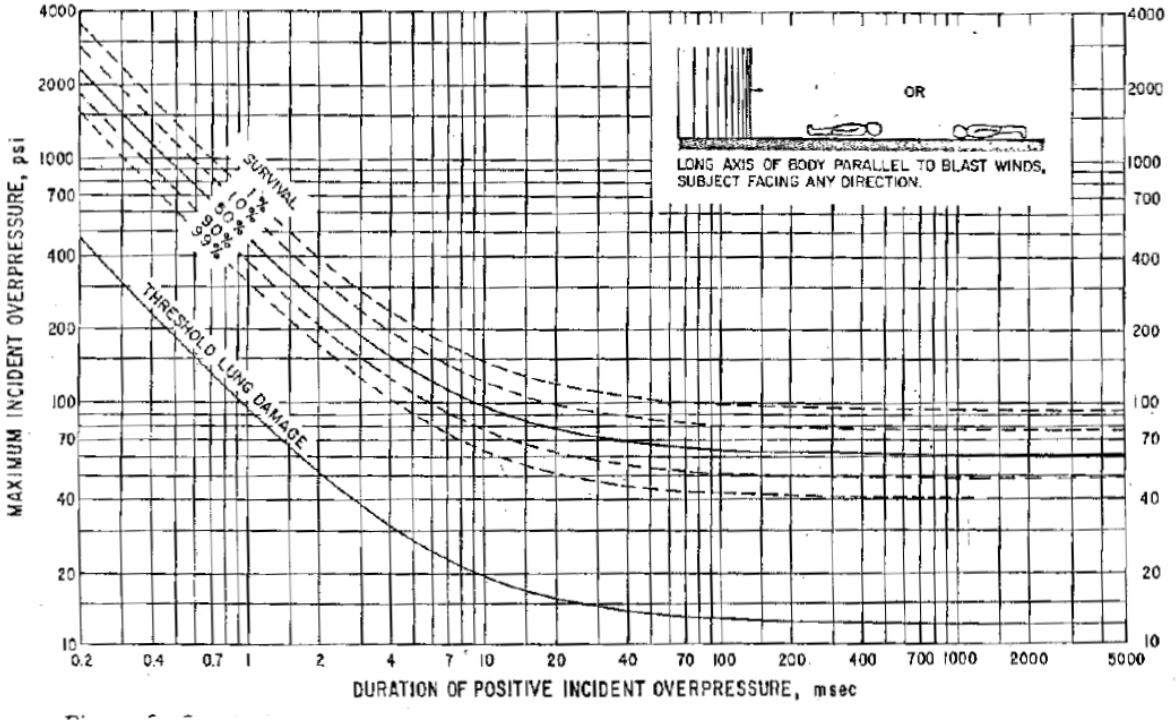

Figure 18: Bowen survivability curve for long axis of body parallel to blast winds [Bowen, 1968]

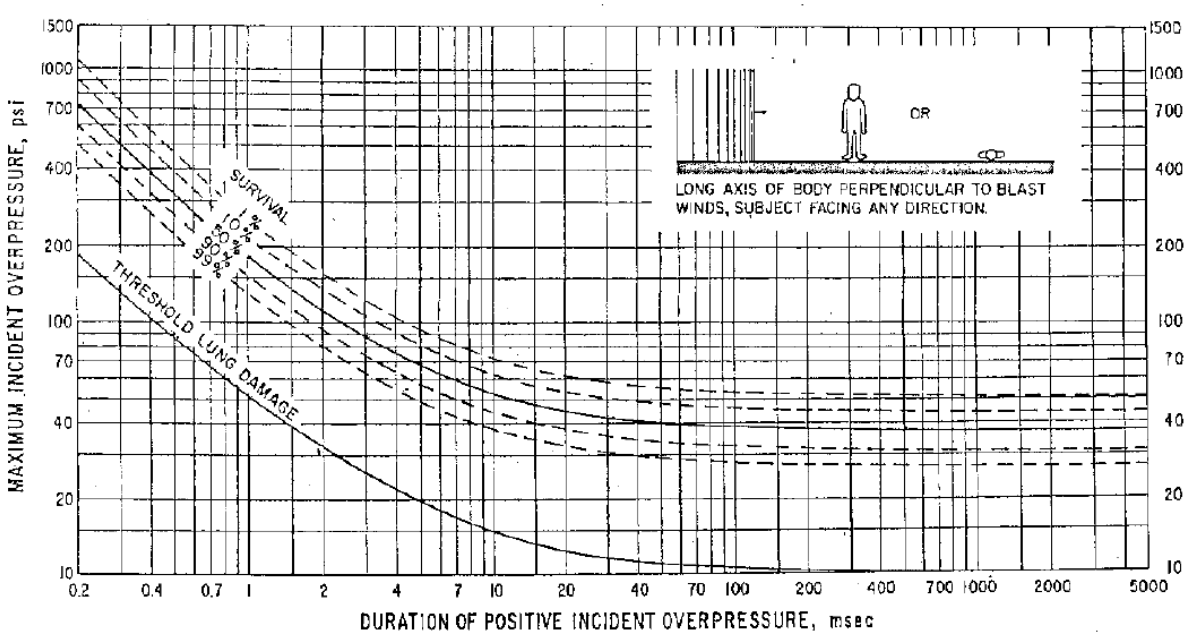

Figure 19: Bowen survivability curve for long axis of body perpendicular to blast winds [Bowen, 1968]

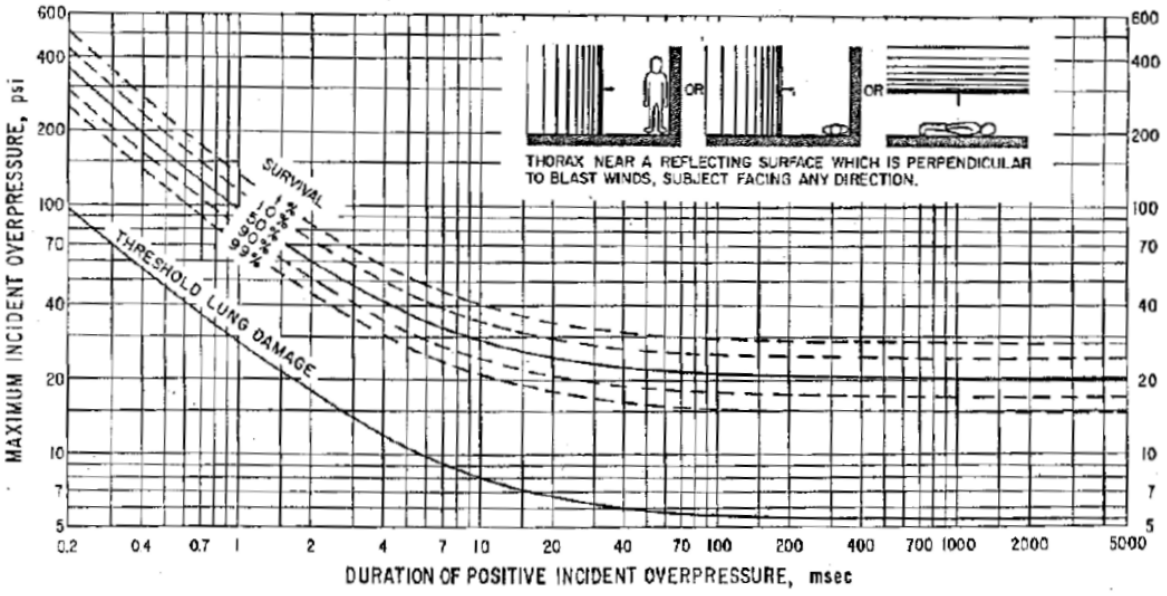

Figure 20: Bowen survivability curve for body near a reflecting surface [Bowen, 1968]

Along with generating curves relating the blast overpressure and duration to injury, Bowen produced curves relating the mass of the explosive (in terms of TNT) and the distance from the blast source to the predicted injury level. These generated curves are also based on the orientation of the body to the blast wave. These curves were produced in order to make the injury curve more readily usable as the reader does not need to know the overpressure and duration, but rather the equivalent TNT size of charge and the distance from the charge. The TNT equivalence technique allows for a wide range of explosives to be considered, by scaling them to their TNT equivalence value. [Wharton, 2000] The curves are shown in Figure 21, Figure 22 and Figure 23 for each of the body orientations.

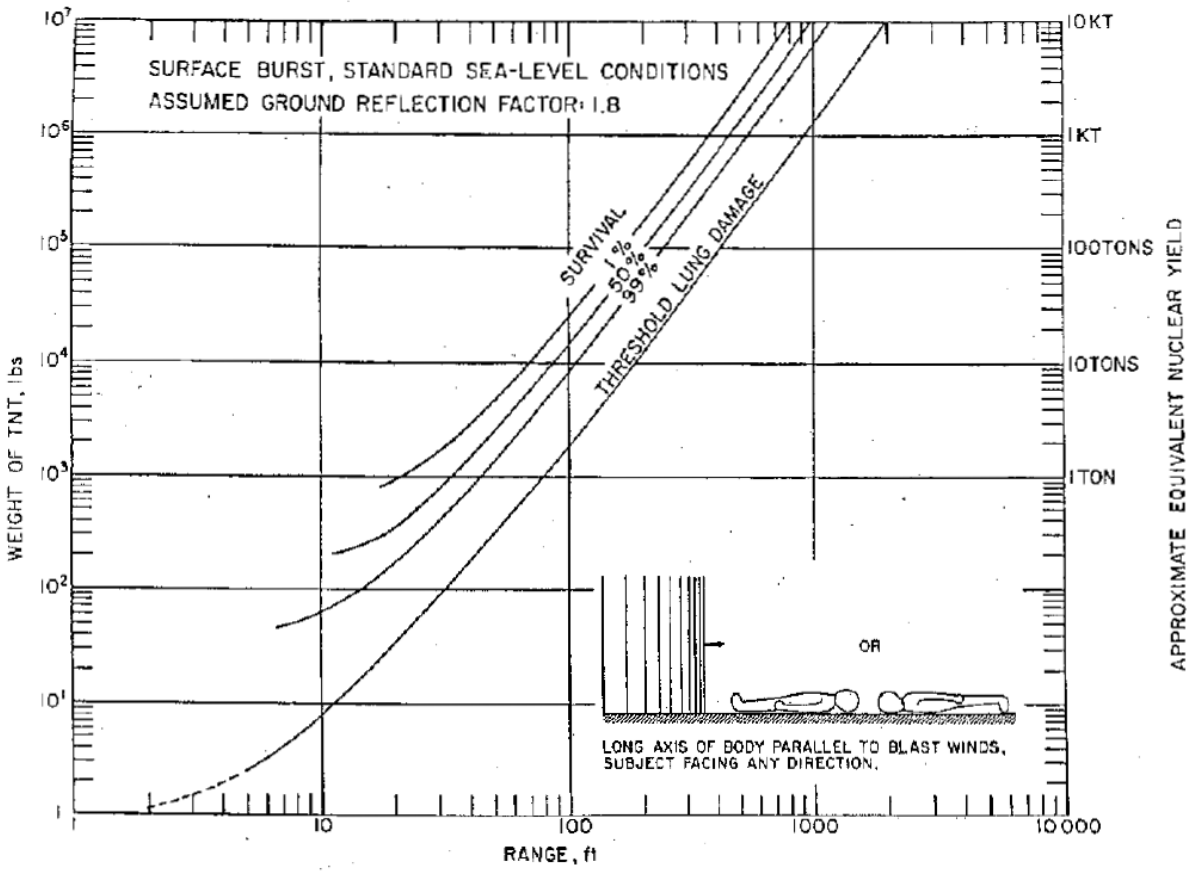

Figure 21: Survivability curves relating charge mass to range for a body parallel to the blast winds [Bowen, 1968]

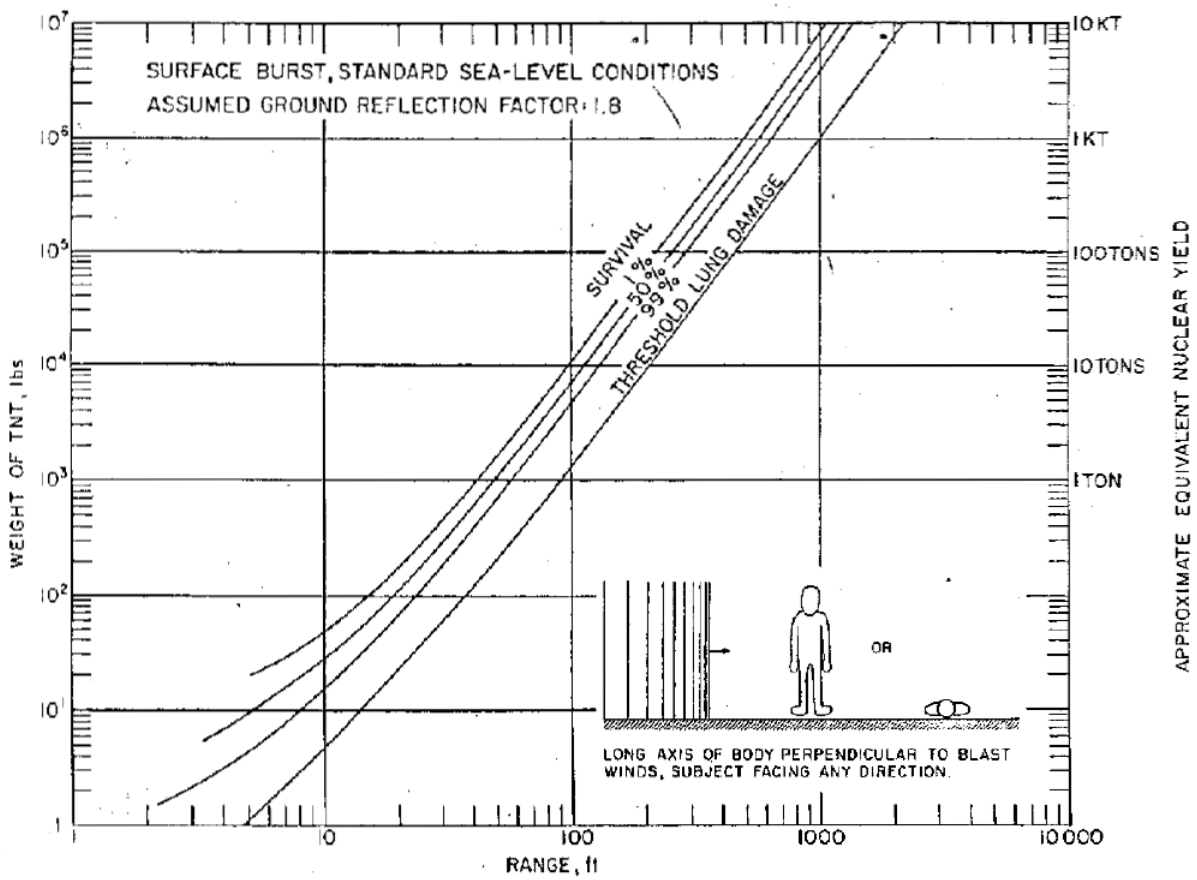

Figure 22: Survivability curves relating charge mass to range for a body perpendicular to the blast winds [Bowen, 1968]

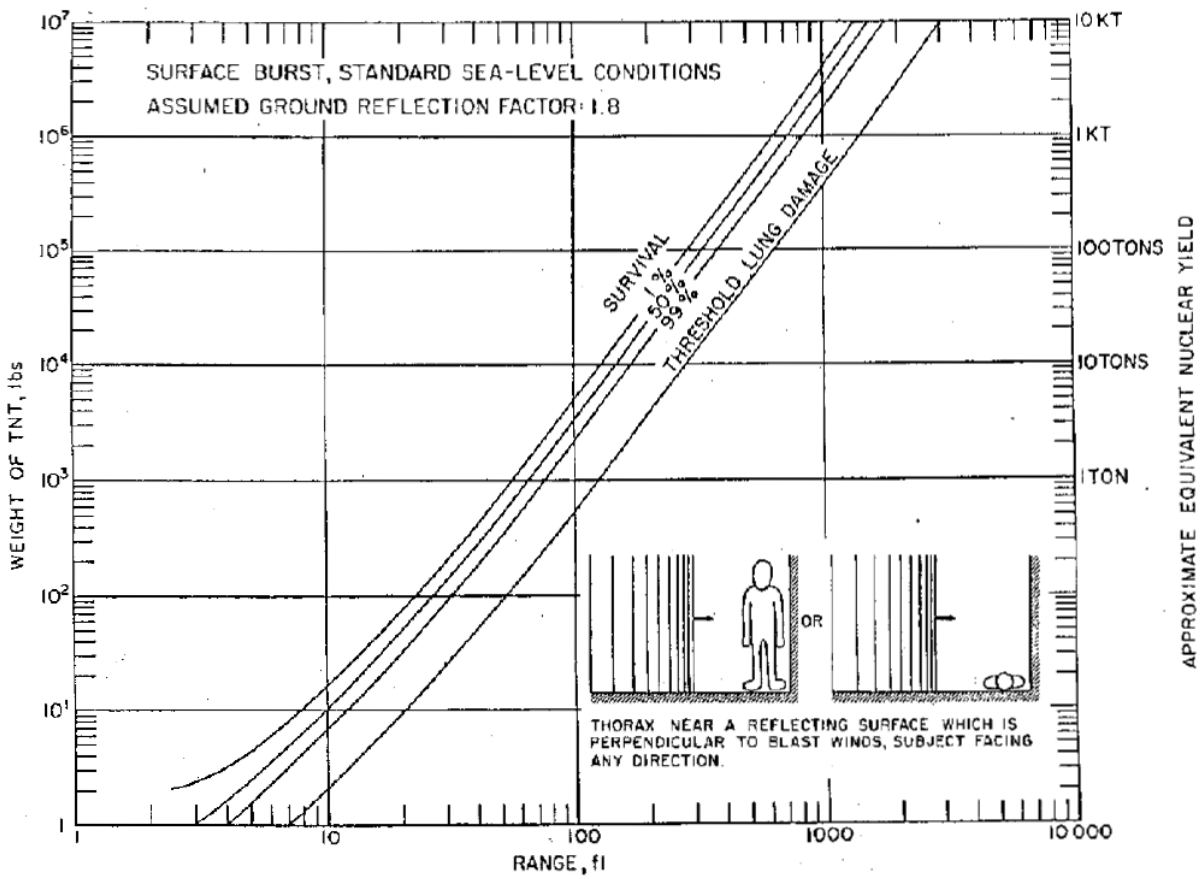

Figure 23: Survivability curves relating charge mass to range for a body near a reflecting surface [Bowen, 1968]

During the compilation of experimental data Bowen noted that the species with large lung volumes relative to their body mass generally had a higher blast tolerance. It was also noted that the body mass was the only parameter required to relate the severity of injury between each of the species. As can be seen from Equation 3 and Equation 4 all things being equal, the body mass is the factor in the equation used to predict injury. The volume or density of the animal's lungs is not required. Bowen also noted that for the same species, individuals with smaller lung volumes have lower blast tolerances.

Bowen's work did not focus on complex blast waves. The studies were done in open air in free field, scenarios without reflecting surface. [Bowen, 1968] The main limitation of the Bowen curves is that they were developed for ideal shock waves. These curves are not directly applicable to complex blast waves. [NATO, 2007] Other limitations of the Bowen curves are the limited data and noting that most of the data obtained was from scenarios where the animal was exposed to the reflected blast wave. The results from the reflected scenario were then used to estimate curves for free-field open air scenarios where the body is either perpendicular or parallel to the blast wave. There were also reported issues in which the pressure transducers were used. It was difficult to place a transducer directly on the animals' thorax, and in most cases it was placed as close as possible to the thorax. As the pressure of the blast wave rapidly decreases as it moves farther from the explosive source it is possible that in many cases, the recorded overpressure was somewhat reduced to that experienced at the animals thorax.

2.6.2 UVa Curves - Revised Bowen Curves

As a result of the increased prevalence of blasts in war and the increased number of soldiers being injured by blast in conflicts a study was launched to investigate the Bowen curves generated by the Lovelace Foundation. The Bowen curves were generated in the 1960s and had not been updated in over 35 years. Since the development of the curves new experimental data has been produced and there have been many questions regarding the validity of these curves for short duration blasts. Bass decided to review the original Bowen curves to investigate there deficiencies for blast durations under 30ms in order to improve the curves and increase their ability to accurately predict human injury from blast waves in air. During the reassessment new injury curves were developed that should replace the original Bowen curves; these curves are commonly known as the Revised Bowen Curves or UVa curves.

The data used by Bowen was also used by Bass, however Bass was much more selective regarding which data points should be included to predict human injury. Bass's study focused on large animals subject to blast waves with durations less than 30ms. The animals reviewed for the study were unprotected and information of the mass, injury and fatality outcome from the experiments was used. As was noted by Bowen, animals fall in two categories, either high or low tolerance to blast waves. Bass limited his study to the high tolerance, lager animals group as this is the group that humans fall under. The animals used for this study were specifically selected as they have similar lung densities as humans. Durations less than 30ms were selected to limit the injury mechanism being studied and to limit the equipment required for the experiments. It is believed that the injury mechanism is different for short and long blast duration. Short duration blasts tend to produce more localized injury as compared to long duration blasts where the entire body may be subjected to a constant high pressure. For experiments requiring a blast wave of long duration a shock tube is generally used, whereas short duration blast experiments generally use a bare HE charge. The experimental setup generally changes at 10ms. [Rafaels, 2008]

The revised Bowen curves also used the scaling laws by Bowen to scale the animal data to the reference mass of 70kg. The selected data was compiled and composed of 1129 animal experiments. A nonlinear logistic regression model was used to characterize the results and a good fit was obtained. The outcome of this study was the development of three new human blast tolerance curves.

The revised Bowen curve for the blast scenario, where the individual is near a reflecting surface correlated well with the original Bowen reflecting-surface curve. The other two curves did not correlate well with the original Bowen curves, where the body is parallel or perpendicular to the blast winds. One of the main findings in this study was that Bowen utilized pressure corrections for local ambient experimental pressures. The findings of this

study indicated that this type of scaling correction for short duration blast experiments at higher altitudes should not be used. The inclusion of this correction factor can lead to the under prediction of injury.

The revised Bowen curves were applied to body orientations similar to Bowen where the body was placed parallel and perpendicular to the blast winds. Bowen had suggested that for bodies parallel to the blast wave the overpressure used for the calculations should be the incident overpressure and for bodies perpendicular to the blast waves the combination of the incident and dynamic overpressures should be used. These revised Bowen curves suggest that this assumption may be valid for long blast durations, however for short durations and durations especially under 4ms that this assumption is not valid. The study suggest that scenarios were the body is parallel to the blast wave and scenarios where the body is near a reflecting surface that the overpressure used for injury prediction should be taken as the reflected pressure. The revised Bowen curves for bodies perpendicular to the blast wave along with the original Bowen curves are shown in Figure 24.

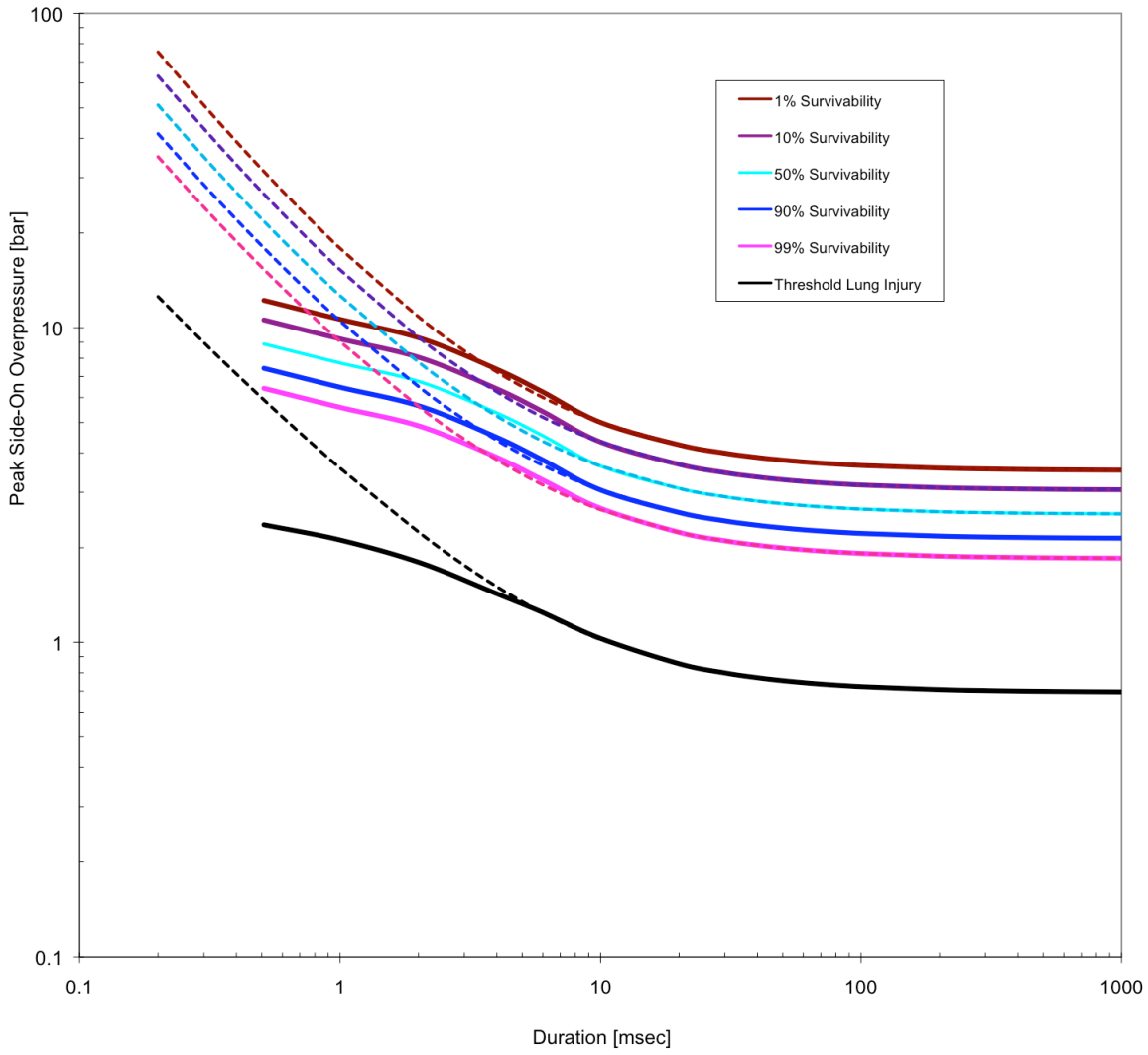

Figure 24: Revised Bowen curves for long axis of the body perpendicular to blast winds. Original Bowen curves shown as dashed lines

The newly generated injury curves from Bowen were compared to the curves and injury predictions for parallel, perpendicular and body near a reflecting wall scenarios. The scenario in which the body was placed near a reflecting wall showed a good correlation between the original Bowen curves and the revised curves. There was however significant discrepancy between the scenarios without a reflecting surface. The majority of Bowen's

original experimental data was obtained from animal data near a reflecting surface and this data was interpreted in order to obtain data for parallel and perpendicular body orientations to blast winds. The interpretation of the reflected wall case to the parallel and perpendicular cases is where the revised Bowen curves improve on the originals. [Bass, 2006]

Additional studies by Gruss also concluded that the original Bowen curves were under predicting the injury level for short duration blasts. Another study of the original Bowen curves involved examining the original data and using state of the art blast calculations to reassess the results calculated by Bowen. The study found that using the original Bowen curves with real blast pulse duration data, resulted in a more severe blast injury being predicted, than that, which would occur in reality. [Gruss, 2006]

2.6.3 Mathematical Modeling

There have been some numerical models and mathematical models used to simulate and predict primary blast lung injury, with limited success.

In the late 1960s Bowen presented a mathematical model of the thorax consisting of a two-chamber spring-mass system. Two chambers were used to simulate each of the lungs. This model was used by Josephson in 1988 to predict thoraco-abdominal response to complex blast waves. The model used is shown in Figure 25. [Josephson, 1988] In this model the chest wall was represented as a piston and the lungs are represented as air filled volumes. When a high external pressure was encountered the piston (chest-wall) accelerated and moved inwards compressing the gas of the lungs. The movement of the model terminated by the combination of the damper, pressure in the lung and spring stiffness. [Stuhmiller, 1988]

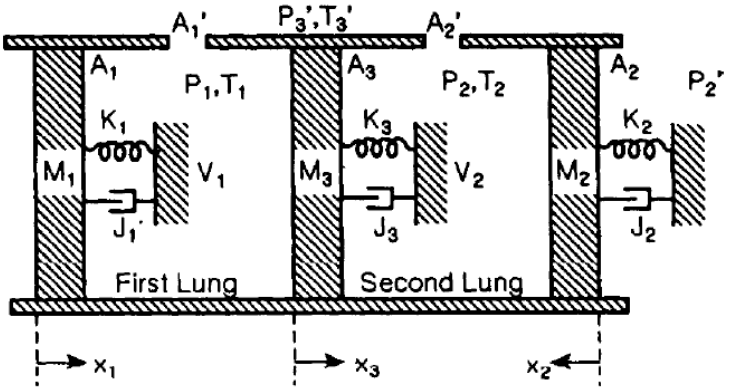

A_i	Effective Area	J_i	Damping Factor
A_i'	Effective Orifice Area	K_i	Spring Constant
M_i	Effective Mass	P_i	Internal Air Pressure
V_i	Gaseous Volume	P_i'	External Air Pressure
x_i	Displacement	T_i	Internal Temperature
		T_i'	External Temperature

Figure 25: Mathematic model of the thorax to simulate response to rapid changes in external pressure

Josephson subjected this model to simple blast waves consisting of various pressures versus duration values. The maximum values of thorax wall velocities, accelerations and internal pressures were obtained. The results were analyzed and it was noted that the maximum internal pressures correlated well to injury noted by the Bowen curves. Good agreement was made in the cases where a simple blast wave input was used.

In order to predict injury resulting from complex blast waves, this model was used and compared with testing performed on sheep. Sheep were instrumented with pressure transducers in their esophagus and placed in an enclosed space. A charge was detonated in the enclosed space and the complex blast wave was measured inside the thorax. The pressure-time histories from the physical experiments were then compared to the results

obtained by using the two-chamber model. There was a somewhat reasonable agreement between the two methods for predicting pressure over time in the thorax. There was however a good agreement between the maximum predicted internal pressure for both methods. Overall this method was able to capture some of the physics in predicting injury from complex blast waves however the author states that this method should only be used on an interim basis, for immediate needs in predicting injury.

2.6.4 Numerical Modeling

There have been several numerical models and mathematical models used to simulate and predict primary blast lung injury, with limited success. Efforts have been made in producing a more detailed model of the human thorax for use in blast injury prediction. Work has been performed by Stuhmiller in an attempt to create a numerical, finite element model of the internal organs of the thorax. The model developed by Stuhmiller represents the thorax of a sheep. A sheep thorax was chosen to model, as its geometry closely resembles that of a human thorax and there is a large body of knowledge as a result of the many blast tests performed on sheep. Utilizing finite element analysis the model improved on existing mathematical spring-mass models and is able to capture some of the physical properties of the tissue and organs of the thorax.

The finite element model was a two-dimensional model based on the horizontal cross section of the thorax of the sheep. The location of the cross section was chosen as it corresponds to the approximate location that measured the intrathoracic pressure in the physical animal tests. The major organs and their relative locations were captured and the model was divided into computational elements. A schematic of the finite element model is shown in Figure 26. The finite element model uses very large elements and is referred to as a very coarse model using current standards.

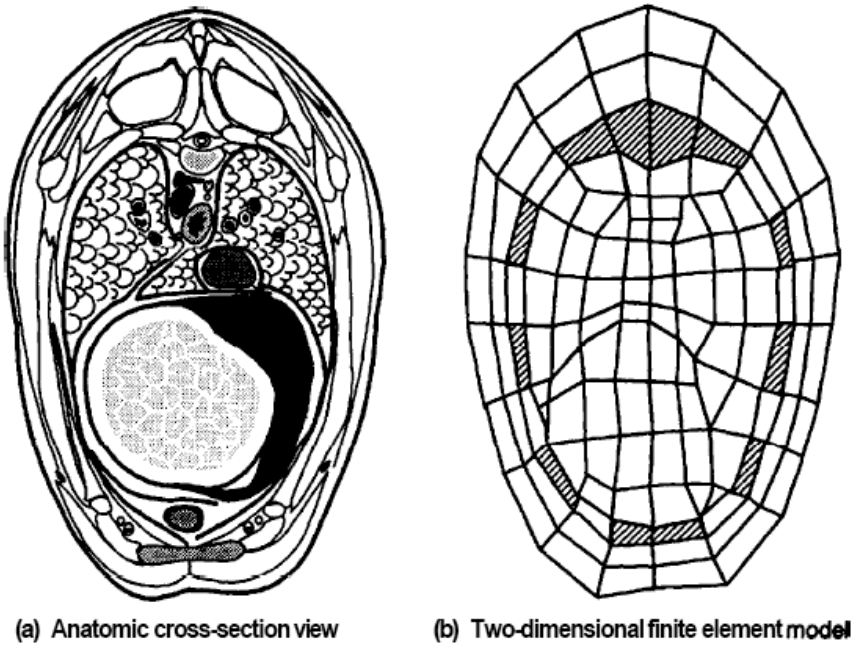

Figure 26: Cross section of sheep thorax and finite element model [Stuhmiller, 1988]

The most important requirement of the finite element model is in obtaining and implementing appropriate material properties to each of the tissue and organ types. This is also reported as being the most challenging aspect. [Stuhmiller, 1988] Through experimental testing it was noted the elastic properties of the rib and heart have a minimal effect in predicting the intrathoracic pressures. Using a lung tissue value that has a greater density or different properties than the actual organ can adversely affect the predicted response. The numerical model of Stuhmiller captured the skeletal muscle, rib, lung and water-filled organs such as the heart. The lung plays an important part in predicting injury and effort was made to obtain appropriate material properties for the lung. This was done by performing laboratory experiments in which the viscoelastic properties of the lung tissue and entire lung were performed along with experiments on the wave propagation through the lung. The finite element model was constructed and simulations were performed based on the existing

sheep experiments. The blast loading from the physical experiments was used as input and applied to the finite element model surface. The numerical simulation calculated the intrathoracic pressures and these values were compared to the experimental results. In general a fair agreement was made between the calculated results from the finite element and the measured results. Based on the coarseness of the model, blast loading uncertainties and numerical approximations, the model was able to capture some of the peaks and trends of the pressure time history in the lung.

The model was correlated to injury by noting from previous experiments that the severity of injury increases as the peak intrathoracic pressure is raised. This numerical model showed potential in using modeling to predict injury from blast waves and improved on the results of the two-chamber mathematical thorax model. [Stuhmiller, 1988]

2.6.5 Physical Test Devices

A thoracic test device, commonly used in experiments to predict primary blast injury is known as a Blast Test Device (BTD). A BTD is an instrumented cylinder used to represent the thorax of a human. The BTD however has a different cross sectional area as compared to a human. This difference in cross sectional area will also lead to the reflected pressure being different as compared to a human. The BTD uses a biomechanical model of the chest wall to compute the force that a blast wave would impart on a human in that location. By measuring the pressure at locations around the BTD cylinder and passing these as inputs to software, an injury value can be determined. Figure 27 shows an instrumented aluminum blast test device with a signal conditioner.

Figure 27: An instrumented Blast Test Device [CHPPM, 2005]

There are currently different software models used to predict injury, such as those of Axelsson and Stuhmiller. These software applications use different methods in predicting injury, however the design of the BTD for both applications is generally the same. Figure 28 shows a schematic of a 30-inch tall BTD approved for use by the U.S. Army Center for Health Promotion and Preventive Medicine. As the BTD only represents the thorax of the

subject it can be mounted in a variety of positions to simulate an individual standing, kneeling or sitting.

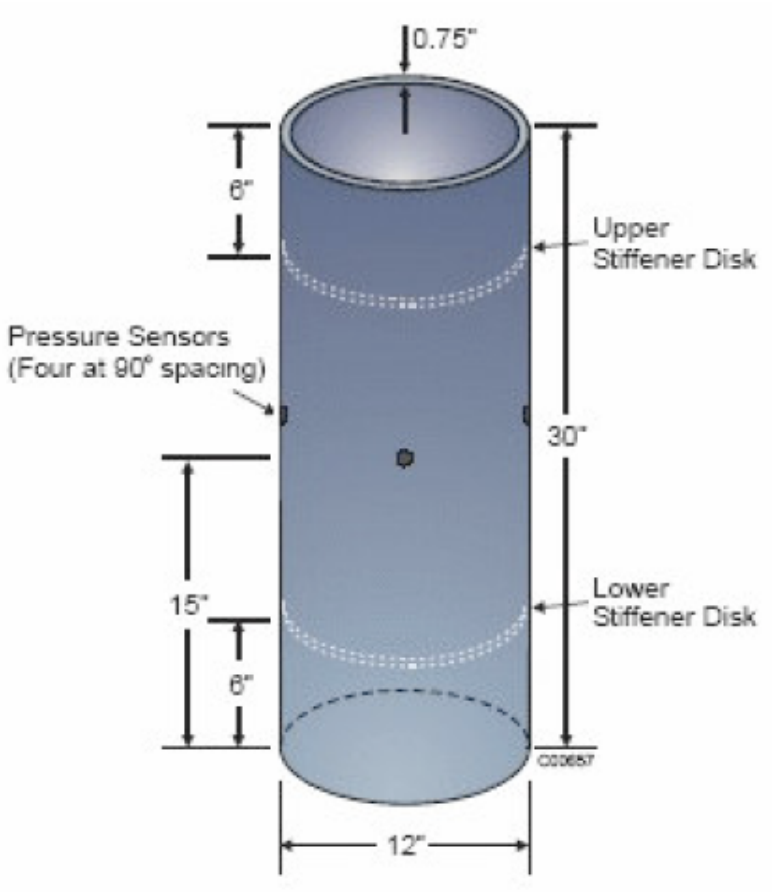

Figure 28: Schematic of a 30" Blast Test Device [CHPPM, 2005]

2.6.6 Stuhmiller Model of Normalized Work - Injury 8.1

The lung is the critical organ in incapacitation resulting from primary blast injury. [NATO, 2007] Utilizing the lung as a predictor of injury levels a mathematical model of the chest wall dynamics was created. The model represents the chest wall movement along with the generation of the pressure waves developed in the lung as a result of the blast wave impact. It has been theorized that these internal waves traveling through the different materials of the

thorax ad into the lungs are responsible for injury. [Stuhmiller, 1996] The mechanical properties of the chest wall and lungs have been studied and used in the development of the model in order to ensure that the model is anatomically and mechanically correct, rather than relying on empirical predictions for injury.

The model developed incorporates the forces acting on the chest by the blast waves, the resultant rise in internal pressure of the lungs and the compression wave generated from the chest motion. This theory assumes that the lung behaves as a compressible material and a relationship that relates the pressure wave in a compressible gas to the motion of a piston is used. The equation of this relationship is shown in Equation 6.

$$p(t) = p_0\left(1 + \frac{1}{2}(\gamma - 1)\frac{\upsilon}{c_0}\right)^{\frac{2\gamma}{\gamma - 1}}$$

where:

p is the pressure

p_0 is the pressure in the undisturbed lung

c_0 is the speed of sound in the undisturbed lung

ν is the velocity of the piston

γ is the ratio of specific heats

Equation 6: Relationship between pressure wave to the motion of a piston

If the piston velocity is very small compared with the speed of sound, then the equation can be shown in the linear for as shown in Equation 7 where the adiabatic relation of Equation 8 is used.

$$p(t) \cong p_0 + \rho_0 c_0 v$$

where:

ρ_0 is the density in the undisturbed lung

Equation 7: Simplified relationship of pressure to motion of piston

$$c_0^{\,2} = \gamma \frac{p_0}{\rho_0}$$

Equation 8: Adiabatic relation

To simplify the model of response of the thorax to blast wave, Stuhmiller assumed a single degree of freedom model for the pleural surface dynamics. The model was further simplified by neglecting the stresses arising from the rib structure and neglecting the internal wave reflections on the thorax movement. By assuming that the chest wall and lung for a rectangular region, Newton's law is applied and the equation of motion is described in Equation 9.

$$m\frac{d\upsilon}{dt} = P_{Load}(t) - p_0\left(1+\frac{1}{2}(\gamma-1)\frac{\upsilon}{c_0}\right)^{\frac{2\gamma}{\gamma-1}} - \frac{p_0 L}{L-x}$$

where:

m is the mass/chest wall area

ν is the velocity

x is the displacement

L is the ratio of the volume of the lung/chest wall area

Equation 9: Chest equation of motion

Assuming that the velocity and displacement are small the equation can be linearized and simplified as shown in Equation 10.

$$m\frac{d\upsilon}{dt} = P_{Load}(t) - \rho c_0 \upsilon - p_0\frac{x}{L}$$

Equation 10: Linearized equation of chest motion

Using the above relationship the normalized work is calculated using Equation 11. Normalized work is defined as the total work done to produce the wave divided by the volume of the lung and ambient pressure. It has been noted that blast injury is caused by local excess strain of the tissue; this phenomenon is not described by this model. Good correlation has been made between injury observed on animals and the irreversible work done on the lung by the motion of the chest wall (normalized work.).

$$W^* = \frac{W}{p_0 V} = \frac{1}{p_0 L}\int_0^\infty \rho_0 c_0 v^2 dt$$

Equation 11: Normalized work on thorax

In order to correlate normalized work to injury a number of tests were conducted. To measure the blast wave pressure experienced on a subject, a blast test device was constructed and placed in the blast flow field. The BTD consisted of a cylinder with four pressure gauges placed at the midpoint of the long axis and at 90 degree increments around the circumference. A charge was selected and initiated and the pressure time histories recorded by the BTD. Tests were conducted for both free field and complex blast scenarios. After recording the pressure using the BTD the experiment was repeated, however this time the BTD was replaced with a sheep. The sheep were then examined and injury scores ranging from no injury, trace, slight, moderate and severe was assigned. Knowing the injuries obtained from the sheep, and recording the corresponding pressures experience at four locations along the torso, as simulated by the BTD, the normalized work for each test case was calculated. The observed injury and normalized work were correlated using a log normal correlation for each injury level. The correlation is shown in Figure 29.

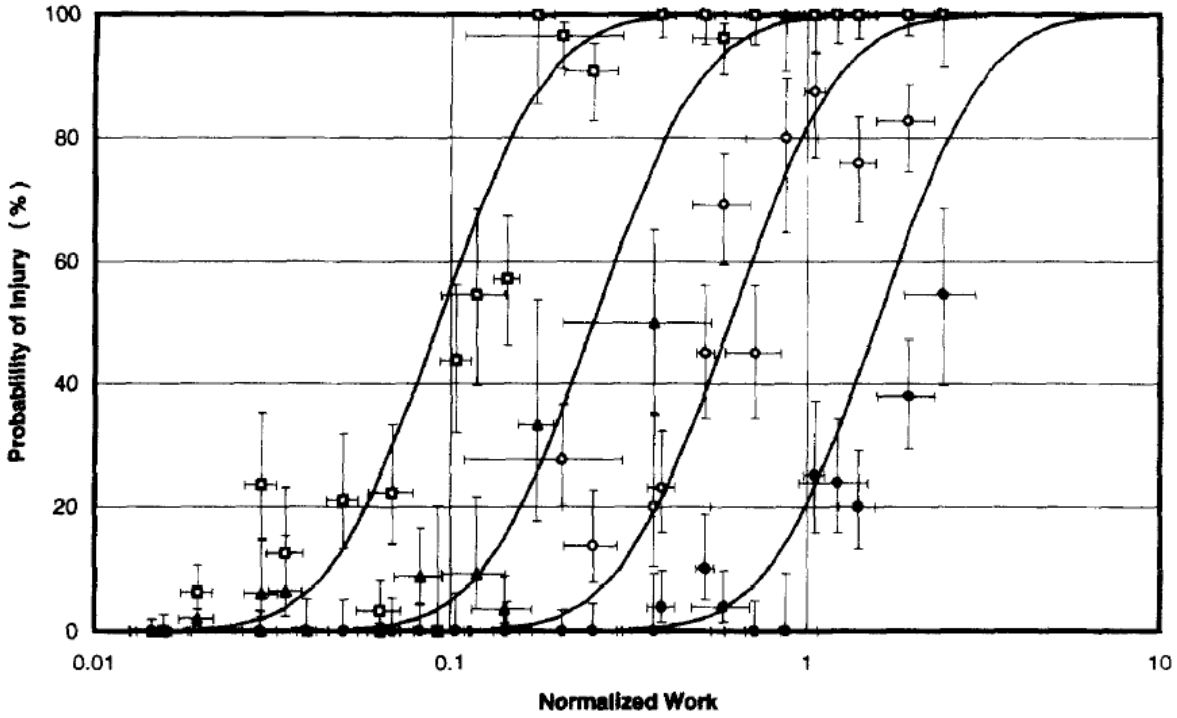

Figure 29: Correlation of normalized work with injury severity
Experimental results were sorted as: (□) trace or greater, (▲) slight or greater, (○) moderate or greater, and (●) severe

Along with the severity of injury predict from a blast wave, Stuhmiller also correlated Normalized work to the area of injury observed in the lung. The correlations are shown in Figure 30.

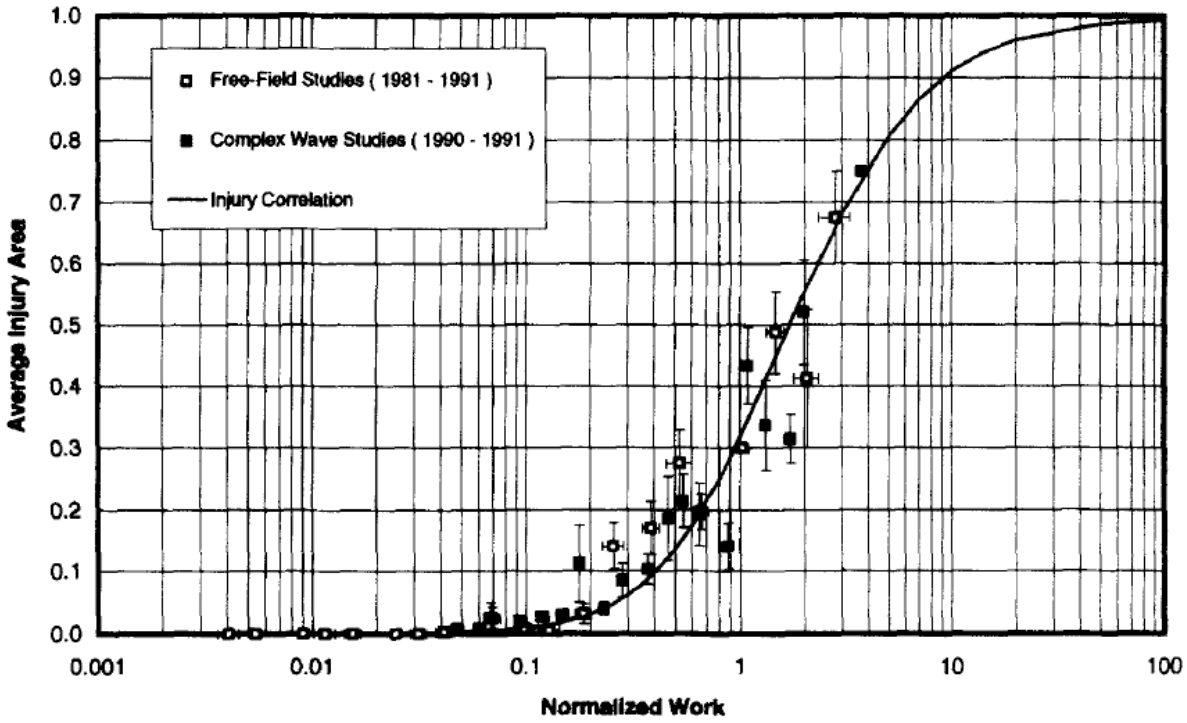

Figure 30: Correlation between normalized work and area of lung injury

To further correlate and test the model, Stuhmiller compared the injury model to results obtained from a wide variety of species of large and small mammals. In order to account for different body masses and size, scaling laws were incorporated into the model. The time scales of the model were scaled in order to account for injury among different species. [Stuhmiller, 1996] Previous work has suggested that mammals may be divided into two groups to predict injury from blast waves. The two groups are generally known as the high tolerance (large mammals) and low tolerance (small animals) group. [Bowen, 1968] Stuhmiller used animal experimental data from the early 1970s in which the injury resulted in 50% fatality, and where the blast overpressure and duration were recorded. Based on the duration and peak overpressure the blast waves were reconstructed assuming either a Friedlander or triangular type waveform. The normalized work for each of the test was

calculated and plotted versus the body weight for each of the mammals groups. The correlation is shown in Figure 31.

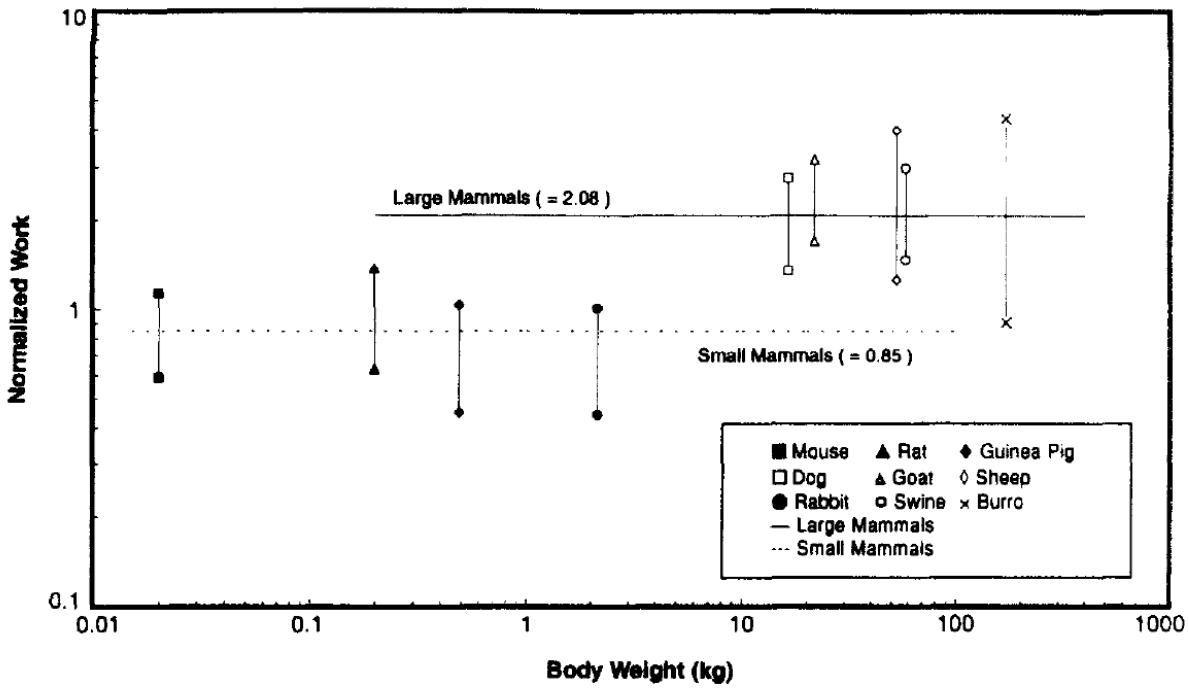

Figure 31: Normalized work associated with 50% lethality for various species of large and small mammals

The model of the thorax presented by Stuhmiller is a simple representation of the thorax of a human, however the correlations presented and the parameters used to model the thorax provides a fair approximation in estimating injury from blast waves. The model does however attempt to predict the compression wave within the lungs, which is believed to be the mediator of injury. Unlike many of the early work, this model has been correlated and can be used to estimate injury from complex blast scenarios.

The injury prediction model by Stuhmiller has been coded into a computer application that is used to predict injury on several species. The application is referred to as INJURY and the current version at this time is 8.1. Using input from four pressure gauges around a BTD the program computes the normalized work based on the blast loading, species, body mass and ambient pressure. The results of the computer code provide probability of lung injury for five injury severities. [Stuhmiller, 2006] These are no injury, trace, slight, moderate and severe levels of injury. The code has been used frequently to predict blast injury; however portions of the code and algorithms have not been made available to the scientific community. The software is available through the Military Operational Medicine Research Program at www.momrp.org.

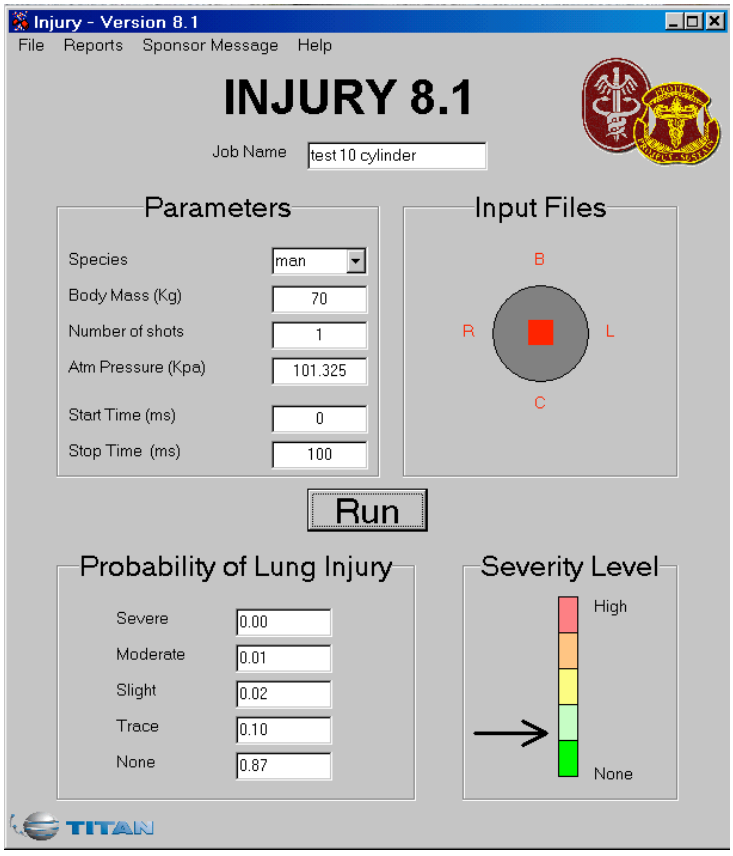

Figure 32: Injury 8.1 application main user interface

2.6.7 Axelsson Injury Model

The majority and most current studies of primary blast lung injury have mainly focused on animal experiments and correlations from idealized, Friedlander blast waves. In reality, when an explosive detonates there is often reflecting surfaces near the charge and the resulting blast flow field does not appear as the idealized blast wave, with an instantaneous rise in pressure and a smooth pressure decay. In enclosed spaces the flow field appears more complex and there will be limitations in applying conventional injury criteria techniques (such as injury curves) to this type of waveform. In order to address the complex blast flow field in regards to human injury a study was performed by the Swedish military, lead by Axelsson. [Axelsson, 1996] The goal was to develop a simple tool for human vulnerability assessment to complex blast waves. Previous techniques to address injury relied on the overpressure and duration of a blast to predict injury; however, with complex blast waves it is not possible to classify the flow field by using only these two parameters. Examining the blast wave generated from an explosion in an enclosed space, in Figure 33 it is incorrect in assuming the wave form behaves like a Friedlander wave.

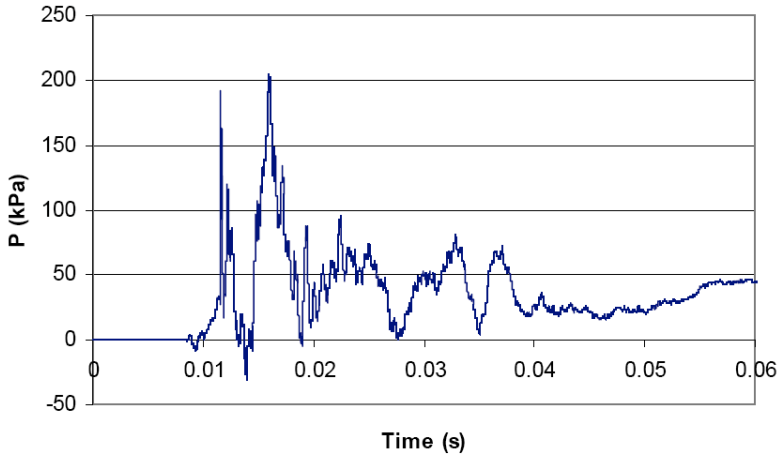

Figure 33: Pressure time histories from a blast in an enclosed vehicle [NATO, 2007]

Previous experiments involving rabbits have indicated that the injury resulting from blast correlates with the maximal inward chest wall velocity. [Axelsson, 1996] In another study chest compression and chest wall velocity have been correlated with injury severity. [Mayorga 1997] Using the hypothesis that the movement of chest wall and its peak inward velocity is a good predictor of the blast injury a mathematical model of the thorax was built. This mathematical model was validated with experiments involving complex blast waves and animal testing. Sheep were chosen for testing purposes as the weight of the sheep thorax is similar to that of a human.

The mathematical model of the thorax consisted of a two chamber spring-mass system to model the two lungs of the thorax. This model is a single degree of freedom system in which the intrathoracic pressure along with the displacement, velocity, and acceleration of the chest wall can be calculated based on a simple or complex blast load input. To further simplify the model a single chamber model was used instead of the two-lung model. The simplified single chamber, one-lung mathematical model of the thorax is shown in Figure 34. The simplified model assumes that the same blast pressure is operating on both, the right and left lungs.

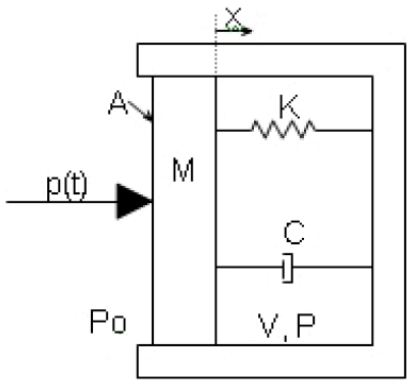

A is the effective area;
M is the effective mass;
V is the initial gaseous volume of the lungs;
x is the displacement;
C is the damper coefficient;
K is the spring constant;
P_o is the ambient pressure;
p(t) is the overpressure over the time; and
γ is the polytropic exponent for gas in lungs.

Figure 34: Mathematical model of the thorax; simplified one-lung model [NATO, 2007]

The equation representing the model is given in Equation 12 whereas the parameters are shown in Table 1. The parameter values listed in the table correspond to a 70kg mammal. In order to account for the mass of other mammals the scaling factors indicated should be used. The behaviour of the model is non-linear, and its response depends on the amplitude and frequency of the pressure load of the blast wave input. A previous study performed by Yelverton subjected 255 sheep to complex blast waves. The results of these findings were used by Axelsson to predict the severity of injury based on complex blast.

$$M\frac{d^2x}{dt^2} + C\frac{dx}{dt} + Kx = A\left[p(t) + P_0 - \left(\frac{V}{V - Ax}\right)^{\gamma} P_0\right]$$

Equation 12: Mathematical formula for thorax model

Table 1: Model parameters for thorax model for a 70kg mammal

Parameter	Units	70-kg body	Scaling Factor
M	Kg	2.03	(m/70)
C	Ns/m	696	$(m/70)^{2/3}$
K	N/m	989	$(m/70)^{1/3}$
A	m^2	0.082	$(m/70)^{2/3}$
V	m^3	0.00182	(m/70)
γ	-	1.2	-

The complex blast waves were generated by placing a charge in various positions in an enclosed space. In total, four different enclosed spaces were used, each consisting of a room with a height of 3.05m. The room dimensions and areas were:

a. 2.44 x 2.44m, 18.2m^3
b. 2.44 x 2.44m, 18.2m^3, access door open
c. 4.88 x 2.44m, 36.3m^3
d. 1.52 x 2.44m, 11.3m^3

The charges were placed at various locations inside the rooms and the charge mass varied from 0.114 to 1.361kg. Various charge weights, room dimensions and charge locations were used in order to produce a variety of complex blast waves. Sheep were placed in harnesses and inserted into the enclosure, suspended 1.22m from the floor and then subjected to a blast. In total 255 sheep were subjected to complex blast waves. Axelsson however only relied on the results from 177 of these sheep tests.

The sheep were assessed for injury and an alphanumeric scoring system was used to in order to classify the severity of the injury. Injuries were scored based on five specific thoracic regions: lung, pharynx and larynx, trachea, gastrointestinal tract and intra-abdominal region. Injuries ranged from lesions, fractures, and the percentage of contusions in the organ. The alphanumeric scoring system for each of the injuries was then converted to obtain the Adjusted Severity of Injury Index (ASII). The ASII levels are shown in Table 2.

To correlate the mathematical model and develop a tool to access injury vulnerability, Axelsson repeated a number of the original animal tests, substituting a BTD (instrumented cylinder) instead of sheep to the blast in the enclosed space. The instrumented cylinder consisted of an aluminum cylinder measuring 0.762m long and 0.305m in diameter. These dimensions were chosen as they approximate the body of a sheep. The cylinder was fitted with four pressure gauges mounted at equal intervals around the circumference at the midpoint of the long axis (a height of 0.381m). Similarly the cylinder was placed 1.22 m from the bottom of the enclosure floor and subjected to a wide variety of complex blast waves. The cylinder was oriented in such a way that one of the pressure gauges was pointed directly at the charge. Figure 35 shows a schematic of the Axelsson blast cylinder used in the experiments. The resultant pressure-time histories recorded by the pressure gauges around the cylinder were used as input to the simple thoracic model. The response of the model was computed for each of the four gauges and the peak inward chest wall velocity was determined based on this input. The average of the four maximum peak inward chest wall velocities were taken and this value was taken to be the maximum peak inward chest wall velocity for the cylinder.

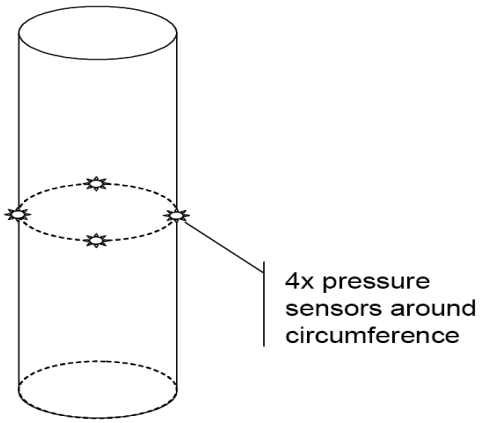

Figure 35: Axelsson instrumented cylinder used to approximate the body of a sheep [Greer, 2006]

The results of the animal cases and instrumented cylinder cases were compared and it was noted that the predicted peak inward chest velocity correlated well with the ASII score assigned to the sheep. In all cases it was observed that placing the individual near a corner while there is a blast in an enclosed space produces a greater level of injury as compared to the individual placed near only one reflecting wall. [Axelsson 1996] The same trend was observed with a numerical study, concluding that the injury obtained on a human increases as the subject is placed near reflecting surfaces. [Dionne 2008; Greer 2008] It was also noted that a lower level of injury can occur if the subject is placed closer to the charge, rather than farther away and in a corner. A correlation relating the ASII and peak inward chest wall velocity is given in Equation 13. The corresponding injury levels relating ASII and peak inward chest wall velocity are shown in Table 2.

$$ASII = (0.124 + 0.117V)^{2.63}$$

Equation 13: Relationship between ASII and peak inward chest wall velocity

Table 2: Injury levels with corresponding ASII and maximum inward chest wall velocity

Injury Level	ASII	V (m/s)
No Injury	0.0 to 0.2	0.0 to 3.6
Trace to Slight	0.2 to 1.0	3.6 to 7.5
Slight to Moderate	0.3 to 1.9	4.3 to 9.8
Moderate to Extensive	1.0 to 7.1	7.5 to 16.9
>50% Lethality	>3.6	>12.8

The Axelsson injury model enables the vulnerability of a human to be assessed in complex blast wave scenarios. Unlike other injury criteria models and curves, the Axelsson model takes the organs of the thorax, rather than just the lungs into consideration when predicting injury. The Axelsson approach has been compared with the original Bowen curves in predicting the injury from Friedlander blast waves and a good correlation has been obtained. [Axelsson, 1996] When comparing the Axelsson model to the revised Bowen curves, the Axelsson model appears to produce levels of greater injury severity for orientations with the subject parallel and perpendicular to the blast wave. The study by Axelsson is based on fewer animal studies at short durations than those of Bass, so it is possible that the Axelsson model is not adequate in producing injury levels for short duration blasts. [Bass, 2006]

2.6.8 Hybrid III

The Hybrid III is a mannequin that can be used in experimental testing to predict injury from a blast. The Hybrid III is an anthropomorphic dummy with component dynamic responses, which approximate biomechanics data. The mannequin is available in a number of configurations, however the standard dummy is the 50th percentile human surrogate. [Foster, 1977] The Hybrid III mannequin is shown in Figure 36.

Figure 36: Hybrid III Mannequin

Blast injury can be computed with the instrumentation (pressure transducers and accelerometers) placed in the mannequin. Using four pressure transducers placed around the torso, the resultant pressure-time histories can be used along with the Axelsson methodology to predict injury. Injury can also be computed by instrumenting the mannequin with accelerometers in the torso. When using accelerometers injury can be computed using the viscous criterion (VC). [Viano, 1988]

The viscous criterion is an injury criterion that predicts chest injury. VC accounts for the compression of the chest and the velocity at which the chest deforms. VC_{max} which is the maximum VC value recorded over the loading period is used and correlates with injury. [Viano, 1985] Neither the Hybrid III nor VC is intended for estimating blast injury. The VC also requires an accurate measurement of displacement, which is difficult to measure

appropriately with the short duration of the blast loading event. Findings have suggested that the anthropomorphic dummies are not well suited for the prediction of blast injury, however if they are to be used they must be well calibrated for each type of trauma source exposure. [Jonsson, 1988]

2.6.9 MABIL

The DRDC Mannequin for the Assessment of Blast Incapacitation and Lethality (MABIL) has been developed to represent the 50th percentile Canadian soldier. This experimental surrogate was developed to access primary blast injury and burns. The surrogate is fabricated from a visco-elastic material, Shore A 70 polyurethane [Anctil 2004]. The surrogate is in the form of a human torso and includes a torso and head. The shape of the torso permits the surrogate to be fitted with personal protective equipment and can be used to investigate the effectiveness of armor. Figure 36 shows the DRDC MABIL mannequin.

Figure 37: DRDC MABIL Surrogate with stand [Bouamoul, 2007]

This surrogate is equipped with two single axis accelerometers; one located at mid sternum and the other is at the level of the belly button in the center of the abdomen. The instrumentation in the torso is used to predict primary blast injury based on the acceleration of the chest wall. [Ouellet, 2008] This experimental device is well suited to measuring blast injury as it was designed and validated for this use.

Chapter 3
Finite Element Modeling of PBI

3.1 Introduction

A numerical modeling approach was taken to investigate blast lung injury. It is not possible to perform physical experiments on live individuals. Performing blast testing on cadavers is not practical as it is very difficult to fully instrument the chest with sensors and these do not provide the appropriate physiological data to estimate or measure lung contusion. The numerical modeling approach allowed for several parameters to be modified in order to access the injury, without the need for physical experiments. Using numerical model allowed for a straightforward change to parameters and values to investigate the effect their change had on blast lung injury. In order to provide appropriate data the numerical model needs to be verified and validate; once this occurs parametric studies can be performed. Numerical modeling allows us to understand constrained parametric studies, investigate local responses and better understand the physics.

3.2 Numerical Methods

3.2.1 Finite Element Analysis

A Finite Element Analysis (FEA) approach was used to model a sheep and a human to investigate blast lung injury. This model was developed at the University of Waterloo. [Greer, 2006] Finite element analysis is a simulation technique used to compute the behavior, interaction and dynamics of components and their surroundings. The finite element method involves dividing the model into a number of elements, known as discretization In order to numerically solve the partial differential equations. Equations are solved for each of these elements and the stresses, forces and displacements are calculated. The calculation run time for finite element analysis is generally proportional to the number of

elements used in the analysis; other issues such as material models and contact can also effect the run time.

Generally two approaches for FEA are used; implicit and explicit calculations. Both approaches may be used to solve time-dependent equations. The implicit approach is used to obtain a solution by solving a set of equations given the state at the starting point and the state at the end point. The implicit solution requires that the dependent variables be defined by a coupled set of equations and these are solved through a matrix or iterative numerical technique to obtain the solution. The explicit approach is an iterative approach that calculates the state of the system at a time based on the state at the previous time. The advantage the explicit approach has over the implicit is that the explicit approach involves a direct computation of the variables without the need for solving equations simultaneously. The disadvantage of the explicit approach is that it requires very small calculation timesteps to remain stable.

In order to limit the calculation run time to a reasonable amount of time the analysis can either involve modeling of large components with large elements or modeling specific components in a higher detail. Using large elements is not recommended for modeling organs as the results are nor reliable since the calculation is not able to accurately resolve the waves travelling through the tissue. This problem is resolved by modeling the cross section of the torso, in detail and modeling the tissue and bone with a high resolution. The elements of the model form a mesh. To model the deformation of the components a Lagrangian mesh is used. The Lagrangian mesh allows for the elements to deform and displace when subjected to appropriate stresses.

3.2.2 ALE Formulation

In the Lagrangian methods the mesh is attached to the material and is translated and deformed along with the material. The elements in this mesh therefore are able to deform depending on the internal stresses of the material. There is no mass flux across the element boundaries and the mass, momentum and energy are transported with the element. [Liu, 2005] The Lagrangian method enables the material to be easily tracked throughout the simulation, as the boundaries are clearly defined. This approach also allows for irregular shapes such as tissues and organs to me modeled easily by using an irregular shaped mesh. Lagrangian methods are however limited to materials that have relatively small amounts of deformation. For example, it is not possible to effectively model the expansion of an explosive charge utilizing a Lagrangian approach, as the deformation is too large.

An Eularian mesh is a fixed, predefined grid, where the material is located and moves across the fixed mesh cells. As the material deforms and moves, the mesh remains fixed and the flux across each of the cells is computed to solve for the mass, momentum and energy of the material. The Eularian approach is suitable for modeling blast waves and fluid flow as the large deformations do not cause any deformations of the mesh itself, leading to numerical instabilities. Some of the disadvantageous of this approach is that it is difficult to track the exact boundaries and interfaces of the materials and it is necessary to have a static grid that is capable of surrounding the deformation of the material throughout the calculation. In LS-Dyna this is an option but can lead to inaccuracies with respect to the advection algorithm.

By combining the Lagrangian and Eularian approaches, the Arbitrary Lagrange Eularian (ALE) formulation is obtained. This ALE formulation operates by a type of coupling between the Lagrangian and Eularian domains. Although this approach is regarded as ‘Arbitrary’ Lagrangian Eularian, suggesting that the fluid domain is capable of an arbitrary

deformation, a full Eularian approach is often used for the fluid, where the fluid mesh is not re-meshed. ALE methods are particularly suited for fluid structure interaction calculations as they allow the benefits of the fluid movement on an Eularian domain and the solids to move on a Lagrangian domain. In ALE, the Lagrangian motion of the mesh is first computed, followed by a step to determine how the Lagrangian elements should be remapped or advected onto the moving ALE mesh. The difference between the ALE approach and the Eularian approach is in the amount of material that is advected between each element; this amount is different since in ALE mesh the mesh is permitted to move. In a pure Lagrangian approach the mesh moves with the material, in a pure Eularian approach the mesh is fixed and the material flows across the elements. In an ALE formulation the mesh is permitted to move independently and arbitrary to the motion of the material. Figure 38 shows the overview of an ALE simulation involving a cross section of a human torso surrounded by air; the ALE mesh overlaps the structural mesh. The ALE mesh is shown with elements that are initially square in shape, whereas the complex structure is made up of many irregular shapes and varying element sizes.

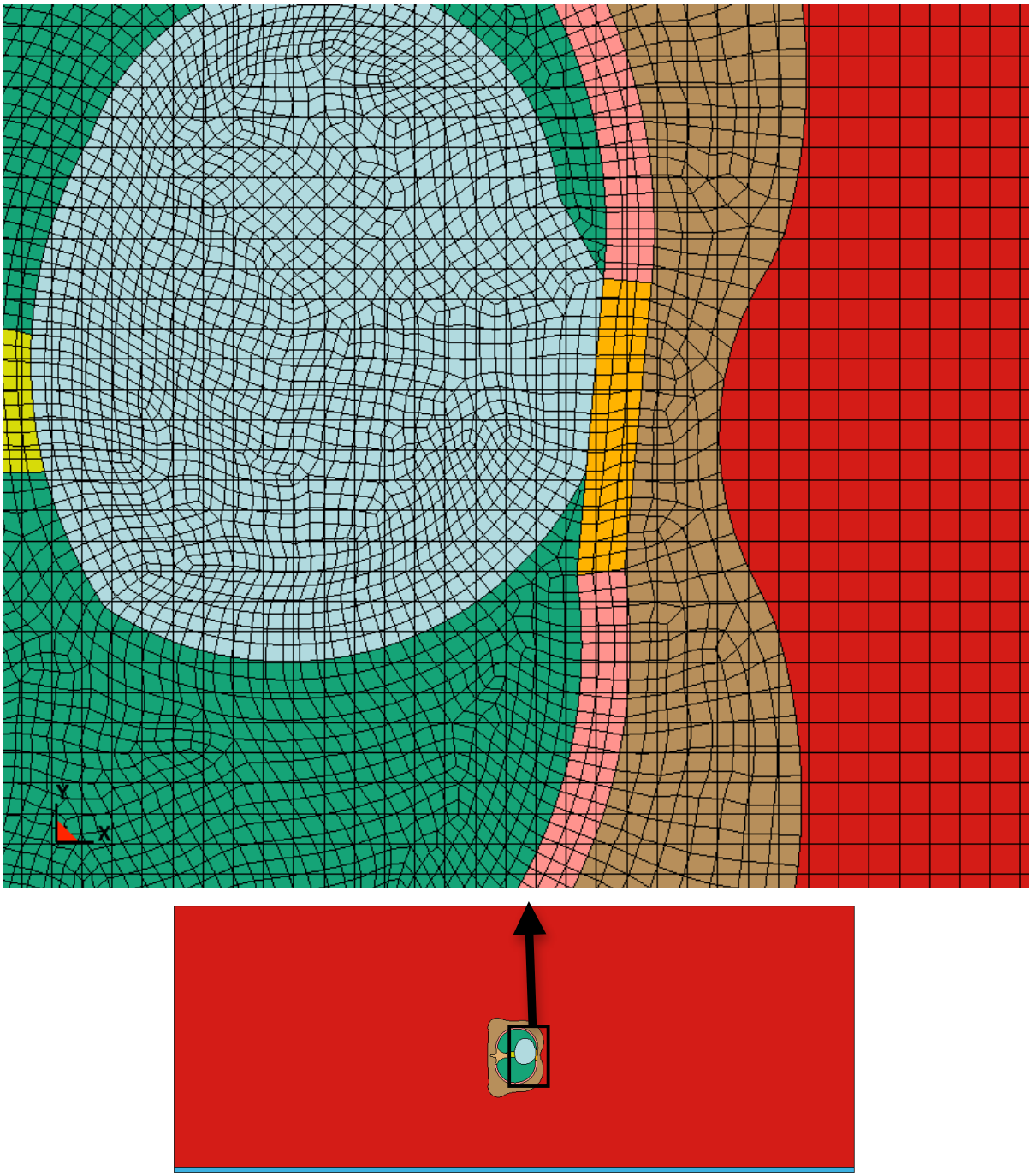

Figure 38: Close-up ALE formulation showing air and solid domains (thorax organs)

3.2.3 ALE Solver

Livermore Software Technology Corporation's (LSTC) LS-Dyna [Halquist, 2003] software was used to perform the ALE calculations. LS-Dyna is a hydrocode, a non-linear finite element analysis code that is capable and suited for solving interaction between fluid and structures. LS-DYNA is one of the few available codes that are able to solve the complex interaction between the blast wave and human torso.

LS-Dyna is able to perform implicit and explicit calculations, however the explicit solver was used as it is more suited for solving the fluid structure interaction. LS-Dyna also has several contact-impact algorithms that allow for the contact between the torso (Lagrangian) and the blast wave (ALE) to be computed along with the contact between the torso tissue and bone. The fluid structure interaction involving the torso and blast wave is complex due to the different densities and stiffness of the materials that compose the torso. A toso model has been developed using LS-Dyna.

3.2.4 Computational Fluid Dynamics

In order to accurately model the result from an explosive charge a numerical method using Computational Fluid Dynamics (CFD) is required. CFD requires that a mesh be created to model the domain including the air surrounding the charge. This discretization of the domain allows the solver to explicitly solve the partial differential equations. In contrast to FEA, not only does the component of interest need to be meshed, the surrounding domain also needs to be meshed as this will be the area that the fluid flows into. Neglecting to fully mesh a significant portion of the domain can lead to the fluid travelling into unwanted boundaries. For modeling of blasts and the resultant pressure wave, it is required that the cell size of the mesh be of a high resolution in order accurately track the blast front and ensure the proper peak blast wave pressure.

There exist a number of CFD computer codes that are used by industry to solve a large variety of problems, from slow speed flows in HVAC scenarios to supersonic flows such in detonation modeling. Many popular commercial CFD codes are limited to slow speed flow and are unable to properly model blast waves, as the solver used to compute the fluxes in the cell is not applicable to blast waves. In contrast many codes that are used to model blast waves are unable to properly model slow moving fluid problems. Martec's Chinook software was chosen to model the resultant blast waves from different explosive charges. This software is a CFD code that specializes in modeling blast and high speed, compressible fluid flow. This code was chosen as it has been experimentally validated against a wide range of experimental blast data. It has been validated using experimental blast data produced by the Research and Development section of the Department of Defence Canada. It is also able to capture advanced blast phenomena such as blast focusing. The blast analysis solver uses an HLLC approximate Riemann solver to compute the cell fluxes.

The mesh used in the blast modeling was an Eularian mesh. The Eularian is a mesh that is created before the CFD calculation and this mesh does not change or adapt as the calculation proceeds. One of the challenges with this type of mesh is that if the mesh is not properly constructed then the blast wave can quickly decay or the shock front can become distorted. It is therefore necessary to create a mesh that follows the shape and profile of the blast wave as it moves across the domain. Figure 39 shows the result of placing a quarter spherical charge at the origin on a Eularian mesh. This results in stepped shape edges rather than a smooth edge on the charge. In order to provide the most accurate solution a "body-fitted" mesh is required; this refers to a mesh that accurately represents the geometry and progress of the blast wave. A more accurate approach to that shown in Figure 39 would be a mesh in which the edges and curves of the sphere would have been captured. This approach would require the use of quadrilateral elements that are not square or rectangular in size. Figure 40 shows

an example of a mesh that can be used to more accurately represent an explosive charge. This mesh is able to capture the curvature of the shape and also includes mesh refinement along the boundary to capture more of the pressure gradients.

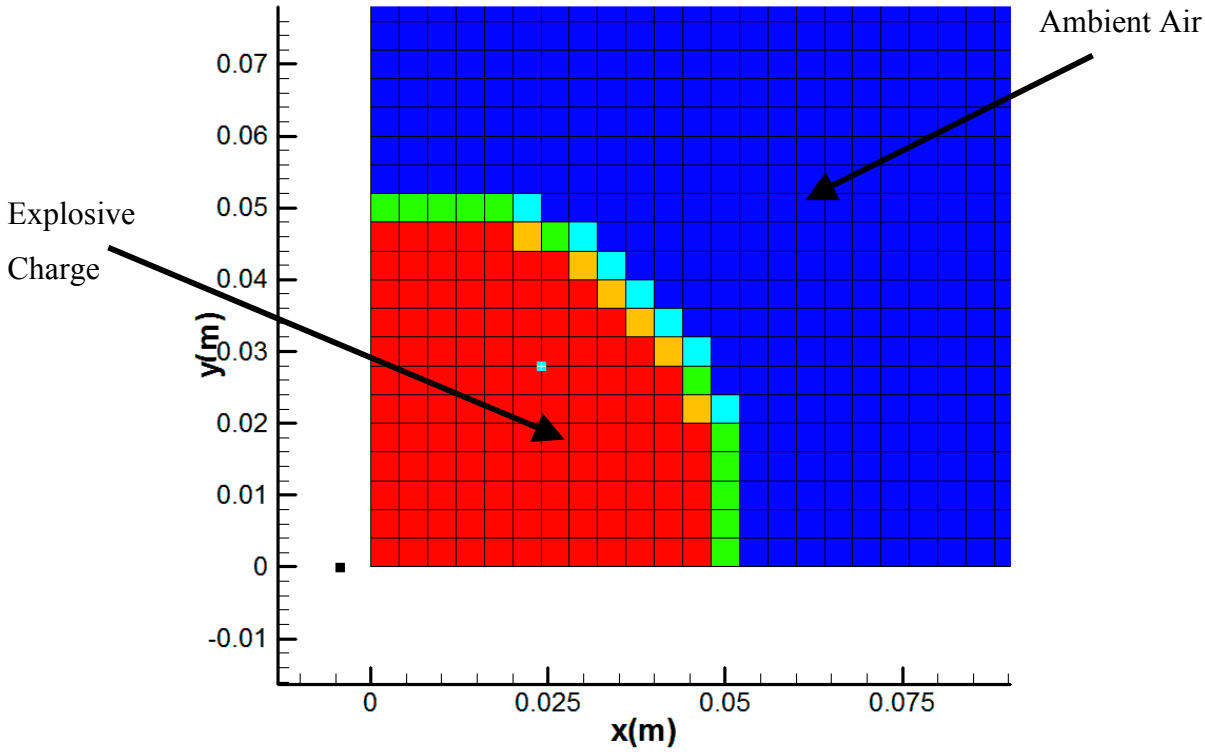

Figure 39: Spherical charge on Eularian grid

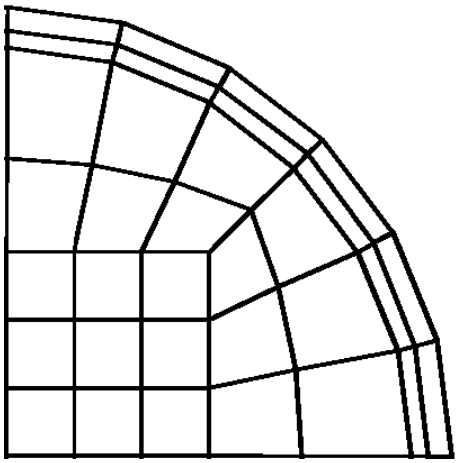

Figure 40: "Body-fitted" mesh of explosive charge

3.3 Blast and Torso Model

The numerical simulations used in this study consisted of a human torso model, an explosive source and an ambient domain (surrounding air). The numerical model was developed at the University of Waterloo [Greer, 2006]. The simulations in this study were carried out using the LS-DYNA software. To model the fluid structure interaction an Arbitrary Lagrangian Eularian (ALE) approach was used.

Blast modeling was used to accurately represent the response and physical properties from the detonation of an explosive device. The use of blast modeling also allows only a subset of the blast to be computed. It is not required to perform a detailed calculation of the entire detonation process of the explosive; only the physics of the blast wave need to be properly modeled before the blast wave contacts the objects of interest. Figure 41 shows a numerically modeled blast wave interacting with a human torso model in the flow field. The

blast wave was modeled by applying a pressure-time history profile used to represent a blast wave; the interaction between the wave and the object (torso) is numerically computed.

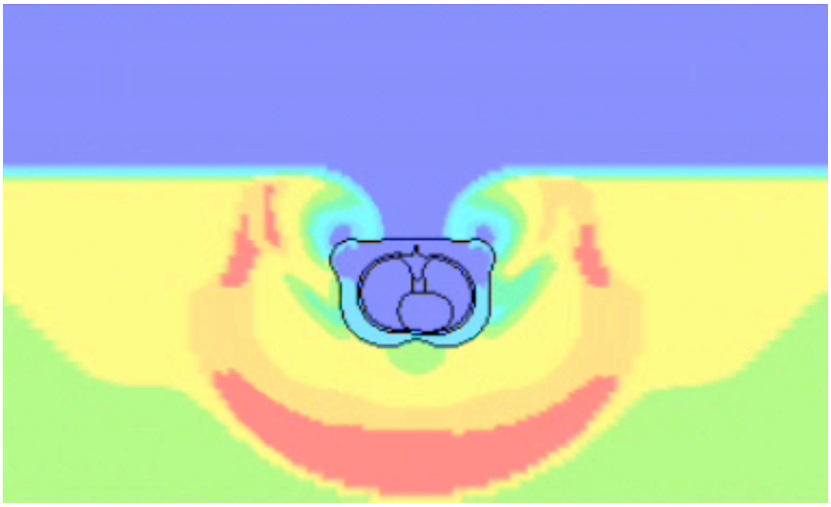

Figure 41: Blast wave modeling, showing wave travelling towards human torso model

The ambient fluid domain (air) completely surrounded the torso model and was required to capture the flow and wave effects between the blast wave and the torso. The domain consisted of three non-reflecting boundary conditions and three reflective boundary conditions. Non-reflecting boundary conditions were placed at the edge of the domain to the right, left and back of the torso model. As the torso model is a slice model the upper and lower surfaces had reflecting-boundary conditions applied to model symmetry. The nodes along these surfaces were also constrained. The other reflective boundary condition was placed downstream of the torso and along the row of high-pressure elements. A large domain size (relative to the torso model) was used to reduce the effect of numerical artifacts that may be caused from the non-reflecting boundary conditions. Figure 42 shows the computational domain along with the human torso model used for the LS-Dyna ALE computations.

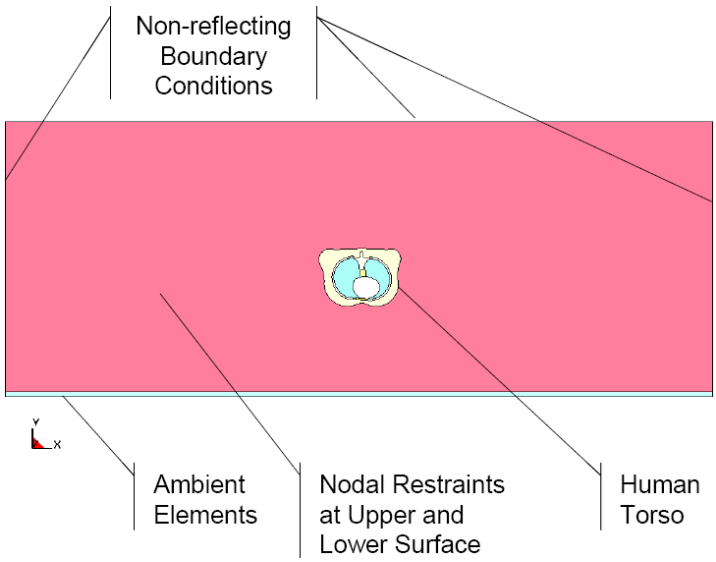

Figure 42: Numerical Model of ALE simulation

The blast wave delivered to the human torso was applied to a fluid (air) domain in LS-Dyna. The blast was modeled as an inflow condition and allowed to travel 0.3m before coming in contact with the torso. The mesh was refined in such a way that the area in contact with the torso was at a high resolution and the area farther from the torso were at a lower resolution. Organizing the mesh in this fashion allowed for a significant reduction in computational run time, while enabling the shock and fluid structure interaction to be captured at a significant level. Figure 43 shows the fluid domain that was meshed for the torso and blast interaction. In the figure, the lower blue cells have a pressure curve applied to them to model the blast inflow. The other boundaries to the left, top and right were modeled as non-reflecting boundaries to permit the blast wave to flow through and out of the domain; the domain was made sufficiently large to ensure that the blast wave was planar and not influenced by the boundaries as it stuck the torso.

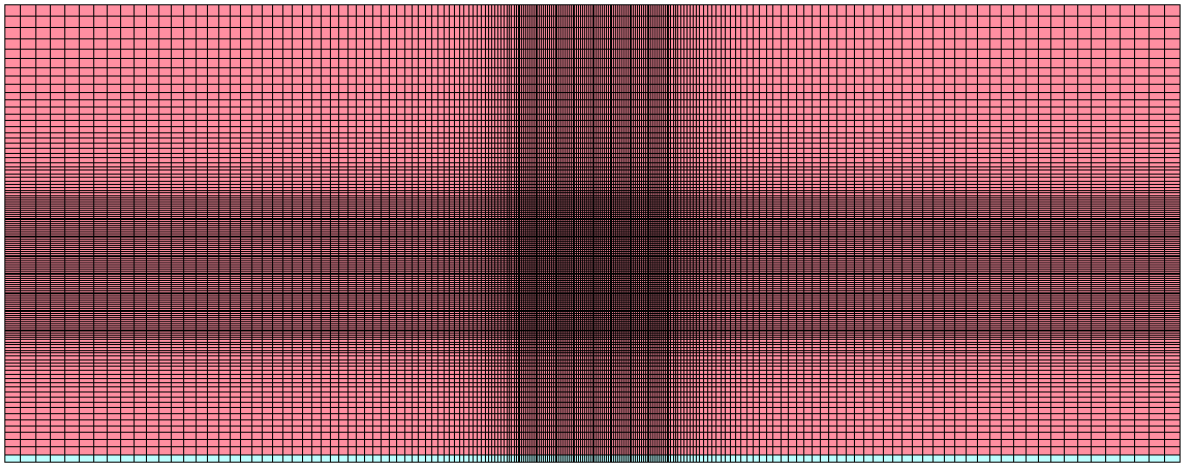

Figure 43: ALE air domain with blast inflow, smallest element size is 0.5mm x 0.5mm

3.3.1 Blast Loads

There are several ways to model the blast load. It is possible to model the charge directly by placing the charge on an ALE domain and using a JWL equation of state along with the explosive material information. Using this method the detonation and the expansion of the charge can be computed. This requires that a high number of ALE elements be used in order to accurately calculate the expansion of the charge. The overall calculation run time would be very long using this approach as the calculation will first need to predict the explosive charge expansion, followed by the blast wave travelling towards the torso, through the air and finally the blast interaction with the torso. The balloon model approach is also used to model a blast, this involves placing a volume of high pressure gas on the ALE domain to simulate the effect of the high pressure expansion explosive products, this approach also results in long calculation run times as the solver needs to further compute the expansion of the high pressure volume. The approach used to model the blast wave and torso interaction utilized a predefined pressure time history placed on a boundary condition that generated the appropriate blast wave. This was implemented as a load curve in LS-Dyna; a temperature-

time curve was created which was used to generate the pressure pulse (temperature was related to pressure through the ideal gas equation). The load curve function decreases calculation run time, as it does not need to explicitly calculate the initial expansion. The blast load input was applied to the cells on the boundary of the domain and the curve contained the necessary values to set the blast wave conditions at this point, using the ideal gas equation, as shown in Equation 14.

$$P = \rho\left(C_p - C_v\right)T$$

where:

Cp is specific heat capacity at constant pressure (1005 J/kg·K)

Cv is specific heat capacity at constant volume (718 J/kg·K)

ρ is density (1.293 kg/m^3)

T is temperature (K)

Equation 14: Ideal gas law used to calculate pressure

To limit the number of cases studied and to ensure that a wide range of injury severities were considered, seven test cases were studied. Theses test cases were selected from the revised Bowen curve and involved examining injury levels for threshold lung injury, LD50 and LD1. [Bowen, 1968] LD(X) is defined as the lethal dose required to fatally injure (X) percent of the subjects. Blast durations ranging from short to long durations were used. The long blast durations were limited to 12ms in duration; longer durations are generally produced in very large, nuclear type explosives and are currently not representative of the smaller charges of interest. Figure 44 shows the test cases of interest identified on the revised Bowen curves.

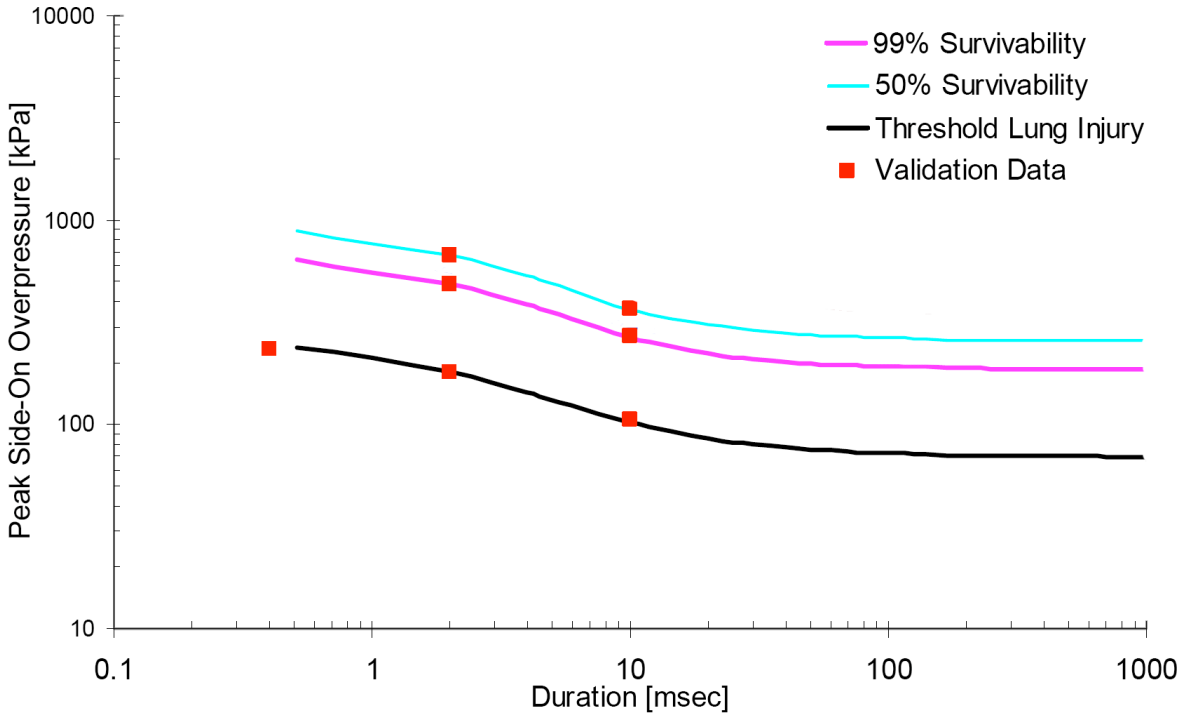

Figure 44: Revised Bowen Curves with selected points for blast loading [Bass, 2006]

The LS-Dyna load curves used to generate the test cases were created such that the resultant pressure and duration test values, shown in Figure 44 occurred at the front of the torso, just before the blast made direct contact with the body. In order to obtain the correct pressure and duration just before impact with the body, the boundary condition was adjusted so that the expansion and pressure decay of the blast load would be accounted for, resulting in the correct pressure and duration wave being delivered to the body. Table 3 shows the important curve values to generate blast loading for threshold, LD1 and LD50 blast lung injury.

Table 3: Test case values for blast duration and peak pressure

Duration (ms)	Peak Overpressure (Pa)	Lung Damage
0.4	250	Threshold
2.0	200	Threshold
10.0	125	Threshold
2.0	500	LD1
10.0	300	LD1
2.0	700	LD50
10.0	400	LD50

The pressure versus time load curve used to generate the blast loading on the torso for an overpressure of 500KPa and duration of 2.0ms is shown in Figure 45. This curve is applied at the boundary of the ALE air mesh to generate the appropriate loading at the location of the torso. This figure shows that the initial load curve placed on the ambient elements needs to have higher pressures and durations to account for the pressure decay as the blast wave travels towards the body. These loading curves were computed through a trial and error process and developed at the University of Waterloo [Salisbury, 2004].

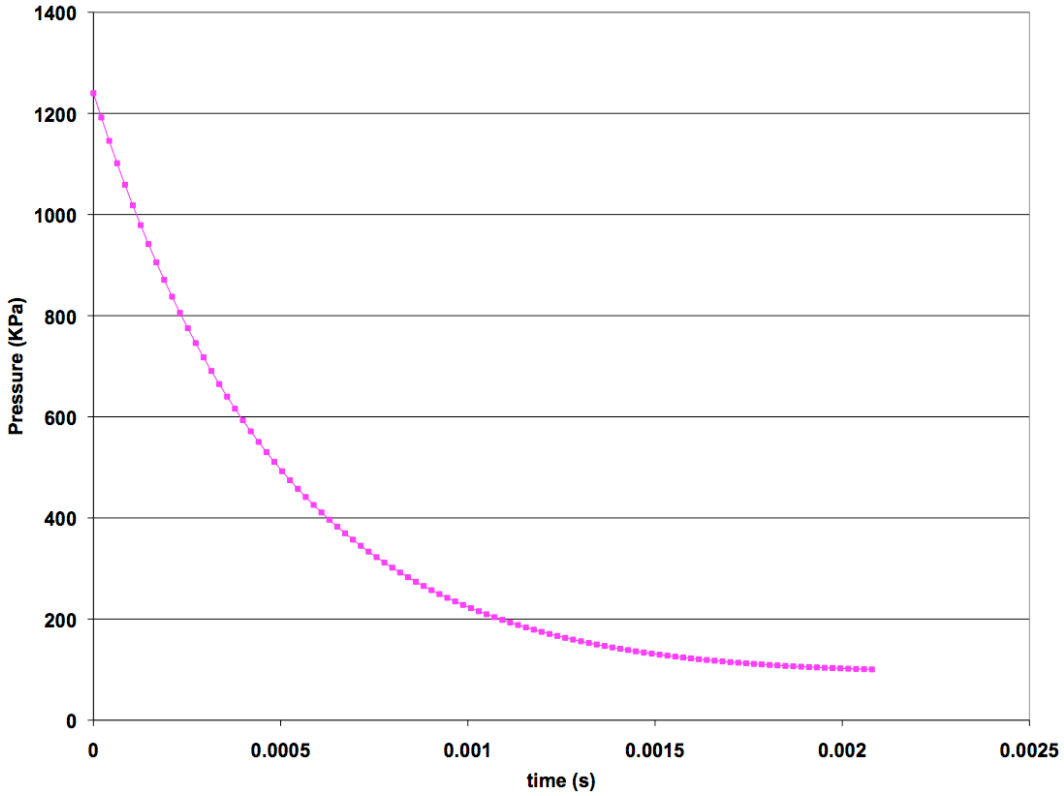

Figure 45: Load Curve for 500KPa, 2ms test case

3.4 Sheep and Human Finite Element Models

The LS-Dyna material models used to model the properties of the organs and bones was the same for both sheep and human thoracic models. The material models used were the same, however there were slight variations in the models parameters to account for the differences between human and sheep bone and tissue. Although there is similarity between the human and sheep thoracic cavities, there are some cross-sectional differences.

3.4.1 Anatomy

The main components of the thorax include the lungs, heart, thoracic cage, vertebrae, muscle tissue and fatty tissue. The Lagrangian reference frame was used to model the torso. To limit the calculation run time to a reasonable amount of time, the model of the sheep and human body was limited to the thorax. The finite element model of the sheep and human needed to have elements of sufficiently high resolution to allow for the tracking of pressure waves inside the lungs and tissues of the body. As the thorax is the main area of interest for blast lung injury, a high element resolution was required. This requirement of having a high resolution through the cross section of the thorax made modeling the complete thorax infeasible as the number of finite elements required to track the stress waves inside the body would be so great that the computer simulation would not be possible with the existing hardware. Therefore, the thorax model uses a cross sectional model at the location of mid sternum. The location of the cross section is shown in Figure 46. At this cross sectional location the lungs have a significant cross sectional area; allowing for the study of primary blast injury.

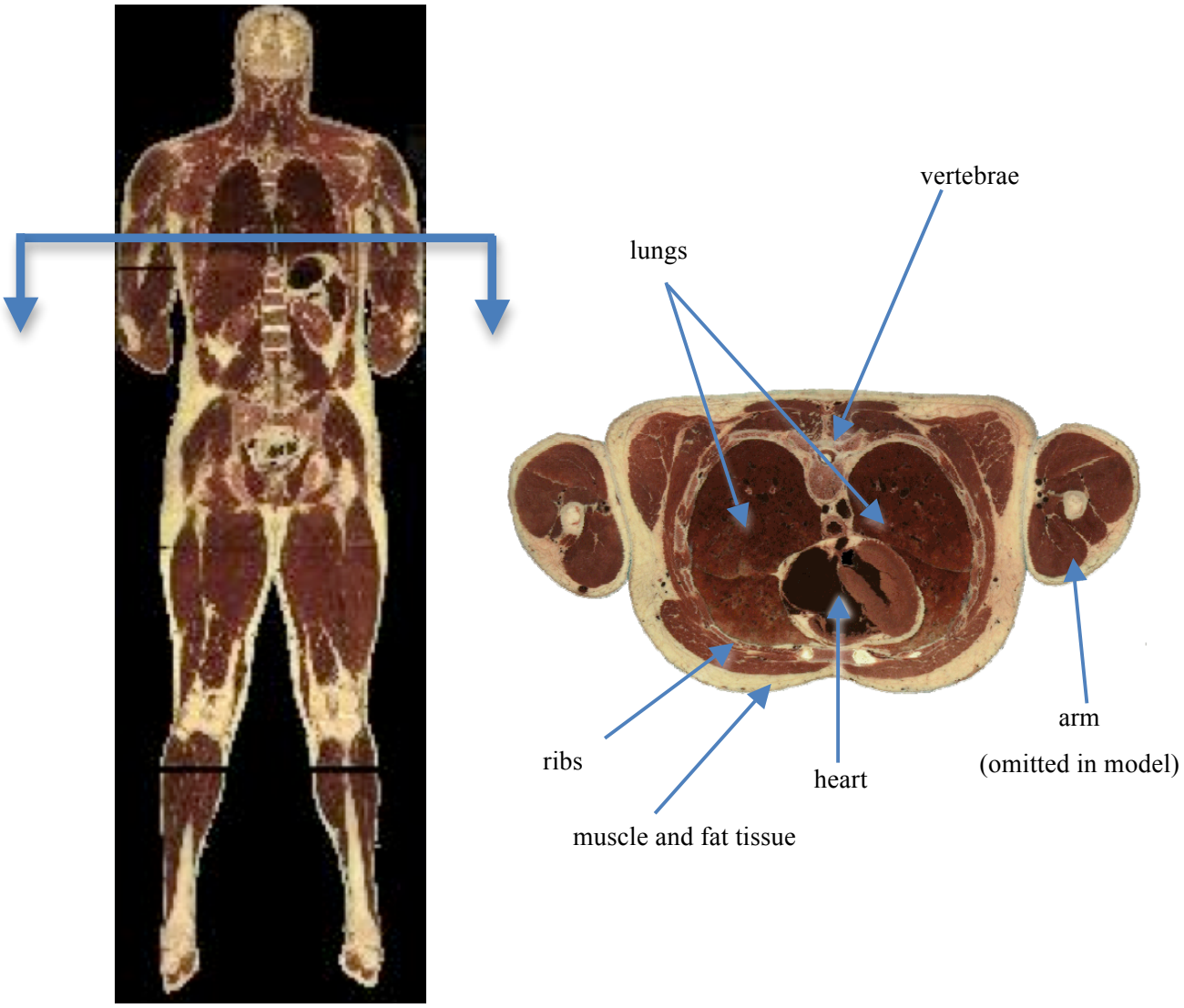

Figure 46: Cross Section of Human Torso

The model is a slice model, and in order to model a section of the torso a portion of the rib and a portion of the intercostals tissue were modeled. This slice model assumes that if it were stacked there would be an alternating layer of tissue and bone. Two elements in the vertical were used to model the intercostals tissue and rib/sternum layers. The cross sectional model consists of two repeating layers; a bone (rib) layer and a tissue (intercostal) layer. The

repeating layers provide a reasonable approximation of the thorax and account for the alternating rib and tissue sections that compose the thorax. The model uses four elements in the vertical direction, two elements for the rib layer and two elements for the intercostal tissue layer. The cross sectional model showing the two layers is shown in Figure 47. The internal organs of the thorax are modeled as a single layer, occupying the four vertical elements. The resultant thorax model is a pseudo-2D model and represents a somewhat infinite cylinder in 3D. The fluid flow interacting with the body at the mid-sternum however behaves as a 2D flow, so modeling the thorax in this fashion is appropriate.

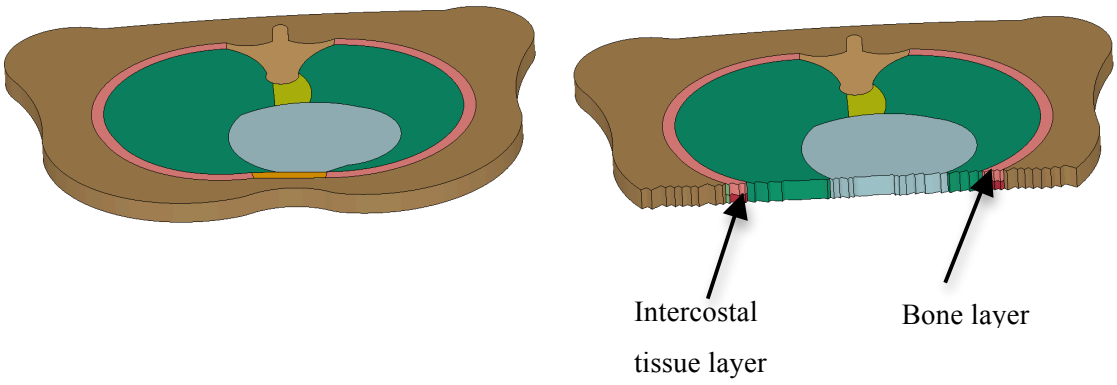

a. Thorax Model b. Slice view showing the two layers.

Figure 47: Cross sectional model showing layers of tissue and bone

3.4.2 Material Properties and Contact Conditions

The material models used for the biological materials were rate sensitive. To model the lung material and equation of state (EOS) model was implemented. The thorax models for each mammal used different material properties in their respective material model, to be consistent with their anatomy.

The numerical models included tissue, which was modeled as a single continuous material, rather than separate materials consisting of fatty tissue, muscle and skin. The heart was modeled as a single macroscopic continuous material. Similarly the lungs were modeled on a macroscopic scale as a single material with appropriate parameters.

Contact between the internal organs of the thorax was handled by using coincident nodes for the separate material components. Using this approach the deformation of the internal components are able to affect the adjacent components, however the calculation run time is decreased as the hydrocode does not need to check and compute contact between these components. Using coincident nodes between the lungs, intercostal tissue and ribs also simplifies the model as the pleural fluid and walls do not have to be explicitly modeled. This approach is acceptable as there is little relative sliding for the duration and deformations associated with blast.

3.4.3 Sheep Thorax Model

The numerical sheep thorax model developed at the University of Waterloo [Greer, 2006], was created for direct comparison to the published blast injury data. Many of the experiments and studies were performed on sheep, so there is a substantial collection of data available. The sheep was selected as a human surrogate as it was defined as one of the mammals that belong to the "high-tolerance group" for blast injury. Humans also belong to this group, so sheep are often chosen as test subjects for direct comparison. [Bowen, 1968]

The sheep model was meshed from CT scan data from the cross section of a sheep thorax. [Davies, 1987] The radiography image used to model the sheep is shown in Figure 48 and corresponds to a cross section between the 5^{th} and 6^{th} vertebrae.

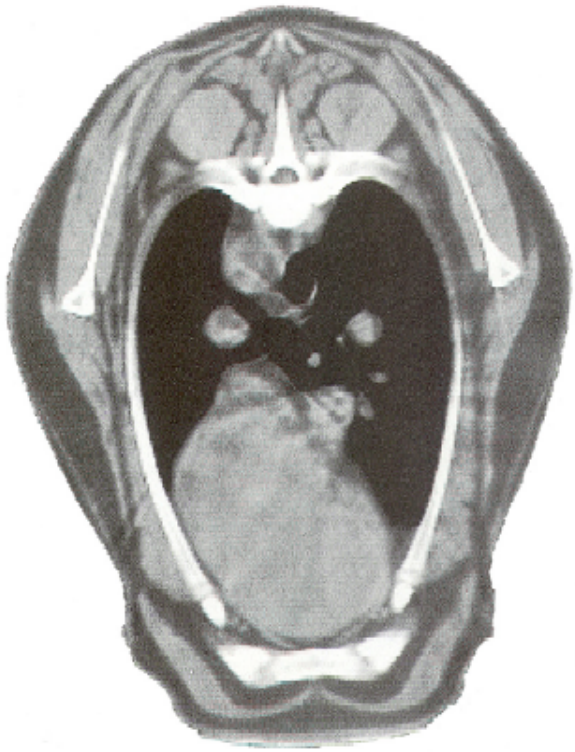

Figure 48: Cross section of sheep thorax from radiography [Davies, 1987]

The sheep numerical model is shown in Figure 49. The mesh in this model clearly shows the components of the sheep thorax. Each component is displayed as a different color or shade in the image. The model shows soft tissue, scapula, ribs, sternum, heart, lungs, vertebra and mediastinum.

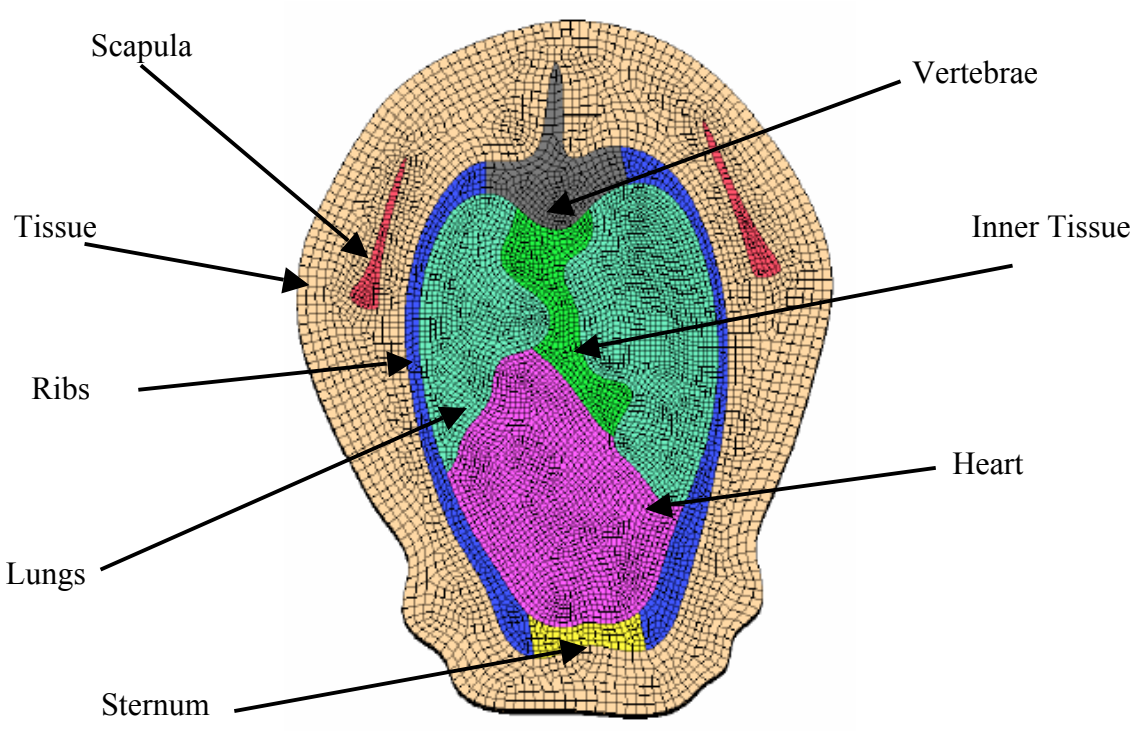

Figure 49: University of Waterloo sheep thorax finite element model

3.4.4 Human Thorax Model

The Visible Human Project (VHP) was used to develop the numerical model of the human thorax. [NLM, 2004; Greer, 2006] The VHP provides a database of cross sectional images from a male who was slightly above the 50th percentile male in size. The size of the 50th percentile male is defined as the mean measurements drawn from a group of data from a particular demographic. The cross section selected for the model was at mid sternum and located between the 5th and 6th thoracic vertebrae. The cross sectional image from the VHP used to model the geometry of the UW human thoracic is shown in Figure 50. The resulting numerical model is shown in Figure 51.

Figure 50: Cross section of human thorax and arms[NLM ,2004]

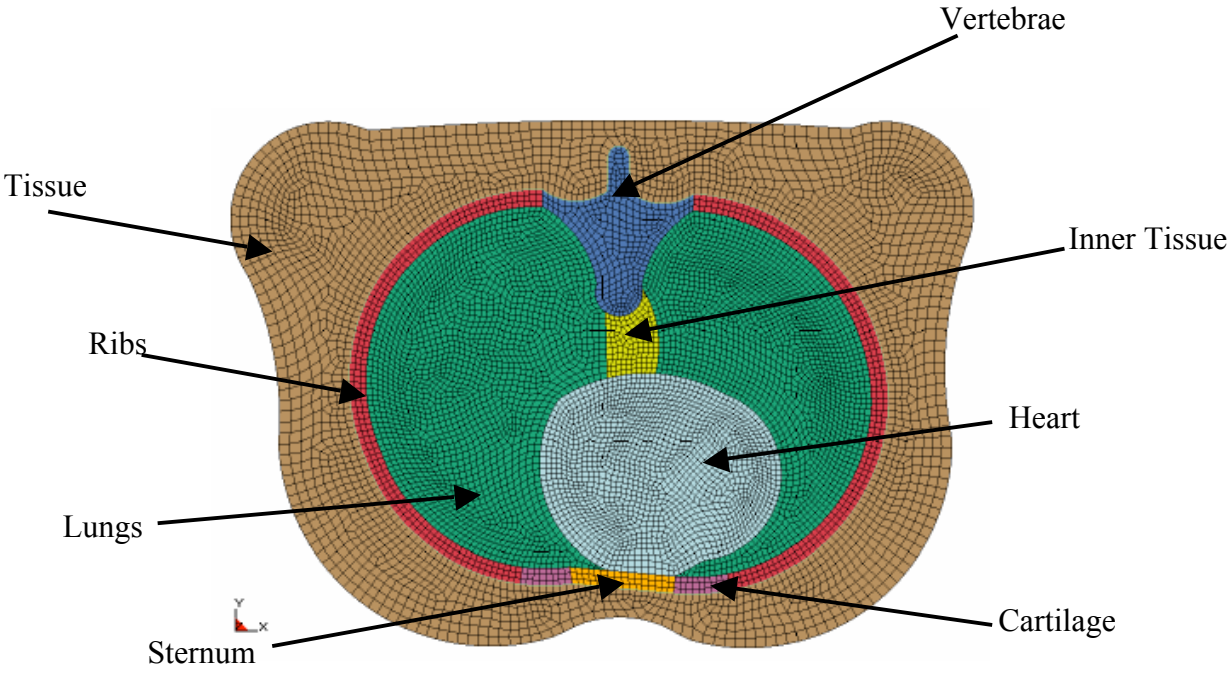

Figure 51: University of Waterloo human thorax finite element model

The numerical model includes the main components of the thorax. The arms shown in the VHP images were not considered in the thoracic model as their location and presence varies, as the subject is moving. The presence of the arms could also lead to injury estimates that under predict the actual injury as they may act as obstacles that direct the blast from the body or act as obstacles impeding the transmission of the blast wave on the torso. Figure 52 shows an exploded view of the torso model displaying all of the computational components. The "Tissue Shell" shown below was used for numerical stability and to enable the lungs to be initially at ambient pressure.

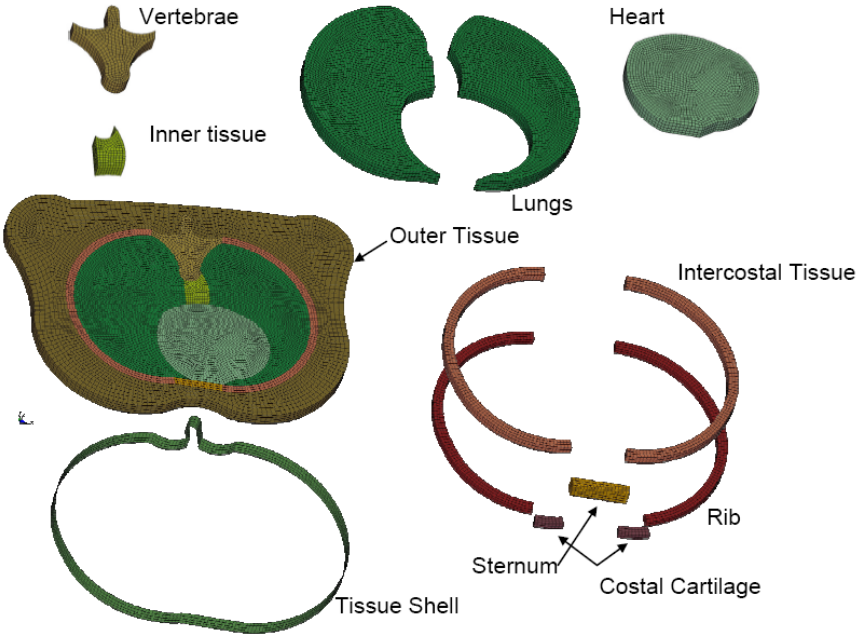

Figure 52: Exploded view of torso model, show all computational components [Cronin, 2004]

3.4.5 Comparison between Sheep and Human Model

The human and sheep thorax anatomy is similar in composition between these two mammals, enabling the numerical models to be similar, there are some discrepancies in the dimensions. The human and sheep thorax models consist of soft tissue, ribs, intercostal tissue, costal cartilage, sternum, vertebrae, heart, mediastinum and lungs.

The sheep and human thorax model are comparable; their material properties and overall size are similar however, the sheep thorax model also includes the scapula bones of the sheep in the soft tissue, where this is not present in the human thorax.

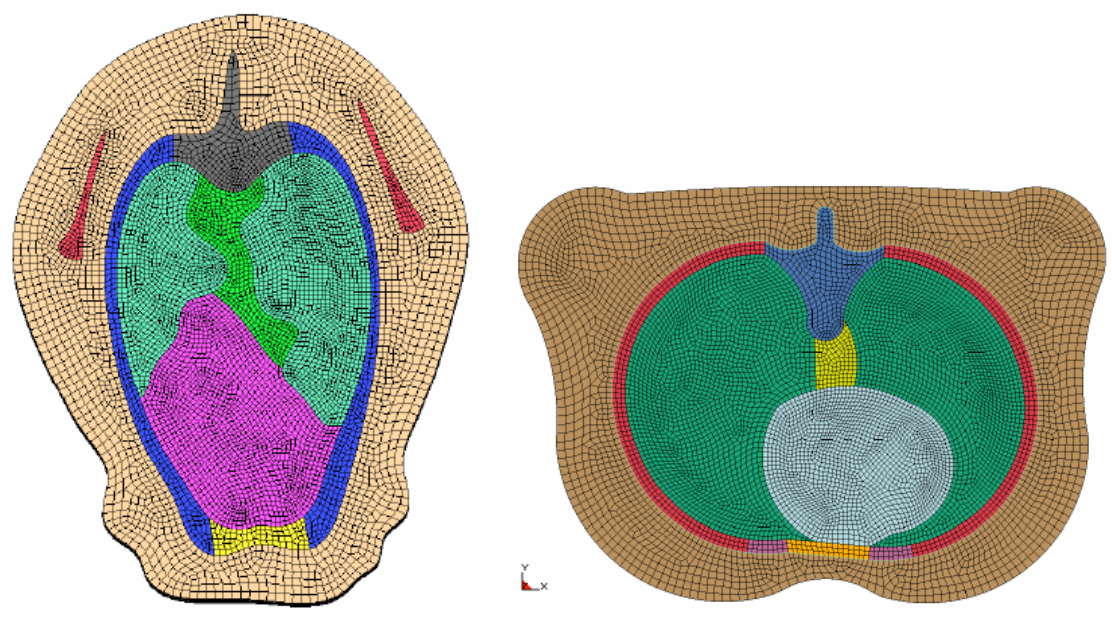

a. b.

Figure 53: Comparison between sheep (a) and human (b) thorax models (same scale)

The sheep thorax section measured approximately 261mm in width and 343mm in depth. In contrast the human thorax measured approximately 347 mm in width and 250 mm in depth. In this orientation the human thorax is wider than the sheep, however it is less deep. When the thoraxes are exposed to a blast wave travelling to the front the sheep thorax is more aerodynamic as there is less surface area exposed to the blast wave as compared to the human thorax. The human thorax would therefore be a larger obstacle in the blast flow field, causing greater reflections. Orienting the sheep thorax at 90 degrees results in the external measurements of both thoraxes roughly being equivalent, however the orientation of the lungs and ribs are inconsistent; the human lungs are oriented right to left, whereas the sheep's are oriented anterior to posterior. This difference is shown in Figure 54.

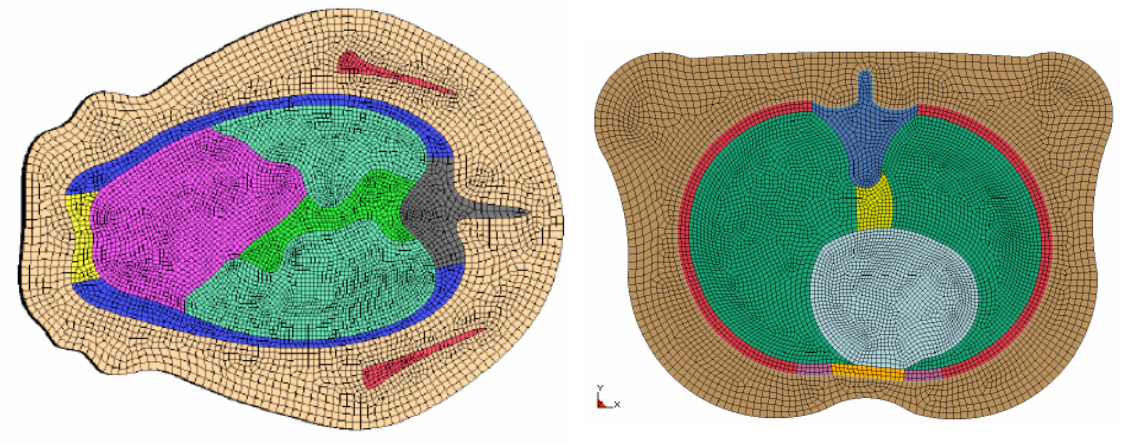

a. b.

Figure 54: Comparison between sheep (a) and human (b) thorax models (same scale)

3.5 Pulmonary Contusion Injury Prediction

The UW model treats the lung as a continuum and does not model the microscopic detail and individual air sacs in the lungs, therefore the actual mechanism of blast lung injury cannot be modeled directly using these numerical thorax models. The model is however capable of capturing the stress waves in the lung that are generated by the blast wave impacting the outer thorax tissue and being transferred into the thoracic cavity. It is postulated that these stress waves that travel through the lungs are responsible for blast lung injury. [Guy, 1998a]

A correlation between injury reported and the use of maximum pressure in the lung element of the University of Waterloo model has been shown. [Greer, 2006]. The UW model predicts injury and damage to the lungs based on maximum transient pressure in a given lung element. It is postulated that high pressures in certain regions of the lung would lead to overstressing of the lung tissue, resulting in injury to the lung and internal hemorrhaging.

The maximum dynamic pressure in the lung elements was used as an injury predictor. To predict the dynamic pressures, the lungs were discretized into a large number of elements; the lungs consisted of 13,947 elements. The UW model also showed good correlation with the different injury levels reported. The injury levels obtained can be further bracketed by pressure ranges. Figure 54 shows the pressure and damage levels obtained in the lung as a result from a blast wave impacting the thorax. The five levels of severity of injury are displayed along with the pressure ranges that correspond to these levels. [Cronin 2004; Greer, 2006]

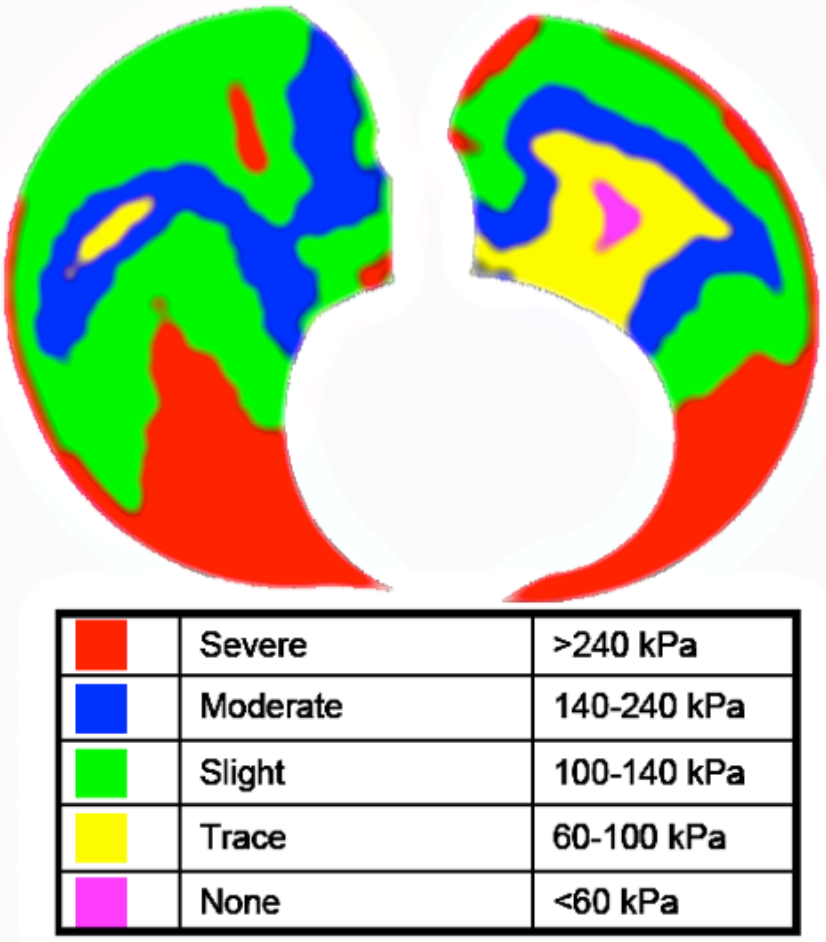

Figure 55: Example of calculated PBI and damage levels inside the lung

Both the predicted injury magnitude and injury locations are in good agreement with the literature. [Greer, 2006] The maximum level of injury is typically observed near the lobes of the lungs, along the ribs and at the locations where the stress waves coalesce. In animal studies where the animals were subjected to blast waves, post analysis has been done on the cadavers of the animals. It was often observed that animals with injury to the lung experience hemorrhaging in the vicinity of the tip of the lobes. [Stuhmiller, 1996]

3.6 Blast Modeling

3.6.1 Torso Response

The sequence of images in Figure 62 through Figure 62 shows the progression of a Friedlander blast wave and interaction with the human torso. Although the results shown are for human thorax and an LD50 case the results shown below reflect those that typically occur with any of the other blast waves studied. An analogous physical response was obtained for the other simulations involving the sheep torso and BTD cylinder.

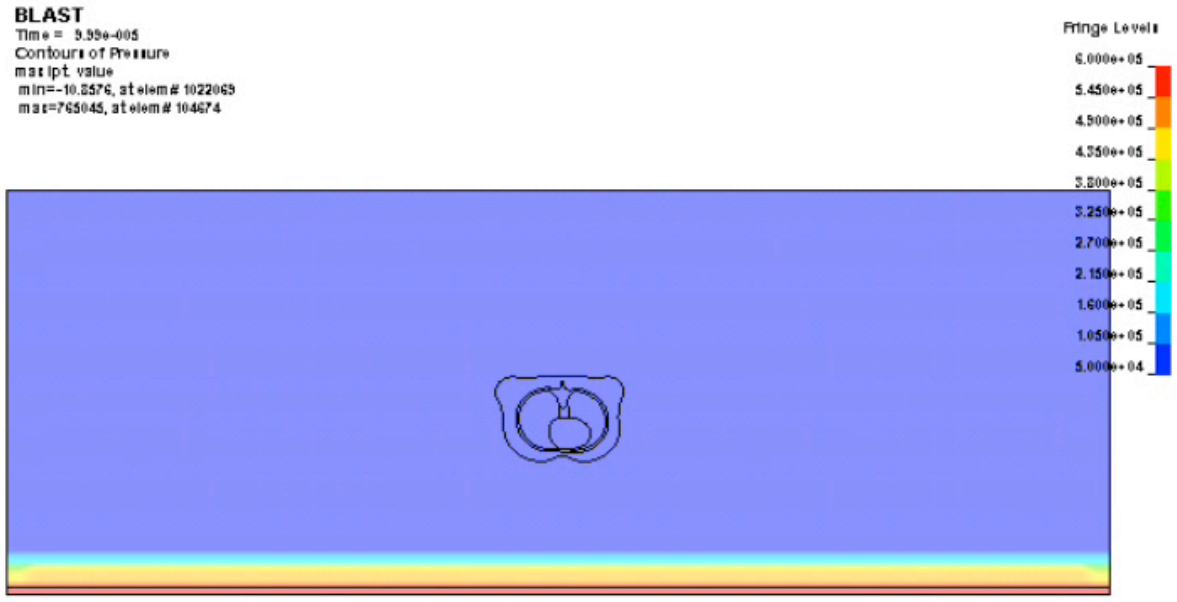

Figure 56: Planar blast wave travelling near bottom of the domain (t=1e-4 s)

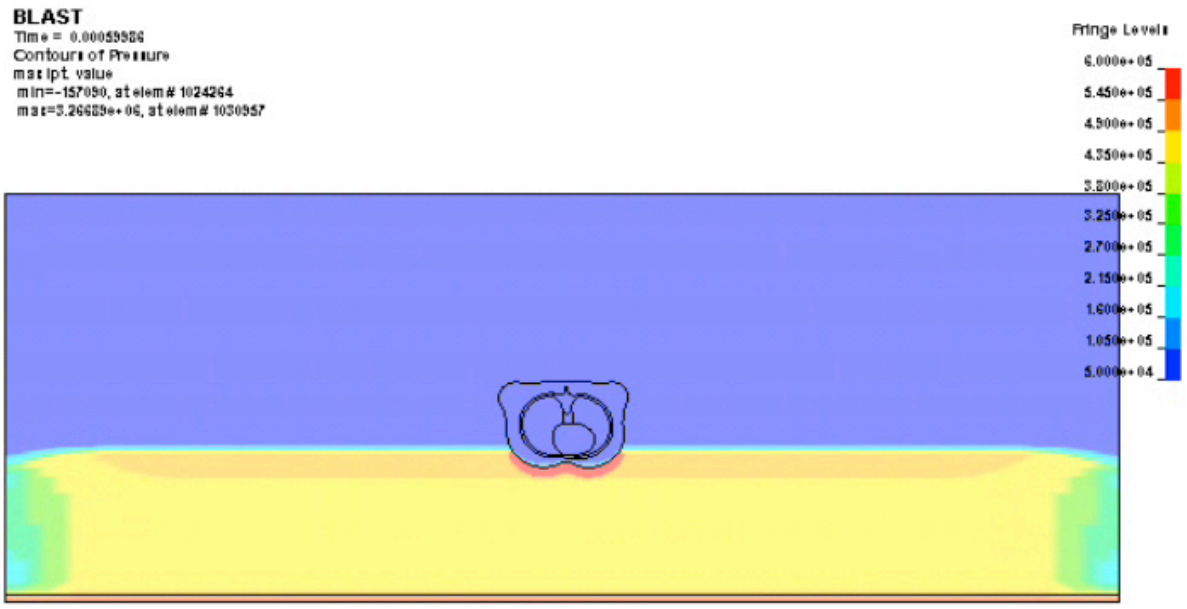

Figure 57: Initial impact of blast wave on torso (t=6e-4 s)

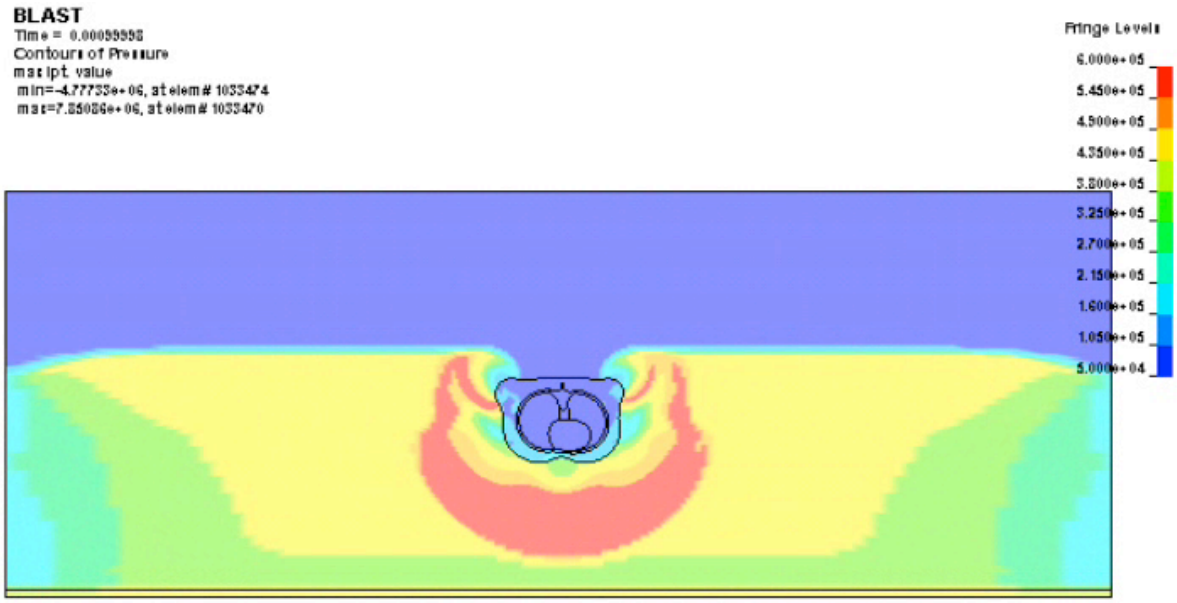

Figure 58: Impact of blast wave on torso and resultant normal reflection off of front of torso (t=1e-3 s)

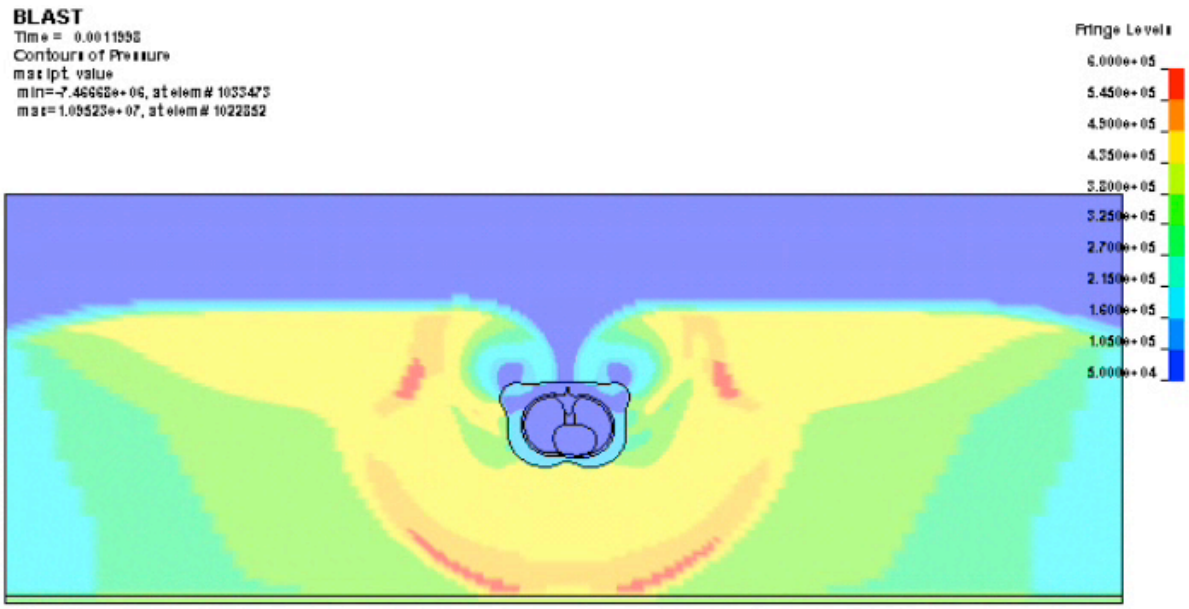

Figure 59: Blast wave reflection from the front of the torso (t=1.2e-3 s)

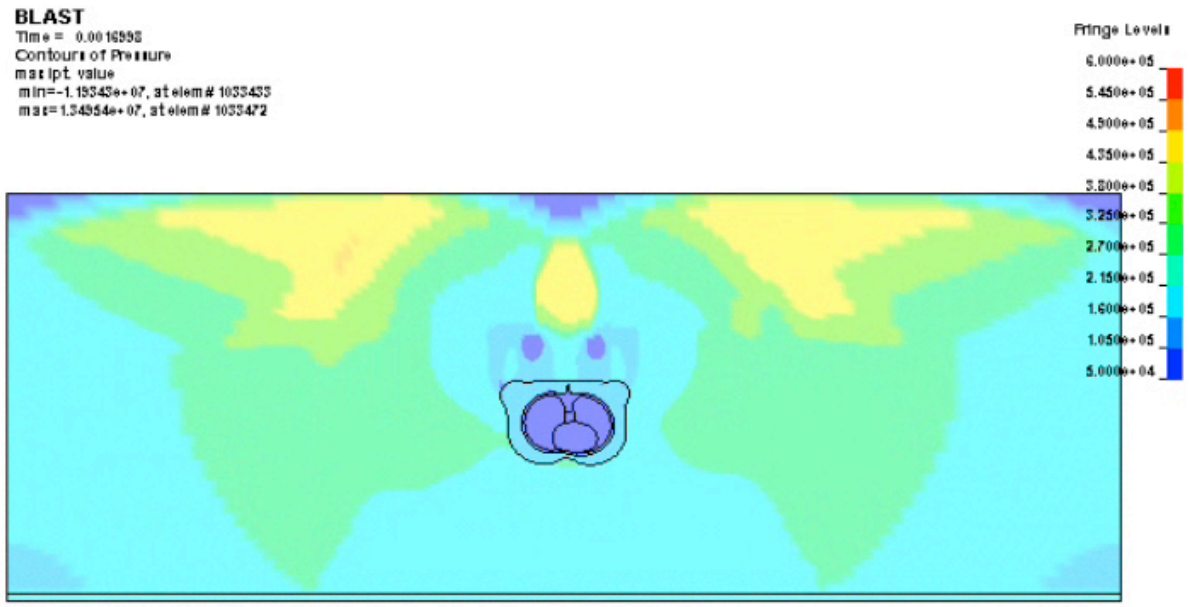

Figure 60: Blast wave completely passing over torso (t=1.7e-3 s)

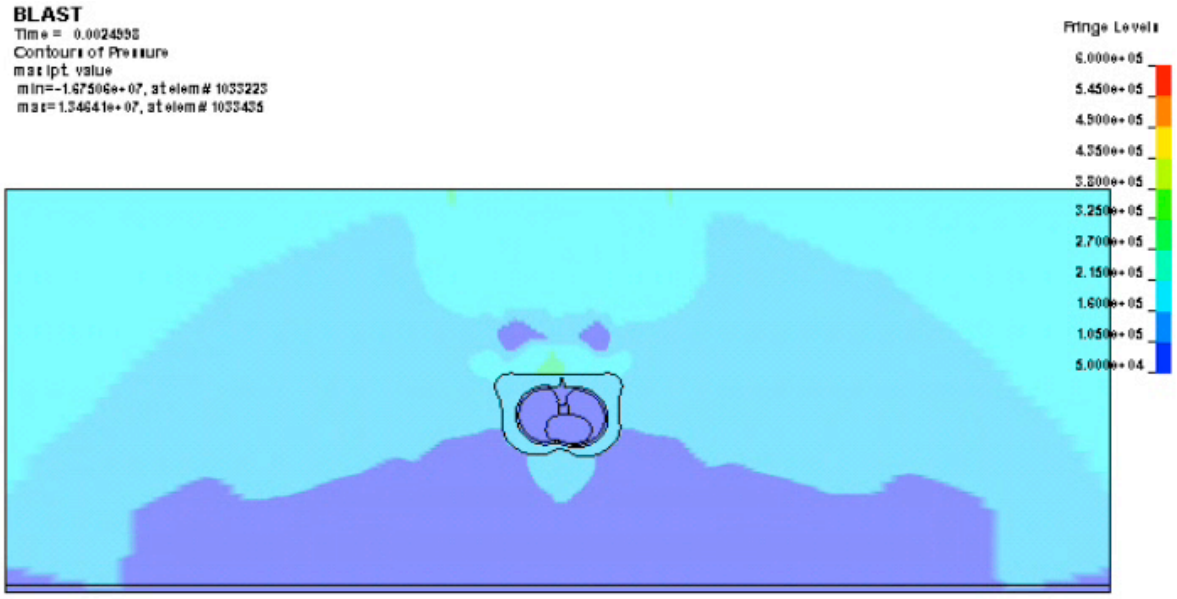

Figure 61: Dissipation of the blast wave, as it expands (t=2.5e-3 s)

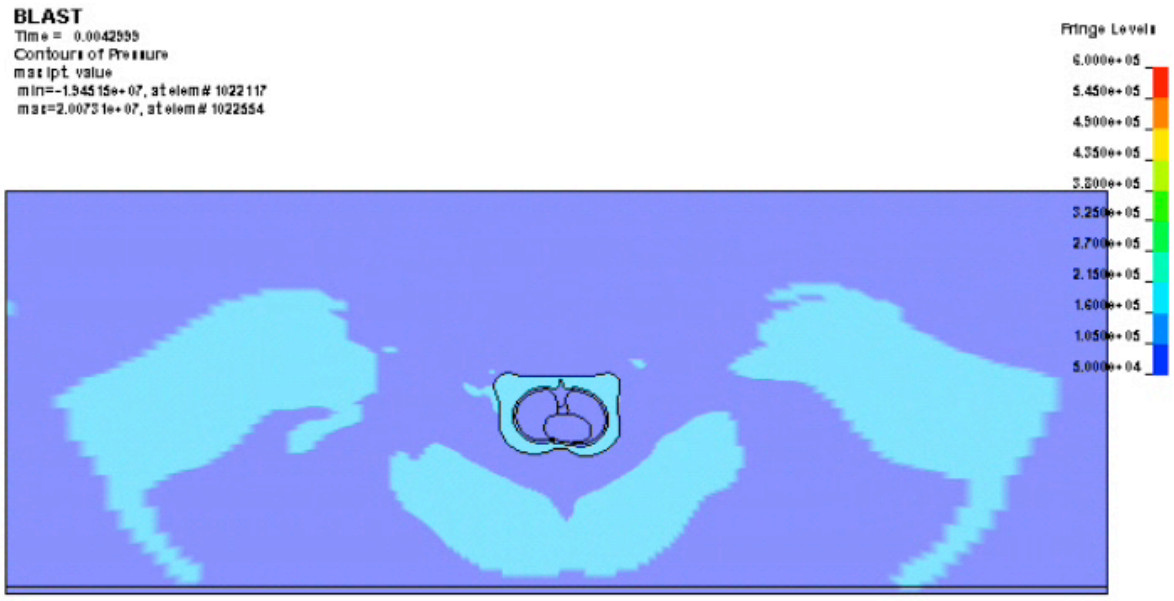

Figure 62: Domain returning to ambient conditions (t=4.3e-3 s)

Examining the pressures and stresses inside the thorax shows how the energy of the blast wave is delivered and absorbed by the thorax, causing injury to the lungs. The sequence of images in Figure 63 shows the resultant stress waves delivered to the body and their progression through the torso. A similar behavior is seen in the case of the sheep thorax. The blast wave impacts the thorax and transmits stress waves to the thorax. These stress waves travel through the soft tissue and muscle of the thorax very quickly due to the higher sound speed as compared to the lungs. The force of the blast wave interacting with the thorax causes the chest to slightly compress. Stress waves are generated in the lungs and travel somewhat parallel to the blast wave, moving along the ribs. The stress waves are highest along the ribs and end up reflecting at areas of sharp radiuses, or near the back where they impact and reflect off of the vertebrae. This internal reflection of the waves increases their magnitude and provides the location of greatest injury. Although the magnitude of pressures inside the lung return to ambient, the lung remains damaged as the high pressures developed were enough to cause excessive damage on strain on the lung material.

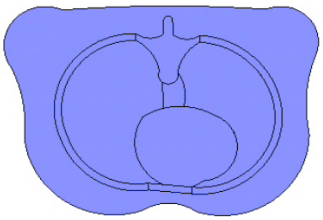

a.) Before impact with blast wave

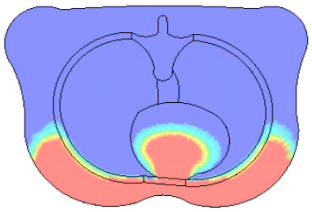

b.) Initial blast impact

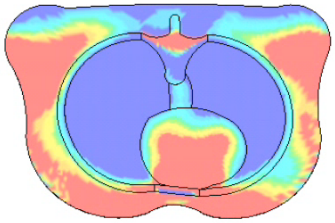

c.) Stress waves traveling along torso tissue

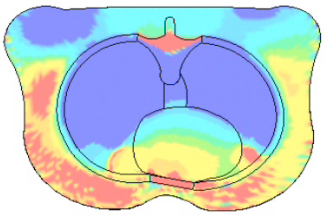

d.) Stress waves forming in the front of the lungs

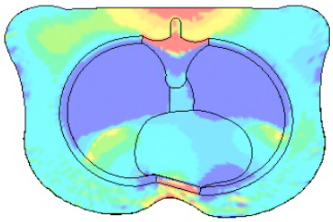

e. Stress waves traveling through the lungs

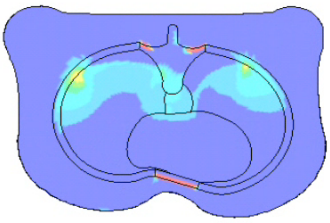

f.) Waves travelling anterior to posterior

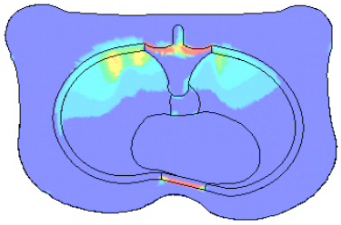

g.) Waves impact vertebrae

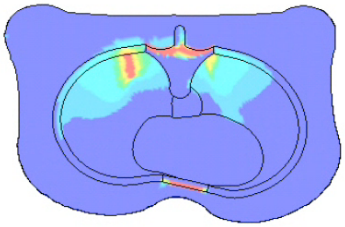

h.) Reflecting stress waves inside the lung

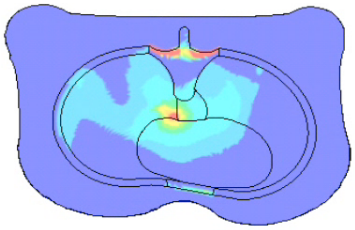

i.) Waves coalesce at sharp radia near the heart

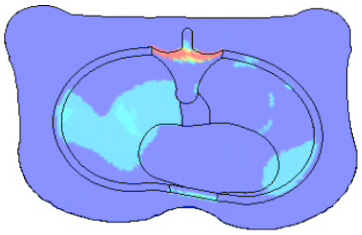

j.) Lower magnitude stress waves traveling

Figure 63: Progression of stress waves inside the torso

3.6.2 CFD Modeling

Martec's Chinook CFD solver was also used to generate blast loading for the numerical torso model. Similar to LS-Dyna this CFD solver is able to compute blast loads by calculating the expansion of an explosive charge by using material properties and an equation of state. [Martec, 2006] Modeling the charge requires a mesh of significantly high resolution and requires long run time to track the expansion. When modeling a small charge on a large domain it would be inefficient to model the entire expansion process, so the Chinook code accounts for this by allowing the results from pre-computed charges to be placed on the domain. This reduces calculation run time and removes the need to use a high resolution grid to model the initial charge. Chinook has a library of pre-computed charges and also allows the user to create their own charge libraries. The pre-computed charges are generally performed on a high resolution 1D or 2D domain and the initial charge is allowed to expand up until a certain radius. A snapshot of the expansion and blast is then taken and values of pressure, density and velocity are then mapped onto the 3D domain, where the remainder of the expansion and blast propagation takes place. [Josey, 2006]

Three CFD simulations were performed to obtain a variety of loading conditions for the body. These simulations were chosen to obtain different blast loading conditions; free field and complex blast loads were considered.

3.6.2.1 Freefield blast

Chinook was used to model a charge placed on the ground representing a free field blast. This charge was modeled using the pre-computed charges available in Chinook, using a charge of 5kg of TNT. The profile was placed on a 3D domain, and the profile selected was set to a large enough size, to reduce the computational time required to calculate the

expansion. The size of the profile was just slightly smaller than the size of the domain, ensuring that there was no interference, contact or overlap with the boundaries of the domain. The profile is shown on the ground in Figure 64. The computational domain was 4m wide, 6m long and 3.5m high and consisted of 325000 cells. The boundaries were set to flow through for all edges except the ground level and the symmetry plane, which were set to solid walls.

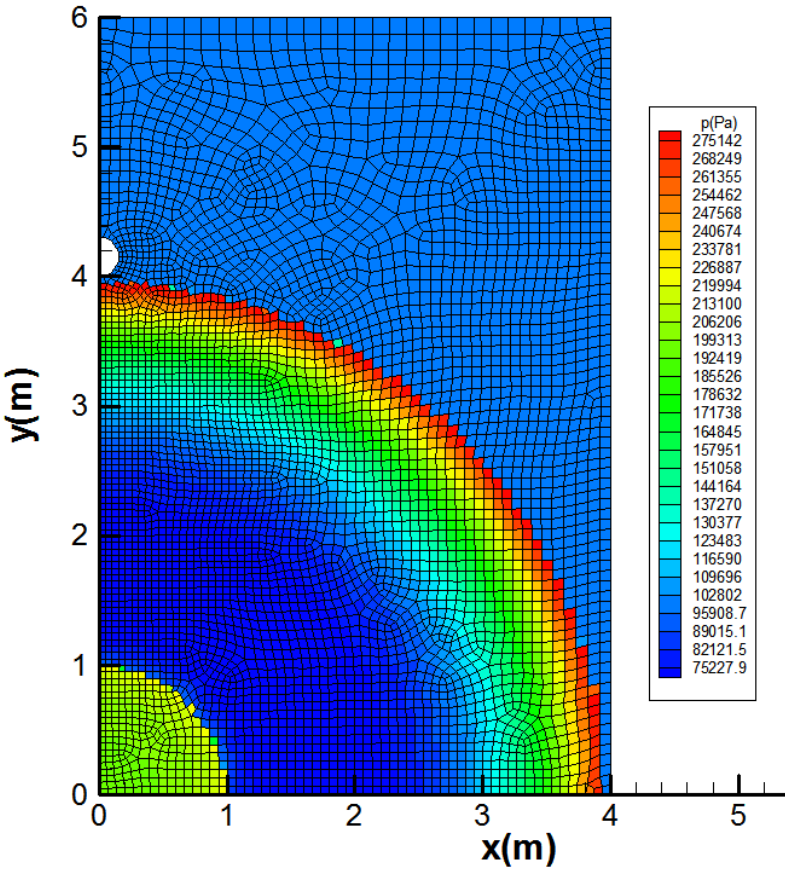

Figure 64: Explosive profile mapped onto Chinook domain at ground (z=0m)

In order to model the effect the torso has on the blast wave a cylinder representing a human torso was placed in the flow field. This cylinder represents a BTD placed in the flow and was instrumented with numerical pressure gauges to record the pressure surrounding the cylinder. The cylinder was 1.78m high, was placed 4m from the center of the blast and has 16 virtual gauges placed around its circumference (equally spaced) at a height of 1.4m. A half symmetry 3D model was used in order to reduce run time and therefore 9 pressure gauges surrounding the cylinder were used.

The pressure histories for blast calculation on the BTD are shown in Figure 65. The results from pressure gauges surrounding the BTD and at a height of 1.4m are shown. It is clearly visible that the gauges near the back of the BTD experience a lower pressure than those located closer to the blast. The blast wave impacts with the gauges on the front of the BTD and the presence of the cylinder allows the blast wave to flow around the BTD. Along with the BTD results, the results for a gauge placed at ground level at the bottom front of the BTD. To compare this reflected value at ground level, the results from a gauge located 4m at the base of a wall and on the ground are shown. The figure shows that the peak pressure is somewhat lower for the case where the gauge is located on the cylinder as compared to the wall. It is also noted that positive phase duration is also lower for the cylinder case, therefore the impulse delivered to an infinite wall is greater than that delivered to a cylinder, as the cylinder allows for the blast wave to flow around the body.

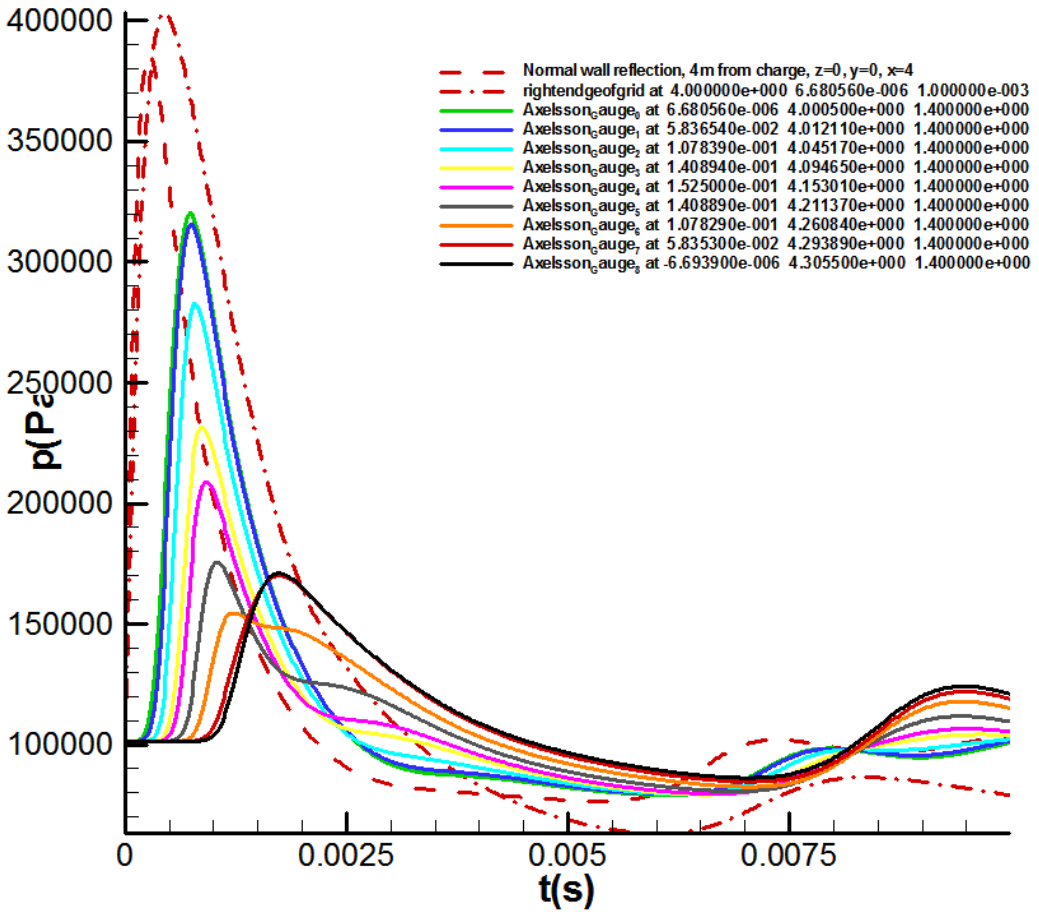

Figure 65: Free field blast loading on BTD

3.6.2.2 HOB

To investigate the effect the charge has when not placed on the ground a blast scenario was computed which involved detonating the charge at a height of 1.4m. This height corresponds to the height of the mid sternum on the 50th percentile man and is the same height that the gauges are placed on the BTD cylinder. By placing the charge at a height above the ground, when the charge detonates the blast wave will initially expand and then hit the ground and reflect. This interaction with the ground produces a somewhat complex blast loading

scenario and is more complex than a simple Friedlander type blast loading wave. Using 5kg of TNT the Chinook solver was used to predict the blast loading on BTD cylinder located 4m from the charge center.

A 3D symmetric calculation CFD calculation was performed using the pre-computed profiles in Chinook to solve for the blast loading. The meshed domain measuring 4m in width, 6m in length and 3.5m high is shown in Figure 66. The mesh consists of 325000 cells. The symmetry of the model is shown in the figure and the profile and BTD boundaries are visible.

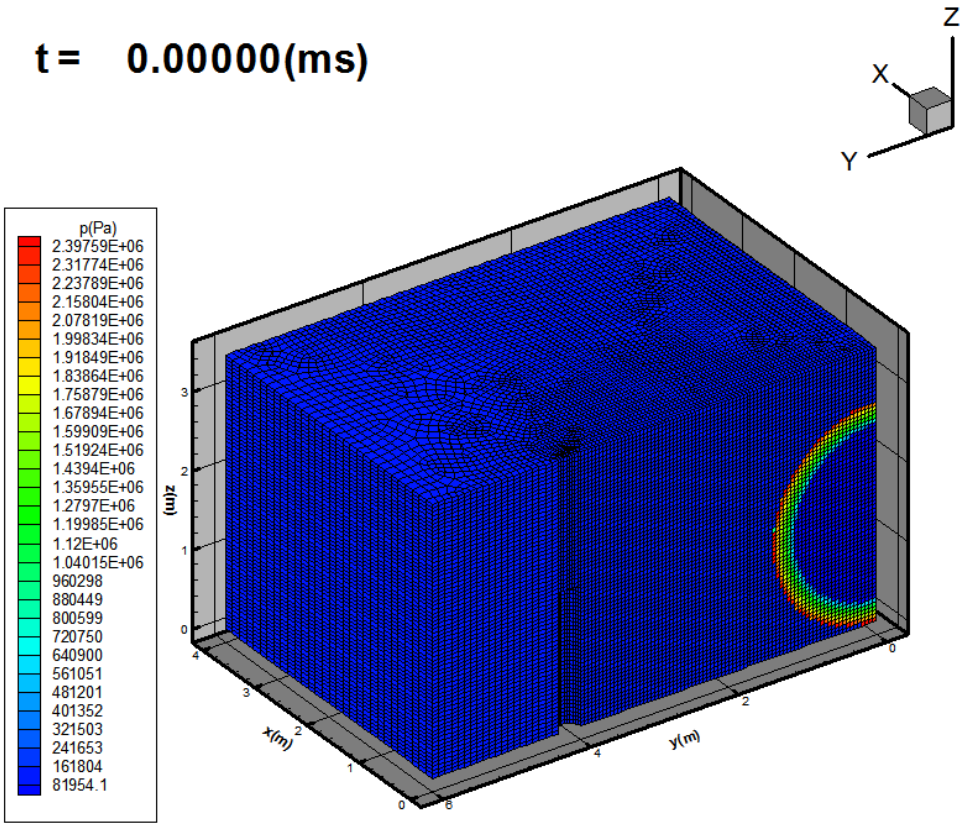

Figure 66: 3D HOB CFD simulation

The blast loading pressure and time results are shown in Figure 67. The results from the simulation show the effect the height of burst has on the blast loading. The blast loading is not a simple Friedlander type loading; the loading has kinks and does not exponentially decay. The complex flow and the reflection the blast wave has on the ground is contributing to these blast loading profiles. For comparison the results of a gauge placed on a rigid wall at a height of 1.4m are shown. The impulse experienced by the rigid wall is much greater than that experienced by the front of the BTD cylinder, as the flat rigid wall creates a more extreme loading case as the flow is not permitted to travel or wrap around the object.

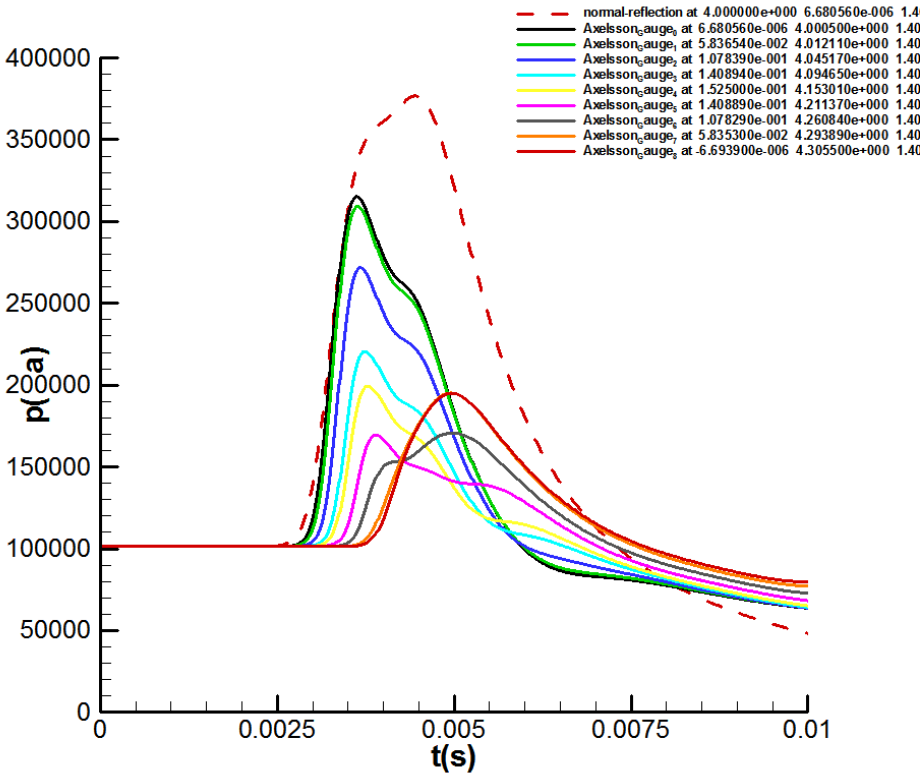

Figure 67: Blast loading results on a BTD from a 1.4 HOB simulation

3.6.2.3 Corridor

To further investigate blast lung injury using complex blasts a scenario involving the detonation of a charge in an alleyway or corridor was investigated. The corridor was modeled with a width of 2m and the boundaries of the corridor were modeled as rigid walls. The top and the ends of the corridor were open and modeled as flow through boundary conditions. In addition to using the rigid walls to create a complex blast scenario, the charge was also placed at a height of 1.4m. Similar to the other scenarios, the torso was located 4m from the center of the charge. A charge of 5kg of c4 was used to model the charge, the initial size of the pre-computed profile used to model the charge was limited to a radius of 1.0m, in order to not have the placement of the charge overlapping the boundary. The 3D model is shown in Figure 68.

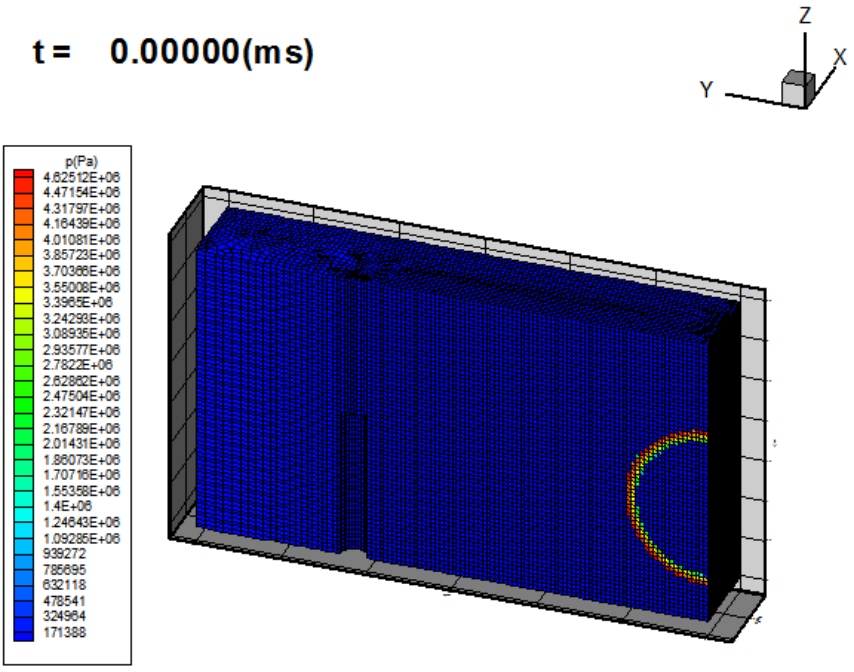

Figure 68: CFD domain for alleyway scenario

The results from the CFD simulation and the resultant blast loading on the BTD cylinder are shown in Figure 69. The alleyway scenario results in a very high blast pressure load on the cylinder. For gauges located near the back of the cylinder, at least two predominant pressure peaks are noted and a result of the complex blast wave generated in the corridor. The resultant impulse delivered to the BTD is much greater in this scenario as compared to the free field or HOB scenario. This increased impulse and higher pressures lead to higher levels of blast lung injury.

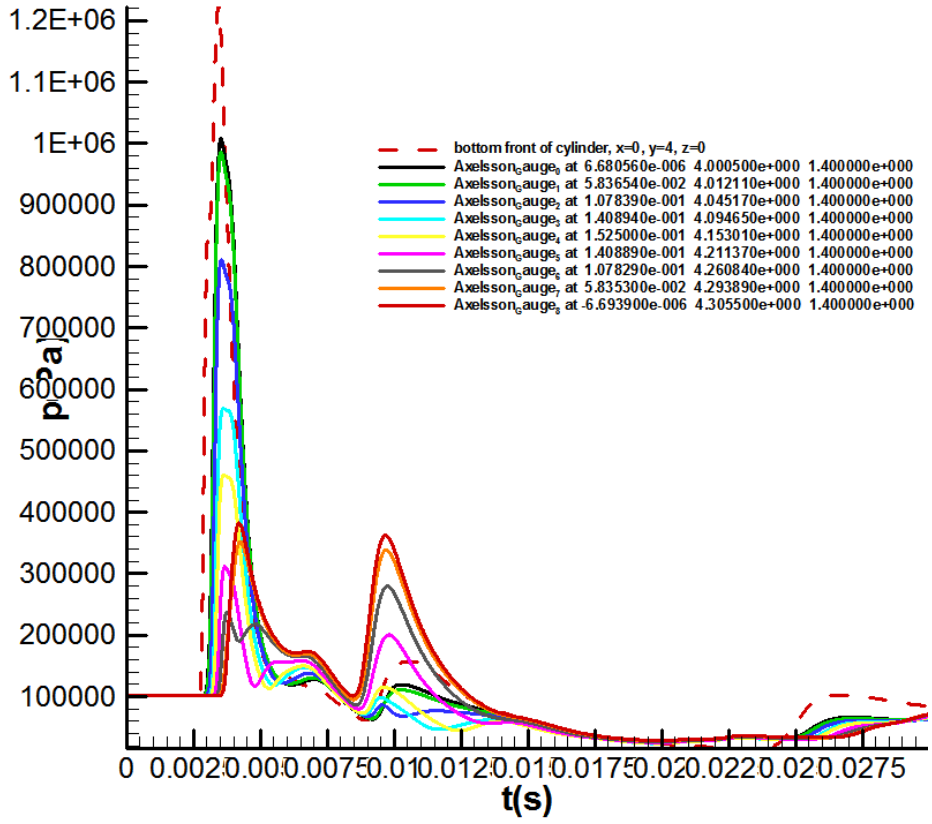

Figure 69: BTD complex blast loading from an alleyway explosion

Chapter 4
Blast Injury Parametric Study

4.1 Introduction

In order to determine the key parameters involved in predicting blast lung injury a study was performed using idealized blast waves to limit the number of uncontrolled variables. The study examined the effects of idealized blast waves on predicted lung injury to determine the importance of peak pressure, blast wave duration and total impulse. Injury was assessed using the finite element model of the human thorax. The parameters examined were peak pressure, blast duration and impulse.

For this study basic and idealized blast waves were used. Using the simplest scenarios, the effect of each of the identified parameters was isolated and its effect measured. Further testing can extend this approach and gradually increase the level of complexity by introducing more complex and non-idealized wave forms. By using a simple approach a fundamental understating of the parameters may be understood. These simple, idealized cases may also then be employed to further validate the numerical torso model.

4.2 Method

A series of simulations were performed using simplified blast waves and changing relevant parameters of the waves to evaluate blast lung injury. Testing involved holding the impulse constant and varying the peak pressure, holding the peak pressure constant and varying the duration, and holding the duration constant and varying the peak pressure. The simplified blast waves, based on the LD 50 Bowen curves, included a right angle triangular shape and a

square wave, which allowed for the different parameters to be considered. The results obtained using the FEA models were compared to the existing Axelsson, Stuhmiller and Bowen injury models.

To investigate the spectrum of injury from no-injury to a lethal level, a variety of explosive charge sizes were modeled. The explosives were modeled as TNT and implemented in LS-Dyna by applying a load curve to the fluid elements. By varying the shape of the load curve a desired waveform was imposed onto the domain. For the purpose of this study, load curves of triangular and square waves were used. These represented simplified waveforms. The loading curve was placed 0.35m from the front of the torso model.

For the square and triangular wave forms the source was modified in three different ways in order to vary the pressure, duration and impulse of the blast source. This was accomplished as follows:

i. Holding the pressure constant and varying the duration (impulse varies indirectly)
ii. Holding the duration constant and varying the pressure (impulse varies indirectly)
iii. Holding the impulse constant and varying the pressure (duration varies indirectly)

Using Bowen curves, a number of duration and peak pressure points were chosen which provide injury levels ranging from threshold to LD50. To round out the study three duration ranges were used: short durations of less than 1 ms, long durations greater than 8 ms and durations between 1 ms and 8 ms were used. Simplified triangular and square waves were modeled as the blast profile simplifies that of the idealistic Friedlander curve. A Friedlander curve is an idealistic blast wave consisting of an instantaneous pressure rise followed by a decay and negative pressure phase. Figure 70 shows a comparison between the blast source

used in this study and the Friedlander curve. Although it was desired to have an exact triangular or square waveform up until the moment of contact with the torso, this was not possible. The triangular and square waveforms were applied to the blast-loading portion of the mesh, located approximately 0.35m away from the torso. As the triangular and square waveforms traveled this distance the shape of the waveform would change, due to the shock physics and attenuation and dispersion of the wave. Placing the blast loading portion of the domain directly in front of the torso would not account for the reflection and wave interaction between the wave and the torso, as the elements in front of the torso would be not be calculated but directly applied with an appropriate load curve value at each time step.

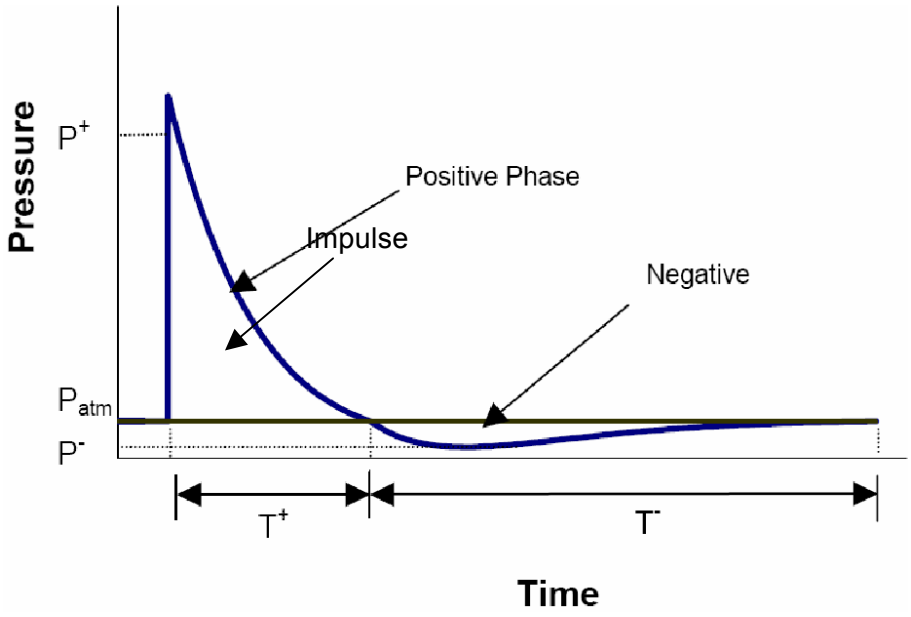

a. Friedlander Curve

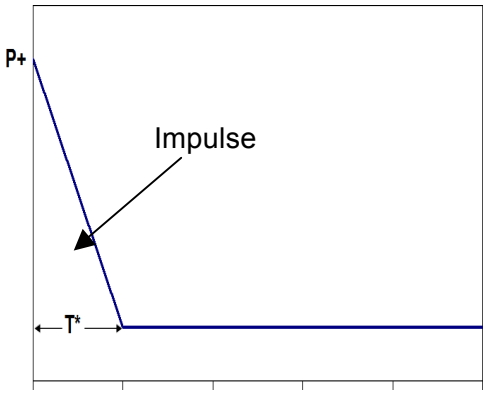

b. Triangular source wave

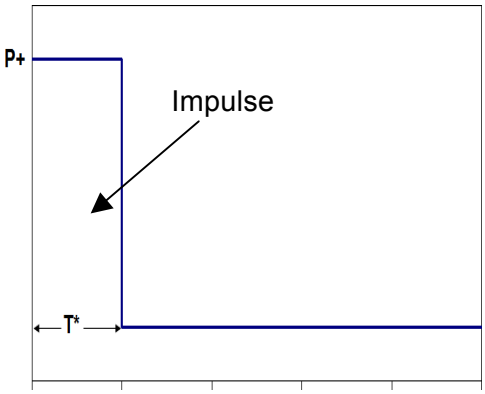

c. Square source wave

Figure 70: Blast Wave Comparison

In total 52 numerical simulations were performed to evaluate the response of the torso model to different blast load scenarios. Pressure and duration values for each of the scenarios were chosen based on the Bowen Curves. Durations between 1 ms and 8 ms were of particular interest as blast durations in these ranges are more typical. In all simulations the location of the torso remained constant and only the blast-loading curve was altered. The test matrix for the triangular and square waveforms is given in Table 4.

Table 4: Parametric Study Test Matrix

P constant, Duration Varies			
	Peak Pressure (Pa)	Positive Phase Duration(s)	Positive Phase Impulse(Pas)
Triangle	2.40E+06	8.00E-04	9.60E+02
	2.40E+06	4.00E-04	4.80E+02
	2.40E+06	2.00E-04	2.40E+02
	2.40E+06	1.00E-04	1.20E+02
	2.40E+06	5.00E-05	6.00E+01
Square	2.40E+06	8.00E-04	1.92E+03
	2.40E+06	4.00E-04	9.60E+02
	2.40E+06	2.00E-04	4.80E+02
	2.40E+06	1.00E-04	2.40E+02
	2.40E+06	5.00E-05	1.20E+02

Duration constant, P Varies (Short Duration)			
	Peak Pressure (Pa)	Positive Phase Duration (s)	Positive Phase Impulse (Pas)
Triangle	4.80E+06	2.00E-04	4.80E+02
	3.60E+06	2.00E-04	3.60E+02
	2.40E+06	2.00E-04	2.40E+02
	1.20E+06	2.00E-04	1.20E+02
	6.00E+05	2.00E-04	6.00E+01
Square	4.80E+06	2.00E-04	9.60E+02
	3.60E+06	2.00E-04	7.20E+02
	2.40E+06	2.00E-04	4.80E+02
	1.20E+06	2.00E-04	2.40E+02
	6.00E+05	2.00E-04	1.20E+02

Duration constant, P Varies			
	Peak Pressure (Pa)	Positive Phase Duration (s)	Positive Phase Impulse (Pas)
Triangle	1.60E+06	2.00E-03	1.60E+03
	1.20E+06	2.00E-03	1.20E+03
	8.00E+05	2.00E-03	8.00E+02
	6.00E+05	2.00E-03	6.00E+02
	4.00E+05	2.00E-03	4.00E+02
Square	1.60E+06	2.00E-03	3.20E+03
	1.20E+06	2.00E-03	2.40E+03
	8.00E+05	2.00E-03	1.60E+03
	6.00E+05	2.00E-03	1.20E+03
	4.00E+05	2.00E-03	8.00E+02

Duration constant, P Varies			
	Peak Pressure (Pa)	Positive Phase Duration (s)	Positive Phase Impulse (Pas)
Triangle	1.20E+06	4.00E-03	2.40E+03
	9.60E+05	4.00E-03	1.92E+03
	7.20E+05	4.00E-03	1.44E+03
	4.80E+05	4.00E-03	9.60E+02
	2.40E+05	4.00E-03	4.80E+02
Square	1.20E+06	4.00E-03	4.80E+03
	9.60E+05	4.00E-03	3.84E+03
	7.20E+05	4.00E-03	2.88E+03
	4.80E+05	4.00E-03	1.92E+03
	2.40E+05	4.00E-03	9.60E+02

Duration constant, P Varies (Long Duration)			
	Peak Pressure (Pa)	Positive Phase Duration (s)	Positive Phase Impulse (Pas)
Triangle	9.60E+05	8.00E-03	3.84E+03
	7.20E+05	8.00E-03	2.88E+03
	4.80E+05	8.00E-03	1.92E+03
	2.40E+05	8.00E-03	9.60E+02
	1.20E+05	8.00E-03	4.80E+02
Square	9.60E+05	8.00E-03	7.68E+03
	7.20E+05	8.00E-03	5.76E+03
	4.80E+05	8.00E-03	3.84E+03
	2.40E+05	8.00E-03	1.92E+03
	1.20E+05	8.00E-03	9.60E+02

Duration constant, P Varies (Long Duration)			
	Peak Pressure (Pa)	Positive Phase Duration (s)	Positive Phase Impulse (Pas)
Triangle	7.20E+05	1.20E-02	4.32E+03
Square	7.20E+05	1.20E-02	8.64E+03

The peak pressure and duration values selected were based on values from the LD50 UVa curves. Using a chosen duration value (or peak pressure value), the corresponding peak pressure value (or duration value) along the LD50 curve was selected. Values for pressure were then increased and decreased by varying amounts to provide a range of inputs for pressure and duration. Several simulations were required in order to cover a wide range of injury and to ensure that the assumptions made from this study were valid and not just based on a few points or findings.

4.3 Results/Discussion

The injury sustained to the torso was calculated for each of the numerical simulations. The injury was assessed by examining the maximum dynamic pressure observed in each of the lung elements, as discussed in Chapter 3. Contours of lung damage were plotted to visualize the injury. Elements that experienced high peak transient pressures were assigned a higher injury score as compared to elements that experienced low-pressure levels. The injury score was subdivided into five injury levels; these levels correspond to a pressure interval. The injury levels and corresponding pressures were:

i. None (less than 60KPa)
ii. Trace (60 to 100KPa)
iii. Slight (100 to 140KPa)
iv. Moderate (140 to 240KPa)
v. Severe (greater than 240 to 140KPa).

Examination of the contours for each of the simulations showed that the typical maximum lung damage occurs near corners and areas where there are sharp radii (where the waves are

focused). These locations were along the front lobes of the lung and the areas that were in contact between the ribcage and intercostals tissue. A contour plot of typical damage predicted by this model is shown in Figure 71 along with the areas that result in the most severe damage.

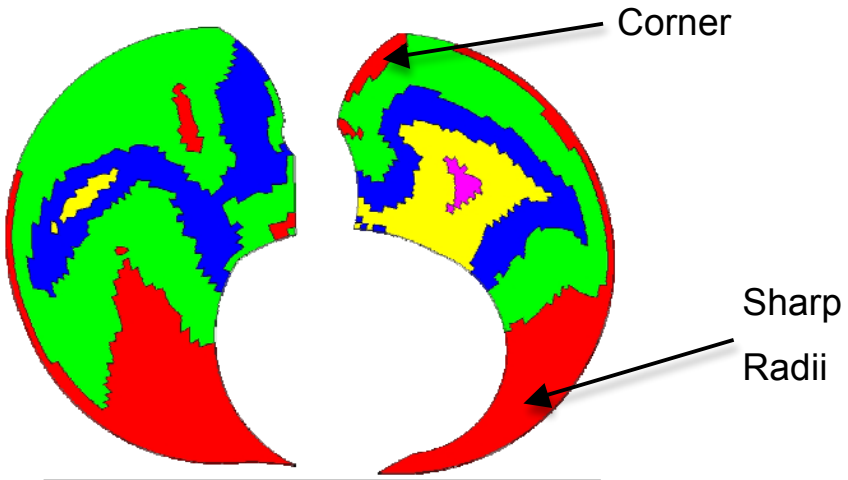

	Severe (Part 117)	>240 kPa
	Moderate (Part 116)	140-240 kPa
	Slight (Part 115)	100-140 kPa
	Trace (Part 114)	60-100 kPa
	None (Part 113)	<60 kPa

Figure 71: Typical damage level contour observed in the lung

The numerical model of the torso allowed for stress and pressure waves to be tracked throughout the organs and components of the torso. As the blast wave came in contact with the torso, the high pressure wave transmitted into the body and in turn transmitted stress waves into the lung. The stress waves were observed during the simulation and higher damage was also observed in locations where the stress waves collided and impacted inside the lung. A plot of the pressure waves inside the lung is superimposed in Figure 72. In this

image the areas of high stress are shown along the rib cage and are traveling from anterior to posterior along the rib cage. The waves were confined mainly in the lungs and followed the rib cage.

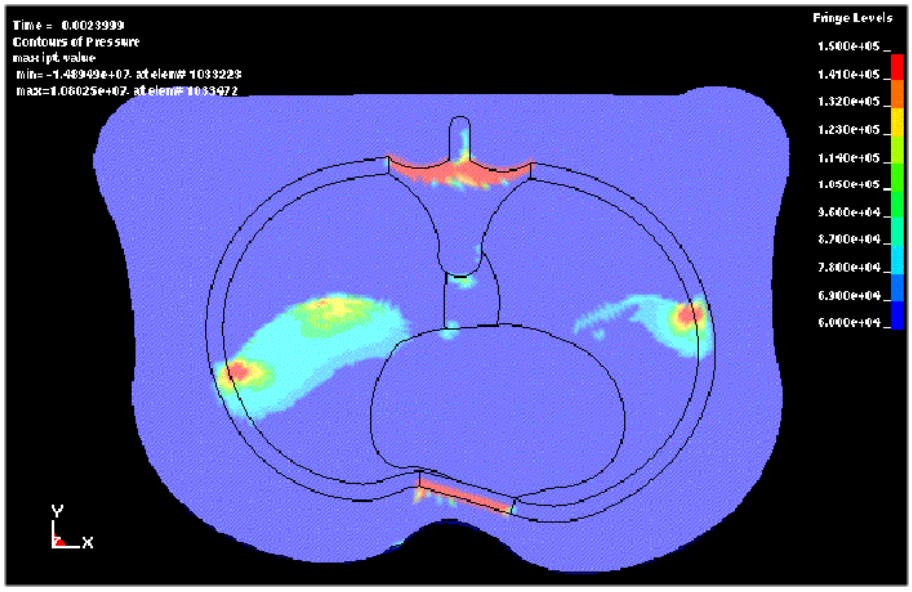

Figure 72: Stress waves inside the lung

The results for the triangular wave form and the square waveform were compared. This was done to correlate the predicted injury level with the effect of duration, pressure, impulse and the shape of the blast wave.

4.3.1 Effect of Varying Pressure

The first phase of the study involved holding the duration constant and varying the pressure of the input blast wave. This procedure was repeated for six different durations, 0.2, 0.8, 2, 4, 8, and 12ms. Six durations were used with five different incident pressure values, for a

total of 30 simulations. Simulations were performed for the triangular wave form and similarly for the rectangular waveform. For this study, resultant injury levels recorded from both the triangular and square wave form behaved similarly. In all cases for holding the duration constant, increasing injury was predicted as the pressure increased. This also in turn increased the impulse of the blast wave. For the same duration level, the injury decreased as the pressure decreased, and as pressure increased the injury increased.

Figure 73 shows the result that the increase in pressure has on the percentage of injury at the five injury levels: none(1), trace(2), slight(3), moderate(4) and severe(5). These results are from a calculation involving a square blast wave form with a duration of 4 ms. As the peak overpressure was increased the blast lung injury increased from predominantly no injury to severe injury.

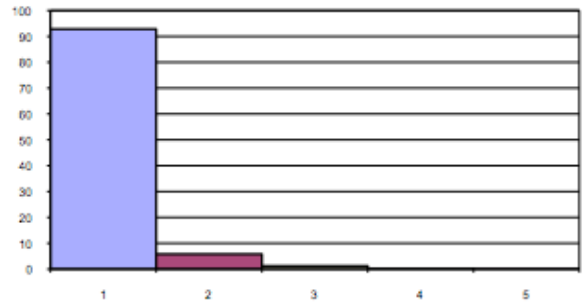

a.) P = 2.4e5 Pa

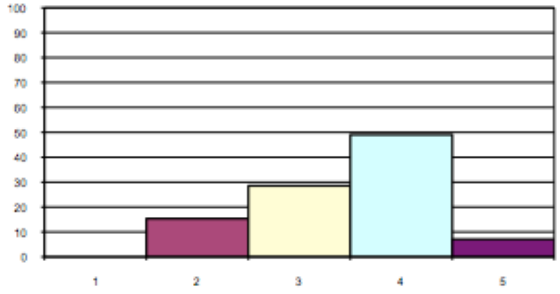

b.) P = 4.8e5 Pa

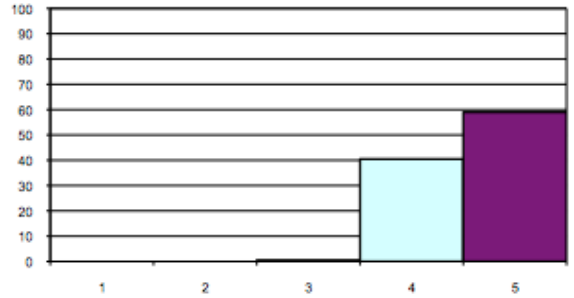

c.) P = 7.2e5 Pa

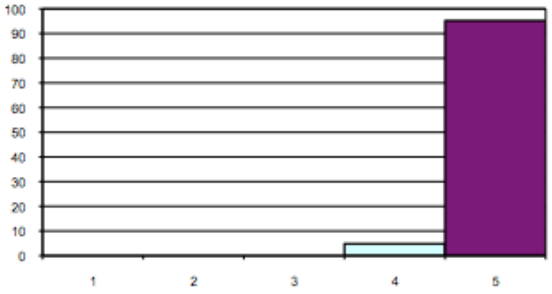

d.) P = 9.6e5 Pa

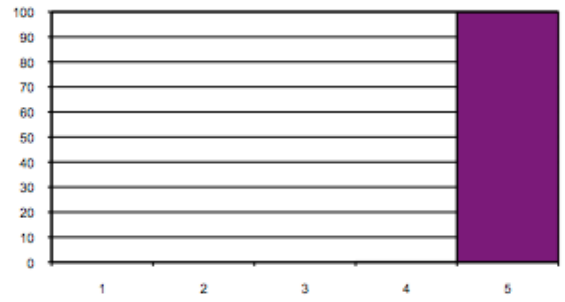

e.) P = 12.0e5 Pa

Legend:

1 = No Injury

2 = Trace Injury

3 = Slight Injury

4 = Moderate Injury

5 = Severe Injury

Figure 73: Increasing percentage of injury levels, Duration=4ms, pressure varies, square waveform

The probability of a severe injury level for a triangular waveform with a duration of 4ms and a peak pressure value from 2.4e5 Pa to 12e5 Pa is shown in Figure 74. As the duration is held constant the figure shows that increasing pressure increases the expected injury.

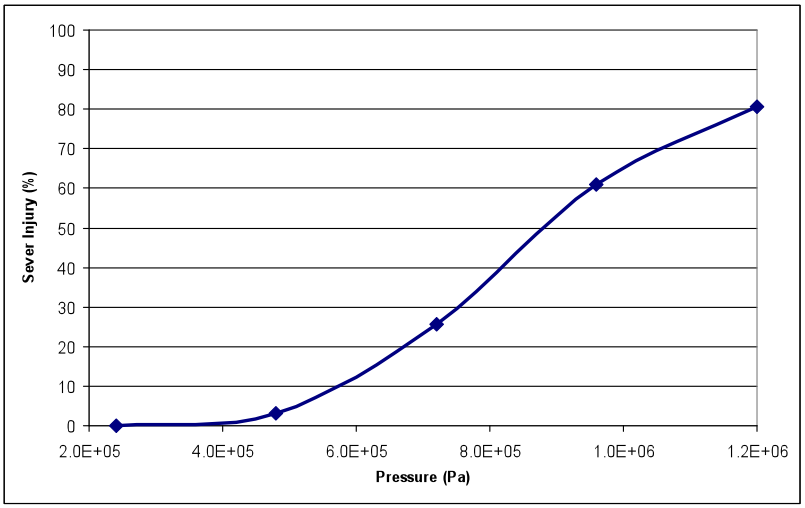

Figure 74: Duration is constant at 4ms, peak pressure varies from 2.4e5 Pa to 12e5 Pa.

4.3.2 Effect of Varying Duration

For both the triangular waveform and square waveform a study was performed where the pressure was held constant and the positive phase duration of the blast source varied. Varying the peak incident pressure and the duration causes a change in the impulse. Both the triangular waveform and square waveform exhibited similar responses. For a given constant pressure value, as the duration increased the injury level increased; the impulse also increased as the duration was increased. The results from the triangular waveform were compared with that of the square waveform. It was concluded that for short durations the injury level recorded was very similar as long as the impulse for the two waveforms was equal. For longer durations there was no direct correlation between the impulse and the resultant injury. A plot of the injury obtained using a triangular waveform is shown in Figure 75. In this simulation the incident pressure of the blast source was held constant at 2.4e6Pa

and the durations used were 0.05, 0.1, 0.2, 0.4 and 0.8ms. This plot shows that as the duration increases the injury varies from essentially no injury for 0.05ms to a moderate/severe level for 0.8ms. The results obtained from a square waveform are shown in Figure 76. The injury obtained from the square waveform involving a duration of 0.8 ms resulted in approximately 100% severe injury to the entire lung. In the following images the vertical axis is the percentage of injury obtained and the horizontal axis represents the injury level classification.

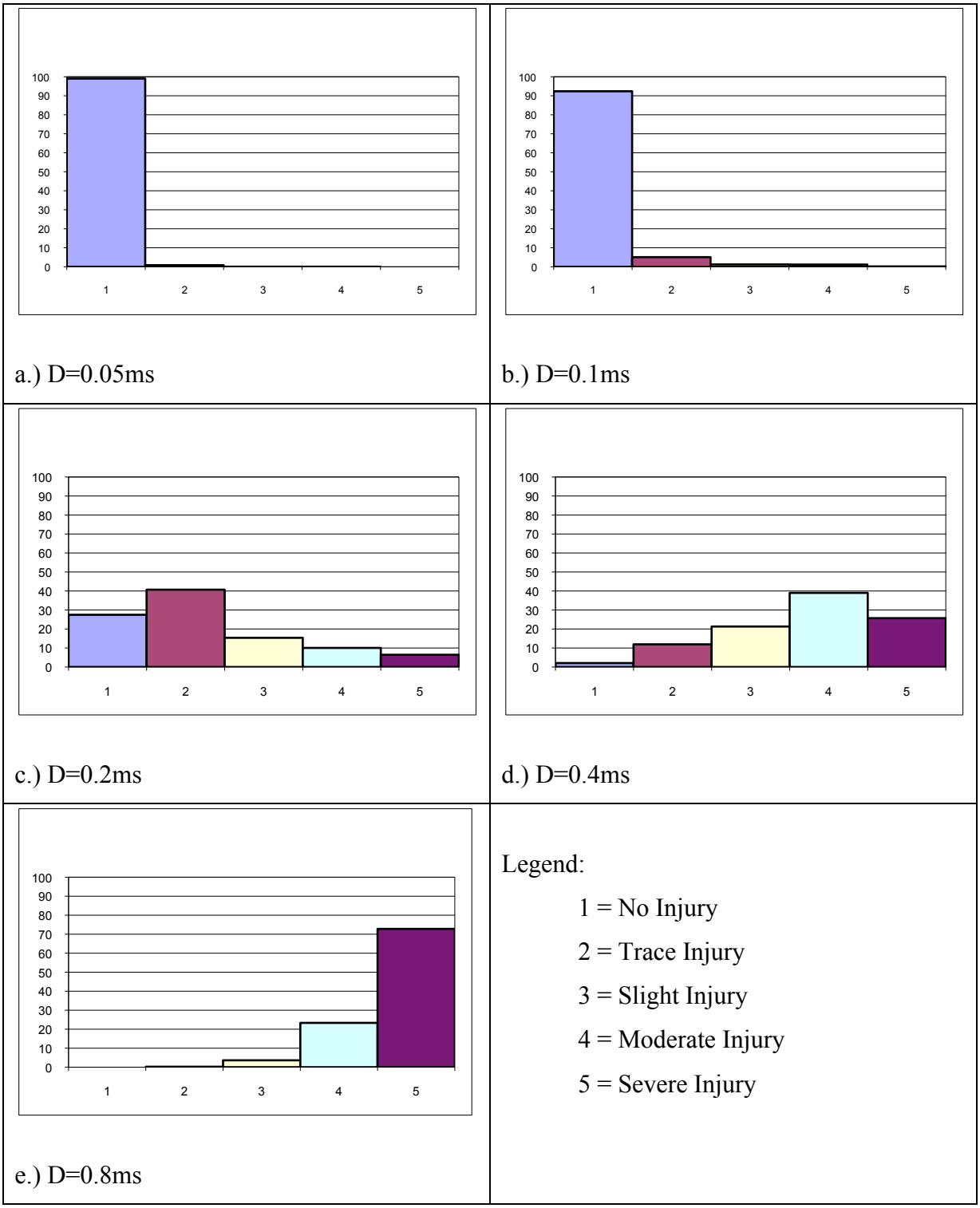

Figure 75: Triangular waveform injury plot for P=2.4e6Pa, duration varies from .05ms to .8ms

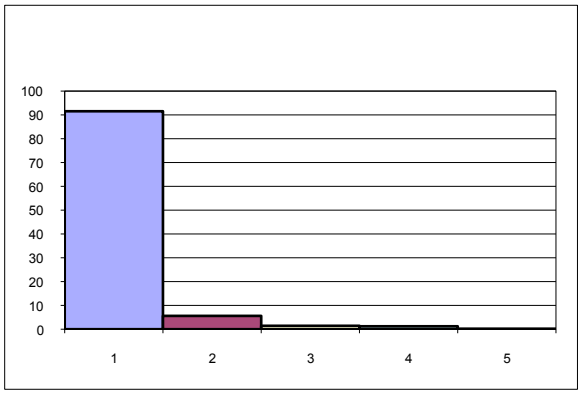

a.) D=0.05ms

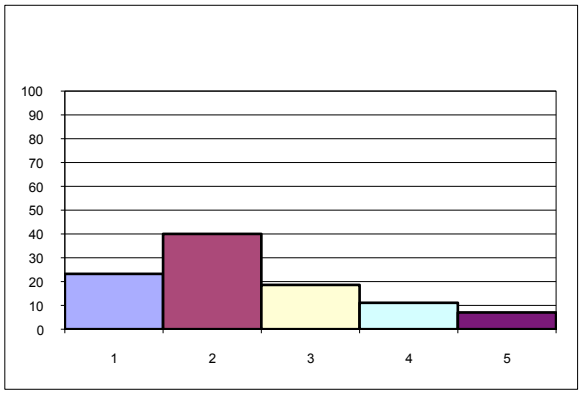

b.) D=0.1ms

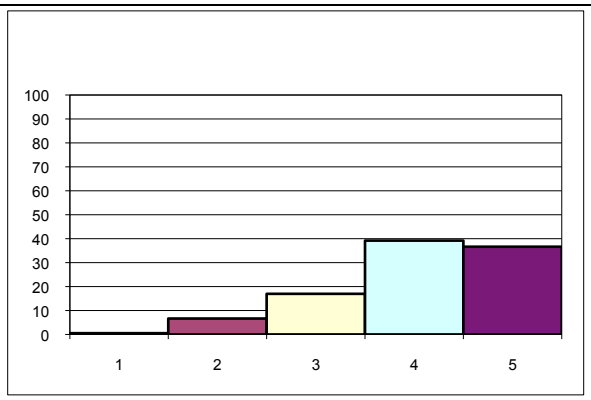

c.) D=0.2ms

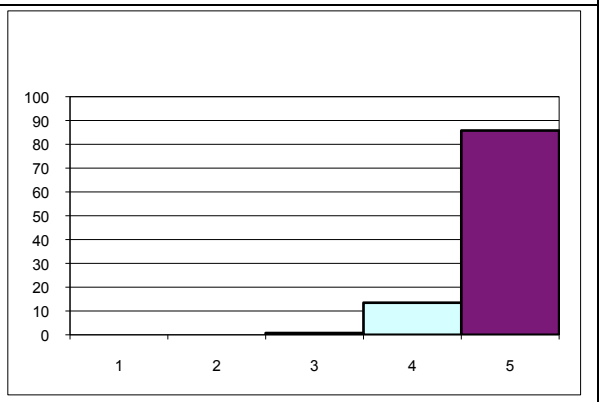

d.) D=0.4ms

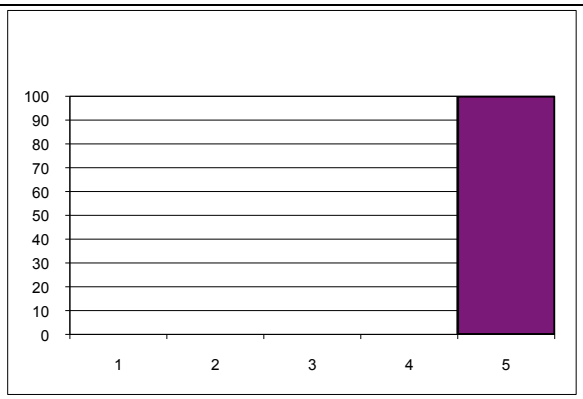

e.) D=0.8ms

Legend:

1 = No Injury

2 = Trace Injury

3 = Slight Injury

4 = Moderate Injury

5 = Severe Injury

Figure 76: Square waveform injury plot for P=2.4e6PA, duration varies from .05ms to .8ms

Figure 77 shows the result of holding the peak pressure of the blast load constant while varying the blast load duration. The results shown in this figure are the results from calculations using a square loading wave with a peak overpressure of 2.4e6 Pa. A similar trend was observed in both waveform cases; triangular and square. As the blast wave duration increased the level of severe injury increased. The increase in severe injury percentage however is not linear.

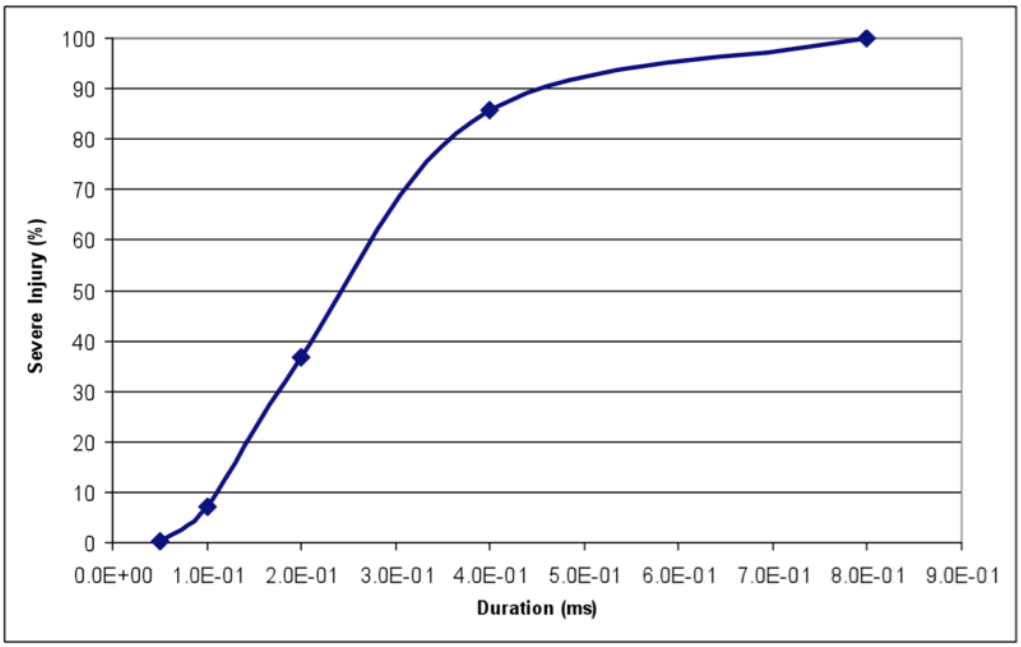

Figure 77: Effect of severe injury obtained by increasing duration and holding pressure constant

4.3.3 Effect of Impulse on Predicting Blast Injury

The impulse values from the blast waves were examined to determine if the impulse was the main factor in predicting blast lung injury. Short (<1 ms), medium(1 ms < 8 ms) and long (>8 ms) durations were compared to investigate the effect of impulse.

For the short duration scenarios, blast loading curves with a pressure impulse of 480Pas were compared. Durations of 0.2 and 0.8ms were used to provide the blast loading curve with the same impulse. Figure 78 shows the percentage of injury predicted for the five injury levels from two calculations with a blast loading impulse of 480Pas. The predicted injury results from these calculations are virtually identical even though the duration of the blast wave was different. This indicates that for short durations the impulse is dominant in predicting injury.

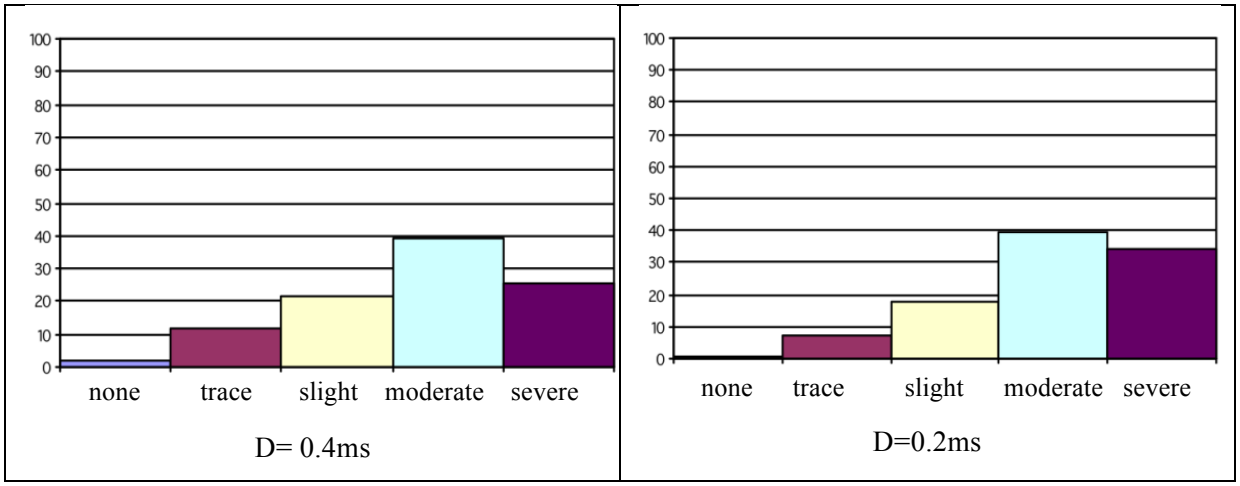

Figure 78: Injury level comparison from calculations with a blast load impulse of 480 Pas (short durations)

Medium length durations (1 ms < 8 ms) were also used to further investigate the effect of blast impulse. Simulations with durations of 2ms and 4ms and a blast impulse of 480Pas and durations of 4ms and 8ms and a blast duration of 960ms were performed. The results of these calculations are shown in Figure 79. The predicted injury is different between these cases, indicating that for longer-medium durations although the impulse is the same the predicted injury is different (this was not the case for short durations)

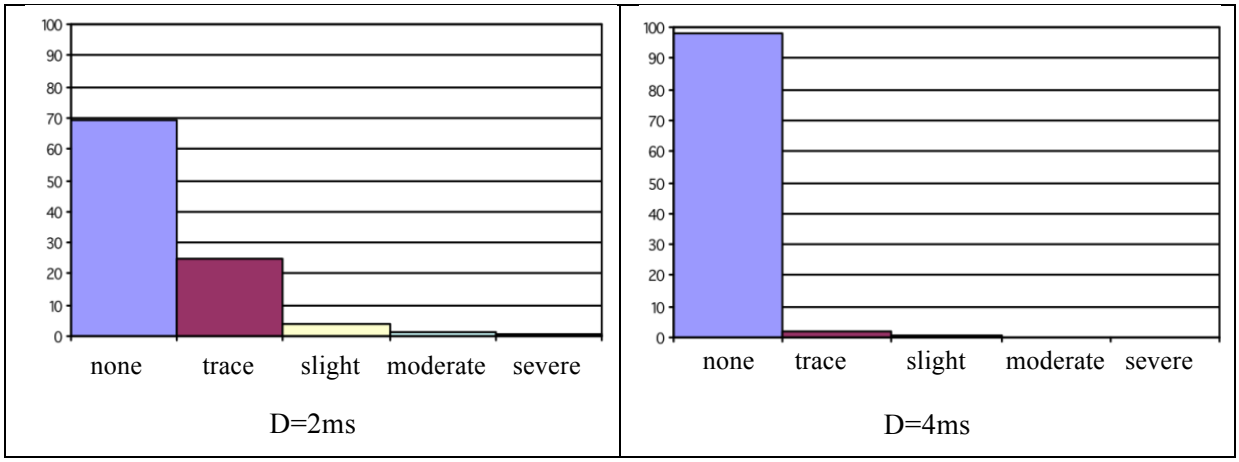

a.) Medium Durations: Impulse 480Pas

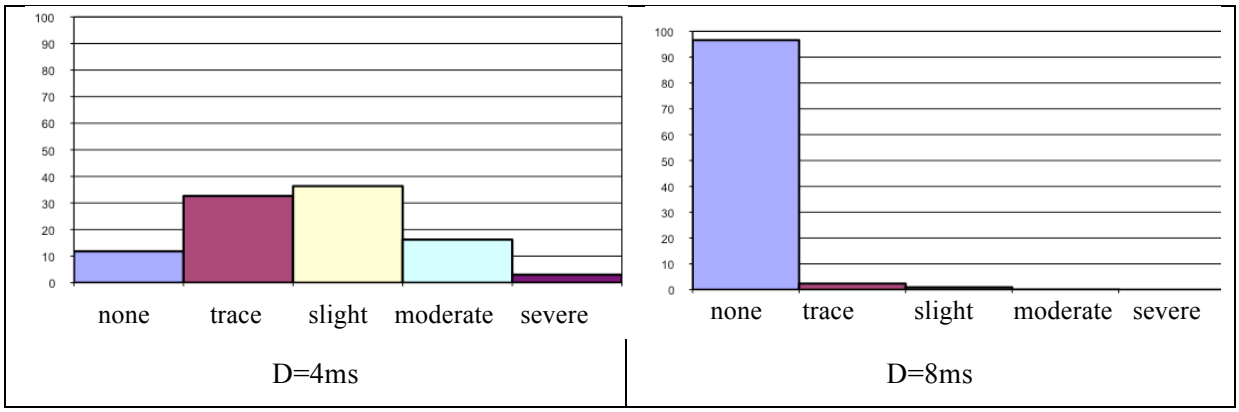

b.) Medium Durations: Impulse 960Pas

Figure 79: Injury level comparison from calculations with the same blast impulse (medium durations)

The results shown in Figure 78 and Figure 79 show that the injury predicted is not similar for all of the test cases; therefore knowing the blast wave impulse alone is not enough to accurately predict blast lung injury. The results however showed that for small duration, (durations under 1ms) that the injury predicted correlates well with the blast load impulse. When comparing the case of the 0.2 ms and 0.4 ms scenarios, a very similar amount of injury is predicted. Each of these cases predict approximately 10% of trace injury, 30% of slight injury, 40% of moderate, injury and 20% of severe injury. In contrast to this the test cases with longer durations predict 0% of severe injury. Comparing the 2 ms and the 4 ms cases and the 4ms and 8ms cases showed that the injury is deviating between these two cases. For waves of durations greater than 1 ms, there was no direct correlation between impulse and predicted injury. Injury only correlates with impulse for short durations.

4.3.4 Effect of Wave Form - Short Durations

It was shown that the predicted injury is related to impulse for blast loading conditions with short durations, for a given blast wave. In cases with these durations, the results were impulse dominant; the impulse was the main factor in predicting blast lung injury. To ensure that the injury obtained for short durations depended on impulse and not the shape of the blast loading wave, the results from the triangular blast load were compared against those of the square wave. The percentage of severe injury predicted from four test cases were compared, at a given impulse with a duration less than 1 ms. The results are shown in Figure 80.

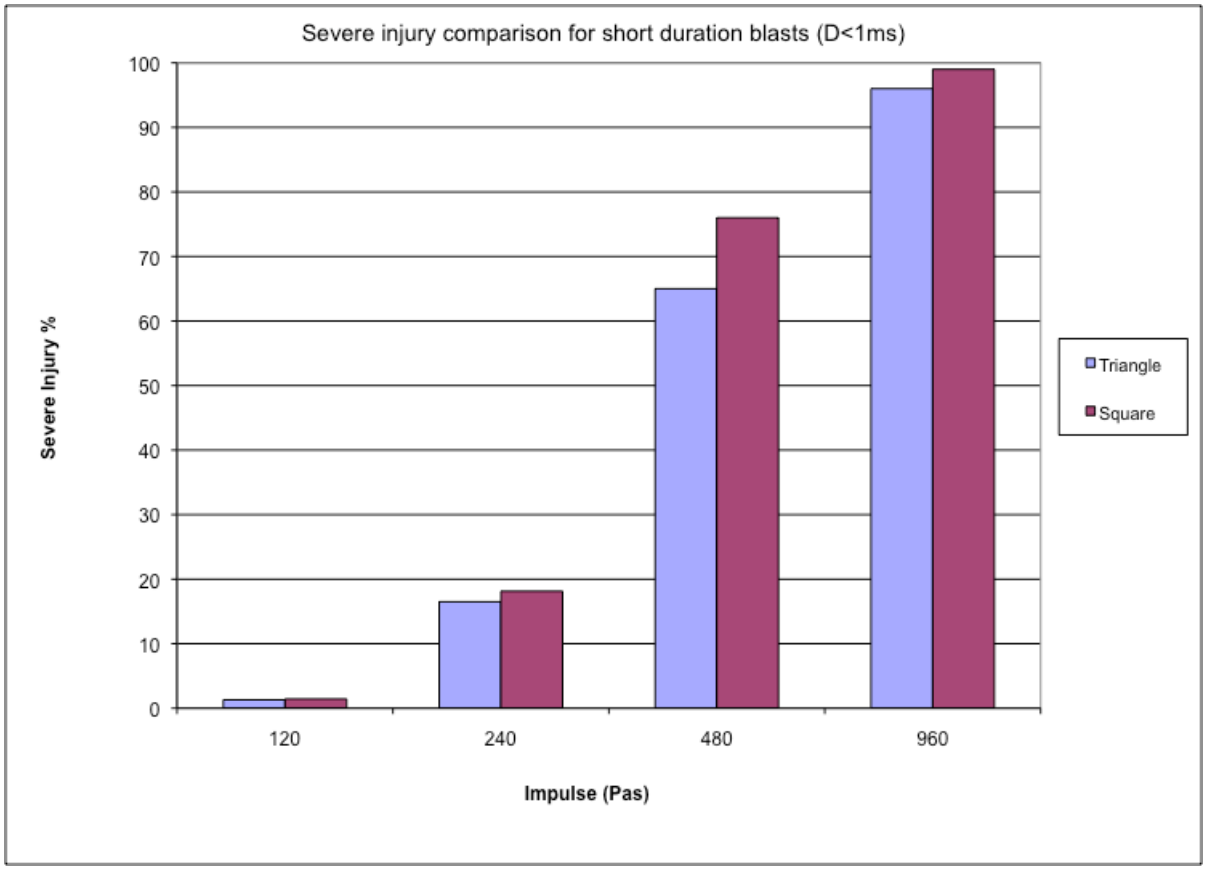

Figure 80: Severe injury comparison for short duration blasts, where duration is less than 1 ms

Comparing these results confirmed that the impulse was dominant in predicting injury for durations less than 1 ms. The results show that equivalent impulse produced similar injury, regardless of the waveform shape.

4.3.5 Effect of Wave Form - Long Durations

For longer durations it was observed that pressure is dominant in predicting injury, this is agreement with the literature [Bowen, 1968; Bass 2006]. The results comparing the

percentage of severe injury from a square blast loading waveforms is shown in Figure 81. The results were obtained by holding the pressure constant at $7.2x10^5$ Pa and varying the duration from 8ms to 12 ms. For both the square and triangular wave there was an insignificant change in injury from 8ms to 12ms when holding the pressure constant; indicating that the pressure was the main factor in predicting injury. These long durations are typically only seen in shock tube experiments and nuclear explosions.

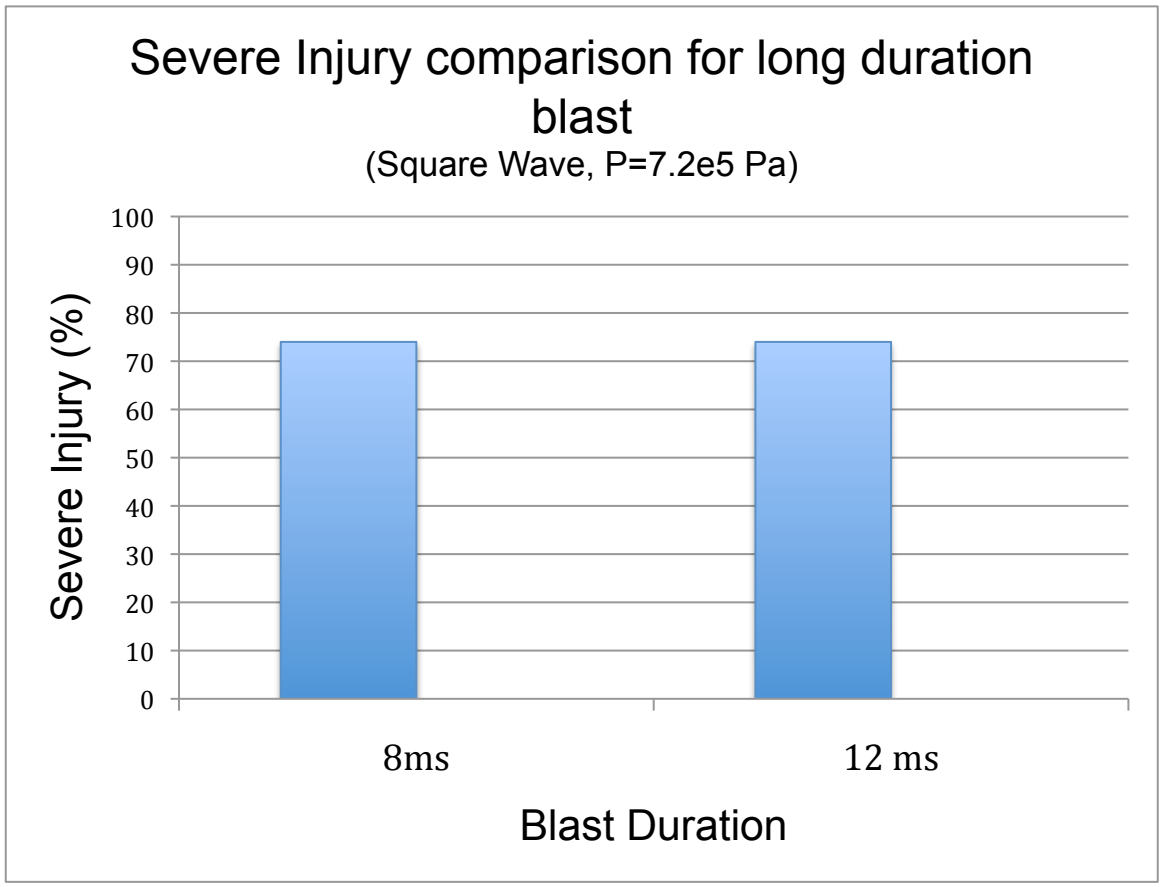

Figure 81: Severe injury comparison for long duration blasts; peak pressure = 7.2e5 Pa

4.4 Comparison with Injury Tolerance Curves

The results of this study compare well with the existing blast injury literature. Examining the classic Bowen curves which relate positive phase blast duration to peak incident overpressure a similar trend is found. On the Bowen chart at durations greater than 10ms to 20ms the shape of the curve tends to become a straight horizontal line. Even as the duration increases the predicted injury level remains constant as the pressure remains constant. This suggests that the pressure is the determinant factor in predicting injury for long durations. Long durations are defined as durations greater than 10ms. [Rafaels 2008]This study focused on short durations and only a few calculations were performed above 10 ms. Calculations using longer durations were not performed as these long durations are typically only observed in nuclear type blasts and fall beyond the scope of this study; this study focuses on durations of small charges. It is important to note that the original Bowen curves have been updated however the latest revisions of the curves also exhibit this similar trend where the shape of the curve approaches horizontal for large durations. Figure 82 shows the original Bowen curves along with the Revised Bowen curves for a blast along the long axis of the body perpendicular to the blast wave. The kink and horizontal portion of the curve where injury is dependant on pressure alone is visible.

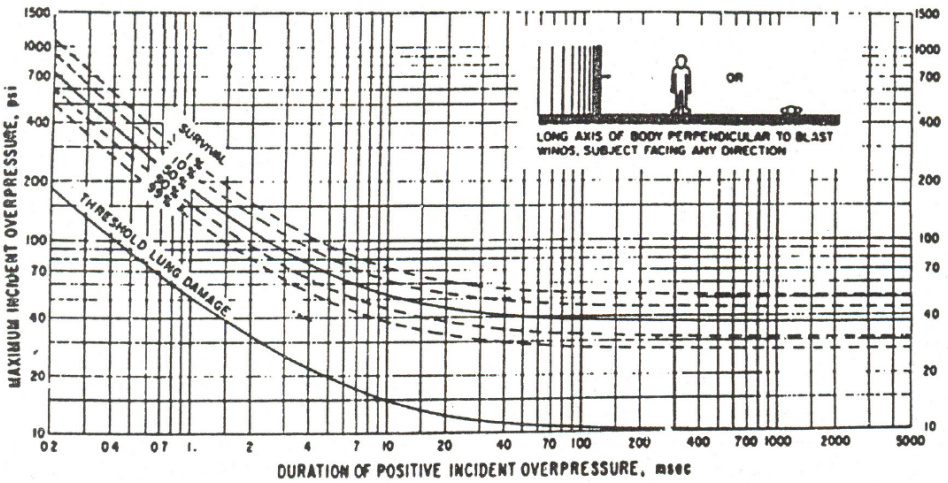

a.) Original Bowen Curves [1968]

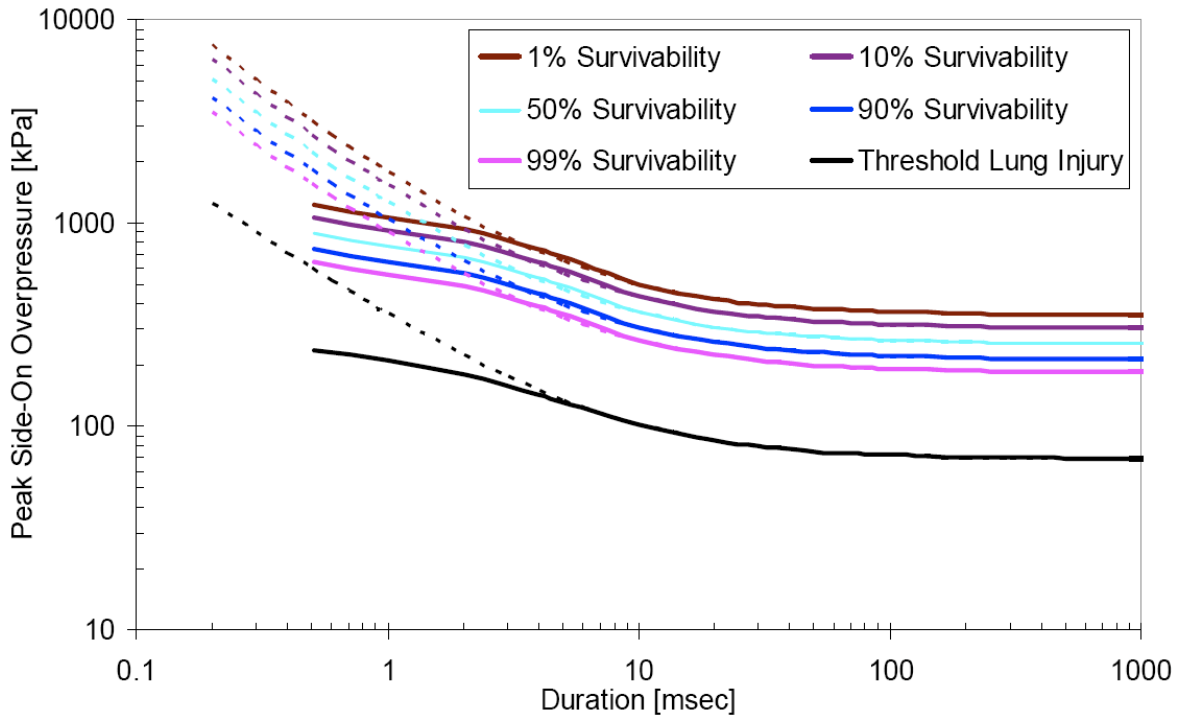

b.) UVa Bowen curves (dashed lines show Original)

Figure 82: Original and Revised Bowen curve for a human in the free field, standing perpendicular to the direction of propagation of the blast wave. [adapted from Bowen, 1968 and Bass, 2005].

A relation pointed out years ago by Schardin indicates that the mammalian response to air blast is mainly depended on overpressure impulse if the durations are short. The mammalian response is dependent of overpressure if the durations are long. [Bowen, 1968] The Waterloo numerical model was able to capture both of these observations.

Chapter 5
Body Orientation Effects

5.1 Introduction

To investigate the effect of the orientation of the thorax on predicted injury a study was conducted in which the thoracic models were orientated differently so the blast would impact the body from 3 orientations: parallel, at an angle of 45 degrees and perpendicular to the blast flow. The orientations were achieved by rotating the body at 0, 45 and 90 degrees on the ALE mesh. Tests were performed using the sheep thoracic model, the human thoracic model, and a blast test device for comparison.

5.2 Individual Lung Damage

The orientation effect was studied to investigate the damage to the individual lungs. It was hypothesized that, if the body is orientated in a way that one lung was closer to the blast wave and the other was further from the blast wave, that the lung closest to the blast wave would experience the most damage. The injury tolerance between a man and a sheep was found to be similar. [Bowen, 1968] However examining the anatomy of the sheep and the human torso it is clear that the position of the lungs and the size of the thorax are not consistent. Figure 53 and Figure 54 show the comparison between the sheep and human thorax anatomy. While human thorax is in a position where the front of the chest is parallel to the blast wave the width of the chest is greater than the depth and the two lungs are oriented left to right. When the sheep has the longer portion of the body parallel to the blast wave, the lungs are oriented front to back. In these orientations the human thorax experienced similar injury in each of the lungs, whereas the sheep thorax experienced greater injury in the lung closest to the blast wave. The relative size of the individual lungs in the sheep and human are also somewhat different. In the case of the sheep the left lung occupies

38.1% and the right lung occupies 61.8% of the lung size. The human torso has a left lung that occupies 42.1% and the right lung occupies 57.9%. [Greer, 2006]

Figure 83 shows a result of the stress contours within the lung of a sheep subjected to a blast loading from the left. [Stuhmiller, 1991] The figure shows that the lung closest to the blast wave experiences the highest stresses and this is consistent with experimental findings.

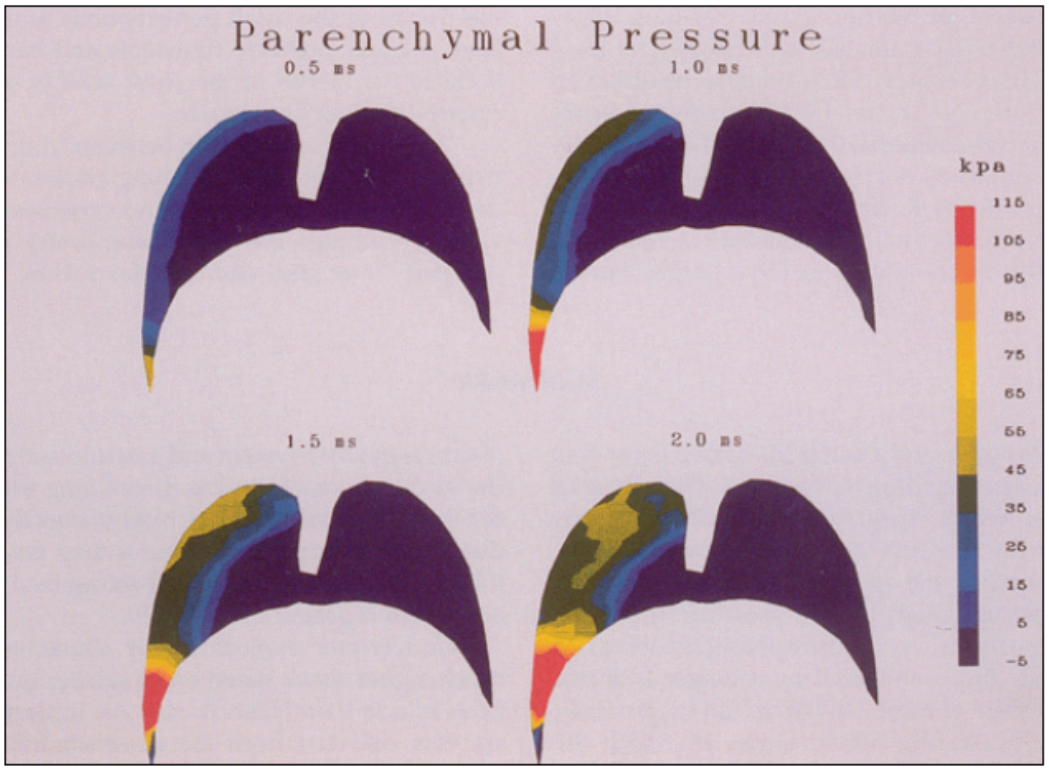

Figure 83: Stress contours within the lung of a sheep, subjected to blast loading from the left [Stuhmiller, 1991]

5.3 Blast Loading

In order to evaluate the model and determine the effect blast waves have on the finite element model a number of free-field calculations were performed. The model has been compared to the injury prediction methods based on the revised Bowen curves and the Axelsson model [Greer, 2006] For each of the models, BTD, sheep and thorax and each of the three orientations 0, 45 and 90 degrees, 8 calculations were performed; a total of 72 simulations.

The calculations that were performed for each torso model (3 different orientations per model) were selected to ensure that blast waves of varying pressures and durations were evaluated. From the study mentioned above it was determined that there are three significant zones were the properties of the blast wave influence the predicted blast lung injury. Therefore the blast loads selected for the orientation study involved short durations (0.5ms), long durations(10ms) and a duration of 5ms. To ensure that a wide range of injury was covered blast loading input was selected for threshold lung damage, LD1 and LD50.

Using the UVa curves, the pressure and duration were selected for the eight blast loading conditions of interest. The blast loading points are shown in Figure 84; the points are displayed as stars in the figure.

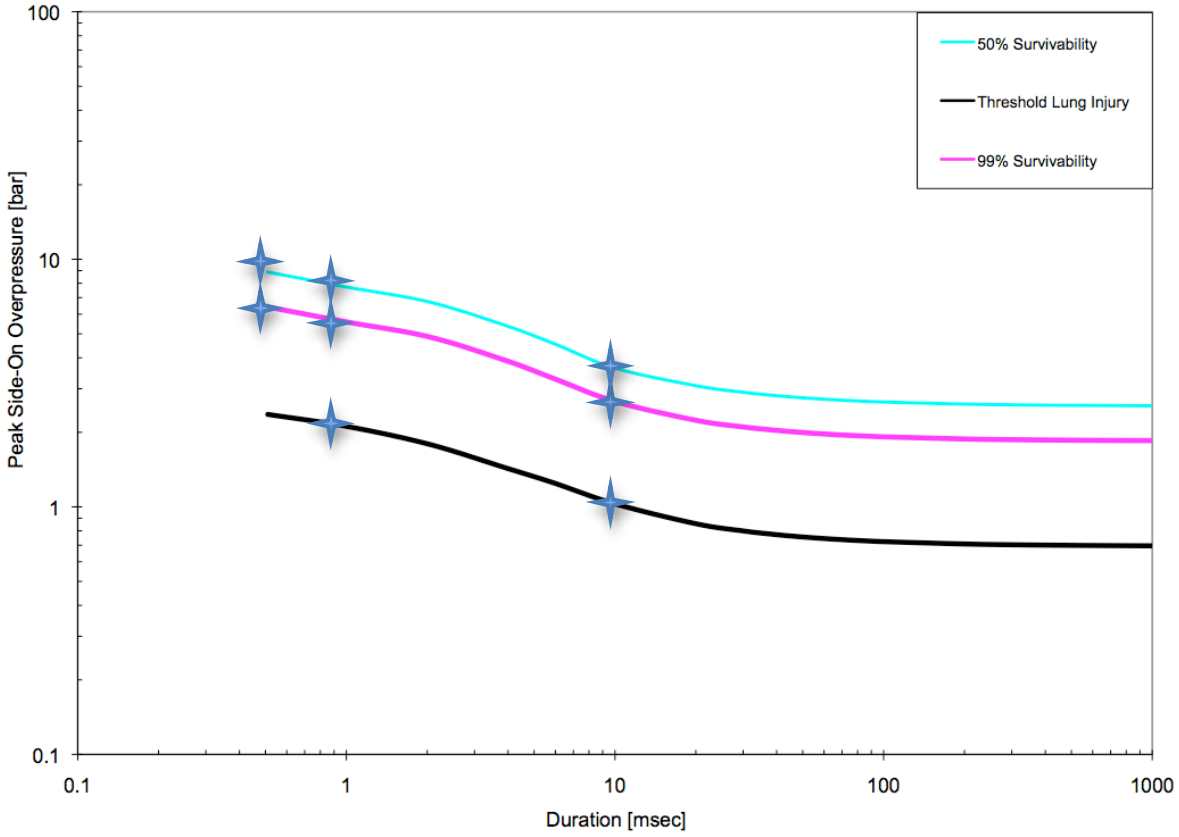

Figure 84: Select blast loading points for Orientation Study

The overpressure and duration values selected from the UVa curves that were used in the calculations for examining the injury based on the body orientation and the injury occurring in each individual lung are shown in Table 5.

Table 5: Pressure and Duration values for injury prediction based on orientation

Injury Severity	Duration (msec)	Overpressure (kPa)
Threshold	1.0	210
	5.0	130
LD 1	0.5	640
	1.0	560
	5.0	350
LD 50	0.5	890
	1.0	770
	5.0	500

In order to obtain the pressure and duration values at the thorax model that corresponded to the locations on the Bowen curve an appropriate blast loading curve was required. A series of calculations using Conwep [Hyde, 1988] and Chinook [Martec, 2006] were performed to determine the blast flow field at the boundary. From these results the Friedlander blast load was created and applied to the boundary condition of the LS-Dyna ALE mesh. An LS-Dyna calculation was then performed to ensure that the pressure and duration values at the distance of the front of the thorax would match those identified on the revised Bowen curves.

5.4 Blast Test Device and Injury 8.1 Model

A series of simulations were performed with a BTD in the flow field to serve as a reference point and to discover if the BTD can predict injury based on orientation. The four gauges on the outside of the BTD recorded the pressure time histories resulting from the blast wave. These four pressure time histories were then used as input to the Injury 8.1 software application to predict injury. Along with the pressures on the thorax, the mass, species type and atmospheric pressure were used as input. For the simulations of the BTD a human with a

mass of a70kg and an atmospheric pressure of 1 bar were used. The exact algorithm and process of predicting injury based on pressure time history is proprietary, however it is based on relating injury to normalized work of the thorax by Stuhmiller. [Stuhmiller, 1988]

Injury 8.1 does not explicitly claim to be able to predict orientation effects with the software and pressure measurements from a BTD. BTDs are used in experiments where the incoming direction of the blast wave may not be know ahead of time; making it difficult to accurately align the front sensor of the BTD perpendicular with the blast wave. This study was performed to provide insight to the applicability of the BTD and to investigate whether it is a tool capable of measuring body orientation effects.

Figure 85, Figure 86 and Figure 87 show the predicted injury results from three LD50 calculations. These calculations were performed using a Friedlander wave with a duration of 1ms, a peak overpressure of 770kPa and a decay constant (b) of 3.3. Figure 85 shows the injury prediction level for the 5 levels of injury as determined by the Injury 8.1 software. These results were representative of the subjecting facing the blast wave at a angle of 0 degrees; an orientation of the body perpendicular to the blast. In the figure the blast will be travelling from bottom to top. Figure 86 represents the body being rotated 45 degrees from the wave. Figure 87 represents the body being rotated 90 degrees from the blast wave; this represents the blast hitting the right side of the body.

Similar simulations were performed for other LD50, LD1 and Threshold injury curves; the same trend and findings were observed in these simulations. Only the results from one of the eight, blast loading simulations are shown in the following figures, as the results from the other blast loading waves provided similar trends.

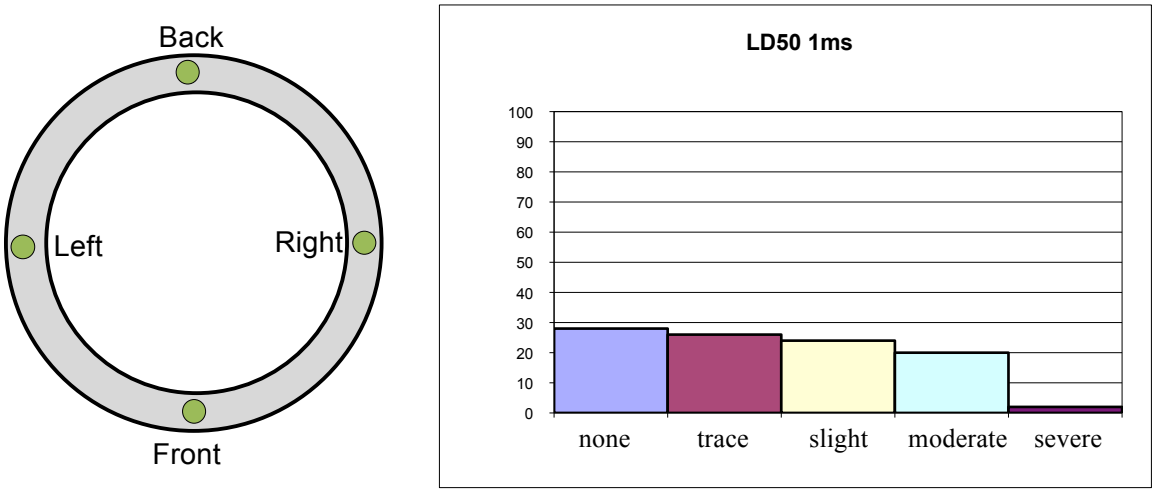

Figure 85: BTD 0 degree rotation – LD 50, 1 ms Blast Duration

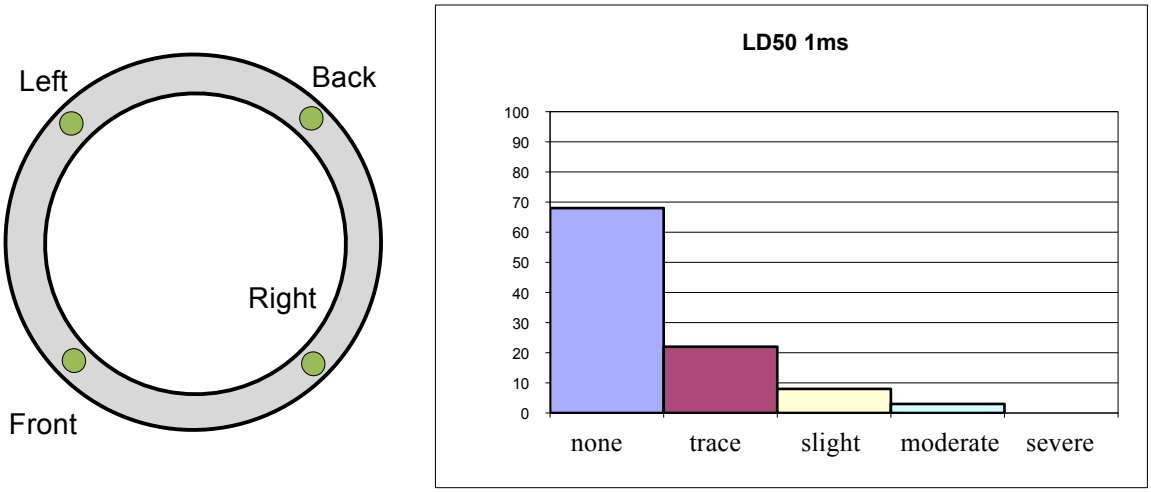

Figure 86: BTD 45 degree rotation – LD 50, 1 ms Blast Duration

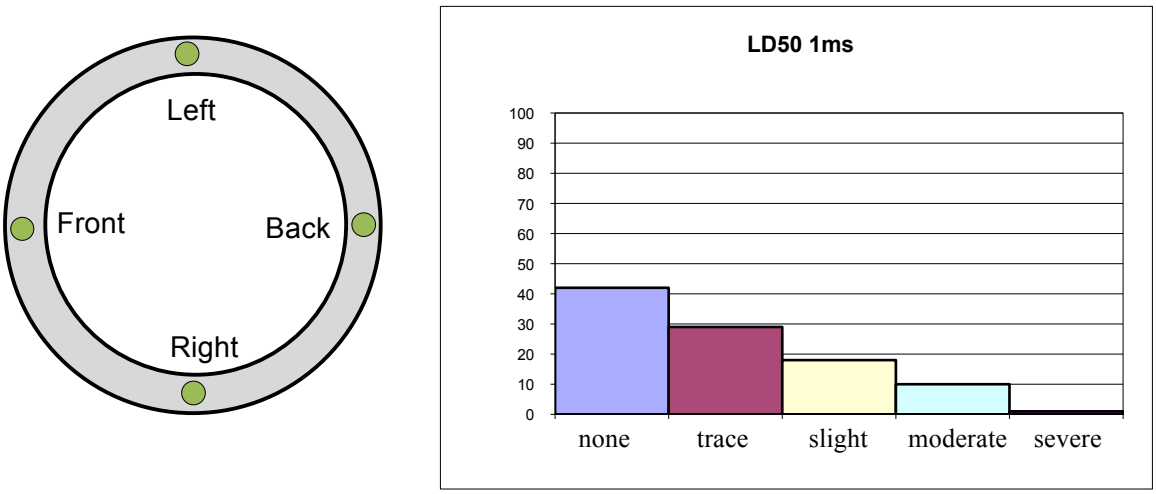

Figure 87: BTD 90 degree rotation – LD 50, 1 ms Blast Duration

The above Figures show that as the BTD is orientated differently the predicted blast lung injury predicted changes. It is important to note that although the orientation changes the distance from the blast loading elements to the closest edge of the BTD remained constant for all simulations. Examining the results from Figure 85 and Figure 87 shows that Injury 8.1 predicts a lower level of injury for the case where the body is oriented 90 degrees from the from the blast. This suggests that if a human is hit by a blast wave, side on they will experience less injury as opposed to being hit with the blast wave directly on the front of the body. Comparing the results from Figure 85, Figure 86 and Figure 87 indicates that when the body is oriented at an angle of 45 degrees the predicted blast lung injury is at a minimum. Although it appears that orienting the body at an angle of 45 degrees provides the lowest injury this may not be the case. The reason for this low level of injury as compared to the other orientations is a result of the gauge placements on the BTD. With the BTD at an angle of 45 degrees the 2 gauges located near the front are located at the farthest distance as possible from the initial point of contact between the BTD and the blast wave. The gauges of the BTD were therefore not able to capture and record the highest pressure, as a result of the initial impact and reflection of the incoming blast wave.

When predicting blast lung injury using the Injury 8.1 software model it appears as though the software applies weighting factors to the gauges based on their location. This weighting factor is not documented with the Injury 8.1 software, so the exact algorithm for predicting injury is not known. The most emphasis is placed on the front gauge, followed by the left and right gauges and then the back gauge. It is for this reason that the blast lung injury predicted from the 0 and 90 degree scenarios varies; the pressure loads observed around the BTD are the same for all simulations.

The drop in injury noted at 45 degrees as compared to the 0 and 90 degree should be further investigated. Ideally it is believed that the injury would decrease gradually as the body is rotated, however the simulations show that the injury appears to be at LD50 for the 0 degree case, then it drops substantially for the 45 degree orientation, then increases for the 90 degree orientation. When the BTD model is used, the orientation of the BTD should be considered and if possible the front gauge of the BTD should be placed perpendicular to the flow field. In complex environments the flow field may not be fully know until a CFD simulation is first performed, based on the results from the CFD simulation the BTD should be oriented appropriately to attempt to have the front gauge perpendicular to the main flow. With the significant change in predicted injury based on the orientation the BTD model, a more appropriate model of the human torso could be used for blast injury prediction.

5.5 Sheep Thorax Model

5.5.1 Sheep Model - Injury Outcome Based on Both Lungs

To validate the numerical sheep model and determine if the model was predicting similar injury to the Bowen curves, calculations were performed with the sheep oriented so the long part of the torso was parallel with the blast wave. This orientation was that which was used by Bowen in the original animal study tests. [Bowen, 1968] In this position the torso of the sheep was oriented such that one of the lungs was physically closer to the blast wave. A schematic of this set up is shown in Figure 88.

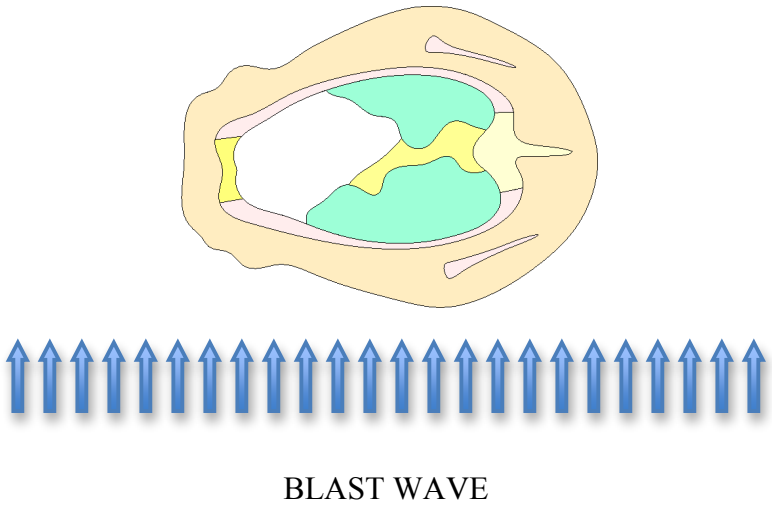

Figure 88: Sheep oriented so the long part of torso is parallel with blast wave

Simulations were performed to investigate how the orientation of the sheep torso affected the predicted injury. As described above, three orientations were used rotating the torso at 0, 45 and 90 degrees to the blast wave. In the 0 degree simulation the right lung was located

closest to the blast wave (shown in Figure 88) and in the 90 degree simulation, both lungs were located approximately the same distance from the blast wave.

The results from the orientation study are shown in Figure 89, Figure 90 and Figure 91. These results are for the LD50 case, with a duration of 1ms. The injury predicted (percentage shown on the vertical axis) by the numerical model is shown in the bar graph, representing the 5 levels of injury (horizontal axis).

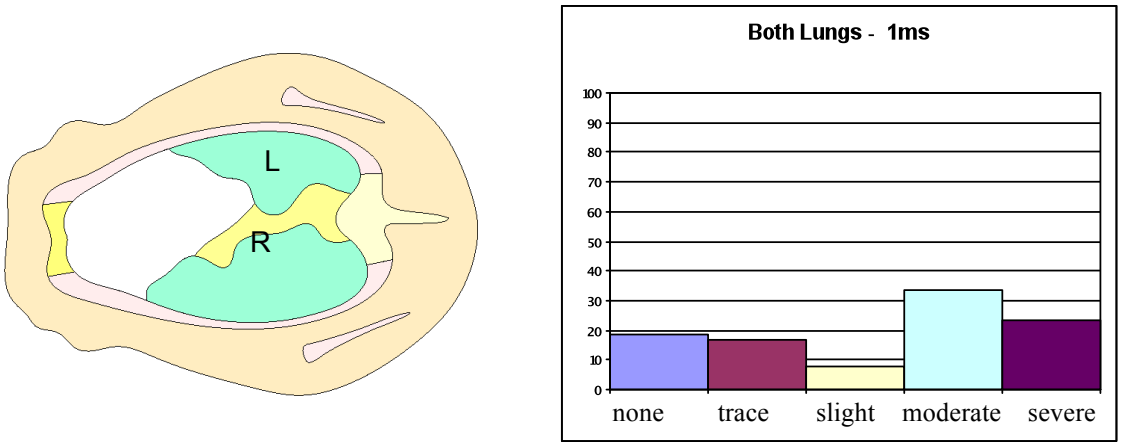

Figure 89: Sheep 0 degree rotation– LD 50, 1 ms Blast Duration (Both Lungs)

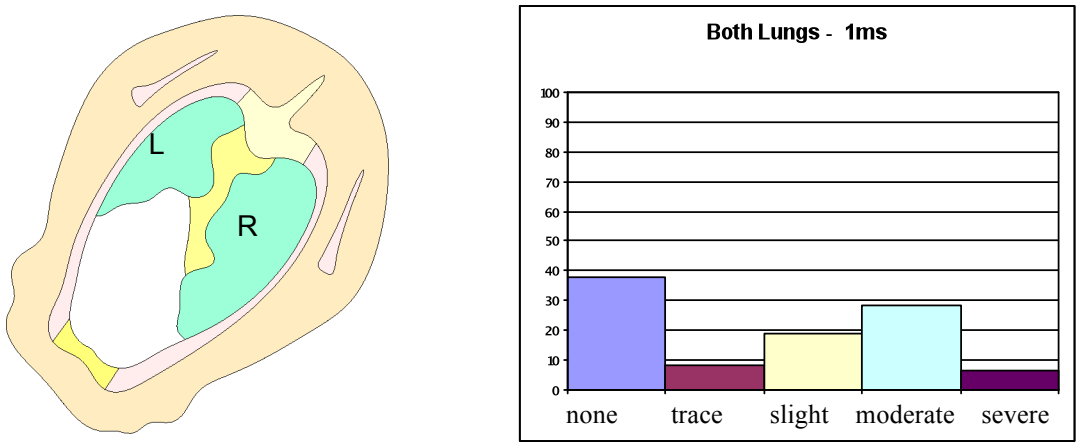

Figure 90: Sheep 45 degree rotation– LD 50, 1 ms Blast Duration (Both Lungs)

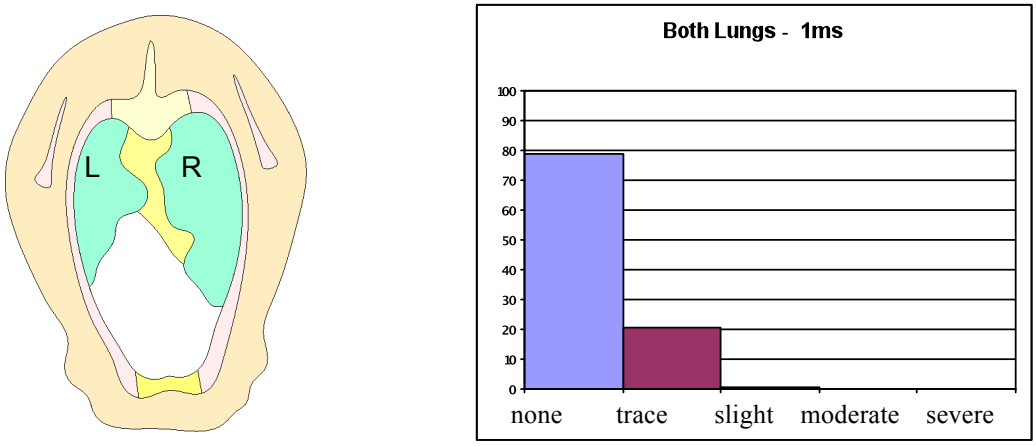

Figure 91: Sheep 90 degree rotation – LD 50, 1 ms Blast Duration (Both Lungs)

The typical results shown in the figures above show that as the sheep torso is rotated from having the long portion of the body of the torso parallel with the blast wave to having the long portion of the body perpendicular to the blast wave the overall predicted injury diminishes.

At an orientation of 0 degrees LD50 is observed, which corresponds to the predictions of the UVa curves and is visible in Figure 89. Comparing the results from the 0 and 45 degree orientation cases, indicated that the percentage of severe injury is reduced. Comparing the results from 45 and 90 degree cases and the 0 and 90 degree cases showed that as the body is further rotated from its original position the predicted injury is reduced. The 90 degree simulation indicated that by orientating the torso perpendicular instead of parallel to the blast wave, the injury predicted diminishes from LD50 to an injury level consisting of trace injury and predominantly no injury.

Although there are few experimental reports examining the effect the orientation of the sheep body has on injury as a result of a blast wave it appears logical that the expected injury would be reduced as the body is oriented at different angles from the blast wave. As the body is rotated there is less surface area in contact with the initial blast wave; the torso is more aerodynamic. As the body is oriented at 90 degrees (long portion is perpendicular to the blast wave) the initial contact area of the torso and the blast wave is reduced by approximately a factor of two. This reduction in area results in a lower impulse being delivered to the body as a result of the blast impact and resultant reflection. The orientation also results in the lungs being located farther from the blast wave source. At a position of 0 degrees the contact with the blast waves transmits stress waves through the soft tissue of the torso, which then pass through the ribs and into the lungs. At a position of 90 degrees the transmitted stress waves must pass through the tissue, the ribs and into the heart before being transmitted into the lungs. The extra tissue and distance that theses stress waves must travel resulted in the stress waves being further diminished as compared to the 0 degree case.. The stiffness of the torso of the sheep is also increased as the body is rotated from a position of 0 to 90 degrees. This increased stiffness resulted in less deformation and compression of the thorax, leading to less stress waves being introduced to the lungs.

5.5.2 Sheep Model – Injury Outcome Based on Individual Lungs

In its current form, the UW injury prediction method predicts injury based on the maximum dynamic pressure observed in the lung elements. This pressure correlates to an injury level for that particular lung element. The lung elements are then looked at as a whole and the injury percentage of the entire lung is computed based on the individual lung elements. The lung injury is computed as a whole and the injury is not separated or distinguished between the individual lungs. In order to predict the injury occurring in each individual lung and to understand the effect that body orientation has on the individual lungs, the injury prediction method was slightly modified to enable the prediction of injury in each individual lung. The

modification allowed each individual lung to be processed and the injury reported separately, rather than providing results for the lung as a whole.

The injury prediction results observed from rotating the torso suggested that, as the lungs are located farther from the blast wave that the predicted injury diminishes. Based on the results it was postulated that if the torso is rotated in such a way where there is one lung closer to the blast wave, that the lung closest to the blast wave will experience the most damage.

Eight simulations for each of the three rotation positions were performed using the sheep torso model. The results from each of the three rotations, with an LD50 blast profile with a duration of 1 ms are shown in Figure 92, Figure 93 and Figure 94.

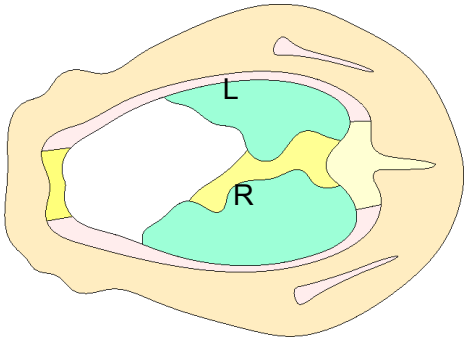

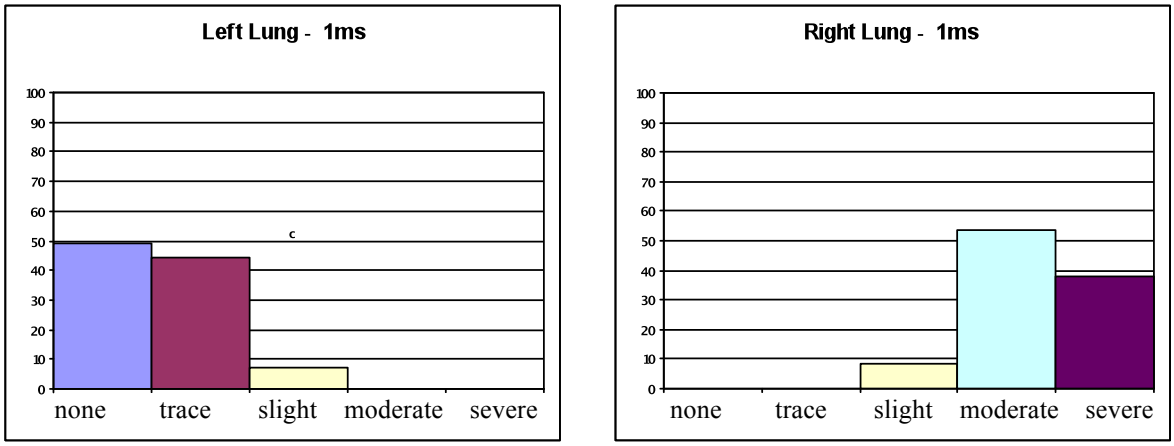

Figure 92: Sheep 0 degree rotation– LD 50, 1 ms Blast Duration (Individual Lungs)

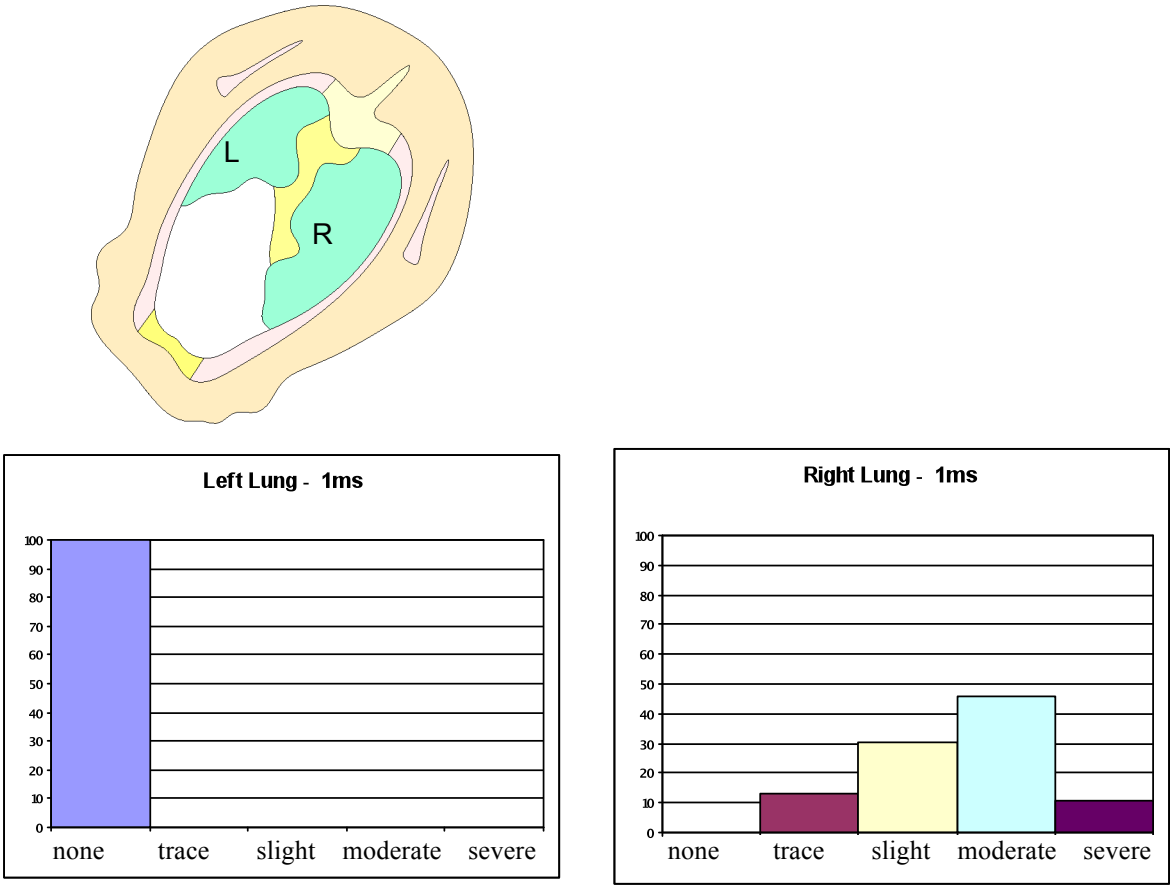

Figure 93: Sheep 45 degree rotation– LD 50, 1 ms Blast Duration (Individual Lungs)

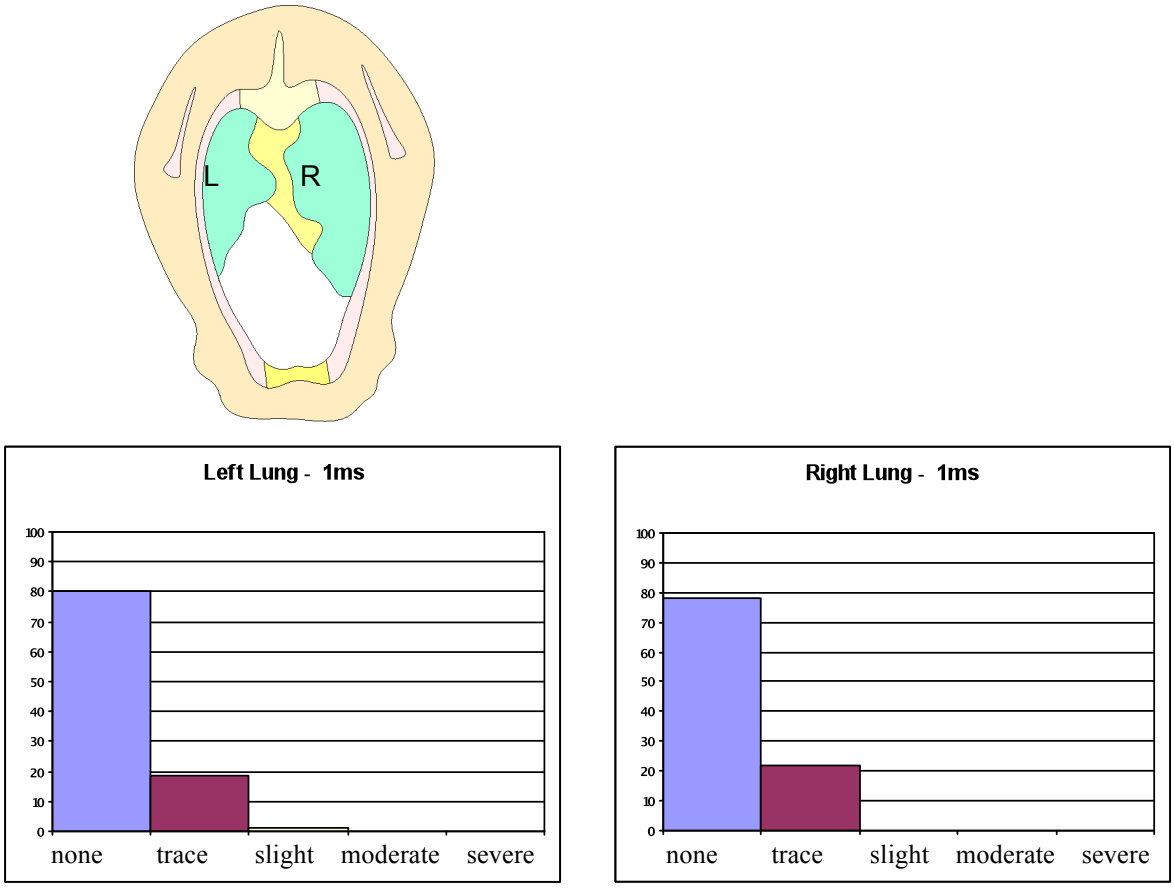

Figure 94: Sheep 90 degree rotation – LD 50, 1 ms Blast Duration (Individual Lungs)

The results of the 0 degree simulations showed that the highest injury is predicted in the right lung; the lung closest to the incoming blast wave. Slight injury is observed in the left lung, however the injury severity is significantly less than the right lung. When the torso is oriented in this way the stiffness of the torso is at a minimum in relation to the blast wave. The rib bones have a small mass moment of inertia in the direction of the blast wave. As the blast wave contacted the torso, the torso was easily compressed, the stress waves passed through the soft tissue, through the ribs and into the right lung. The stress waves were then easily transferred to the left lung, due to the geometry, causing injury in the left lung. These findings were consistent with those observed in physical experiments. In animal tests with

an explosive located near the side of an animal only 1 lung had noticeable injury. The lung with injury was the lung facing the explosion [Hunter, 1941].

The results from the 45 degree simulations showed that the right lung experiences moderate injury, whereas the left lung experiences no injury. The rotated position placed the left lung far away from the blat wave and point of the initial blast wave contact. The right side of the torso was directly exposed to the blast wave, and the left portion of the torso was somewhat shielded from the initial impact and reflection of the blast wave, protecting the left lung. The stress waves were also not as easily transferred into the left lung, since the heart absorbed much of the energy. The stress waves generated in the right lung were not as easily transferred to the left lung as they traveled mainly parallel with the blast wave.

The results from the 90 degree simulation placed both lungs at the same location from the blast wave. As a result the predicted injury in both lungs was virtually identical. The slight differences were a result of the placement of the heart, variations in size and geometry between the two lungs. Although the left lung experienced no predicted injury in the 45 degree simulations, the left lung experienced slight injury in the 90 degree configuration. This was most likely a result of the left lung being located closer to the blast wave, as a result of the anatomy. The relative position between the torso and blast wave also resulted in the torso being very stiff. The blast wave did not easily compress the torso, the long rib bones were the most likely factor. The bones have a large moment of inertia in the direction of the blast wave. There was also a significant amount of tissue and organ that absorbed the blast energy before the stress waves reach the lungs.

5.6 Human Thorax Model

5.6.1 Human Thorax Model – Injury Outcome Based on Both Lungs

The same simulations that were performed with the sheep torso were also performed on the human torso model. The human torso was rotated 0, 45 and 90 degrees in a counter clockwise rotation. The rotations were performed in this manner in order to be consistent with the sheep model; placing the larger, right lung closest to the blast wave in one scenario. In the 0 degree position the long portion of the torso was parallel with the incoming blast wave and both the lungs were approximately the same distance from the blast wave. In the 90 degree case the long portion of the body was perpendicular to the blast wave.

The results from the orientation study are shown in Figure 95, Figure 96 and Figure 97. These results are for the LD50 case, with a duration of 1ms. The injury predicted by the numerical model is shown in the bar graph, representing the 5 levels of injury: none (1), trace (2), slight (3), moderate (4) and severe (5).

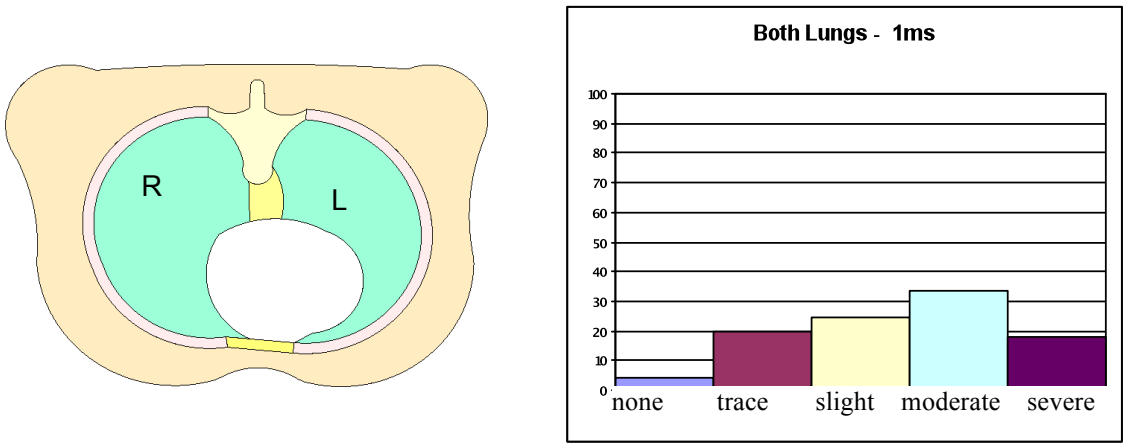

Figure 95: Human 0 degree rotation– LD 50, 1 ms Blast Duration (Both Lungs)

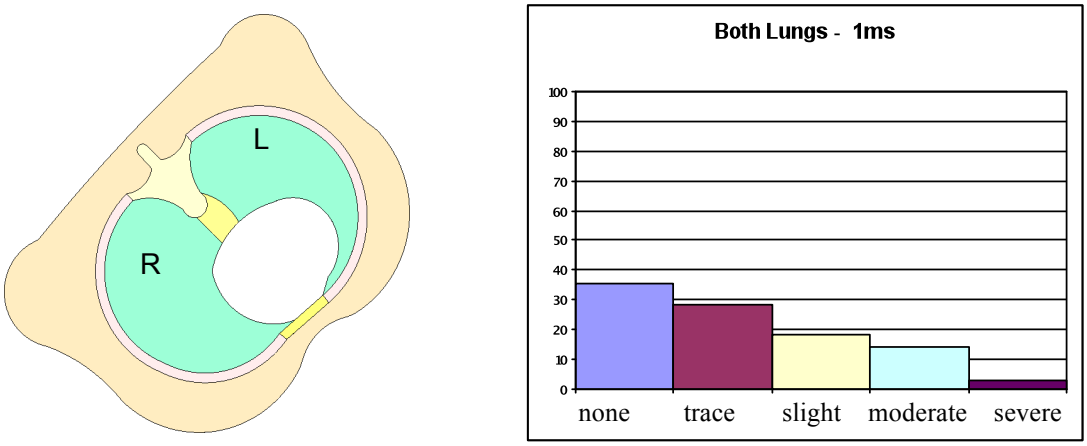

Figure 96: Human 45 degree rotation– LD 50, 1 ms Blast Duration (Both Lungs)

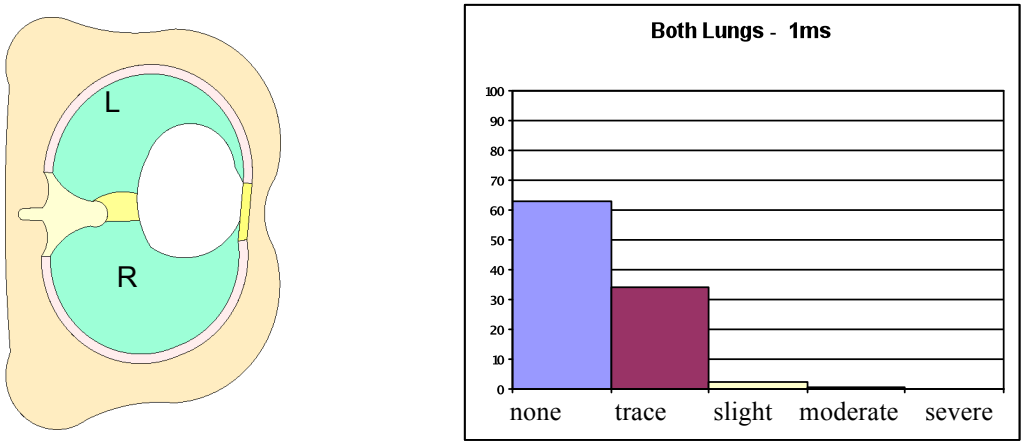

Figure 97: Human 90 degree rotation – LD 50, 1 ms Blast Duration (Both Lungs)

The overall injury results obtained from the human torso were similar to those obtained using the sheep model. As the torso was rotated from having the long axis of the body parallel to the blast wave to the having the long axis perpendicular to the blast wave the predicted injury was lessened with each rotation.

5.6.2 Human Thorax Model – Injury Outcome Based on Individual Lungs

Similar to the sheep model eight simulations for each of the three rotation positions were performed using the human torso model. The results from each of the three rotations, with an LD50 blast profile with a duration of 1 ms are shown in Figure 98, Figure 99 and Figure 100. These results show the typical observations noted from the eight loading curves used at each orientation.

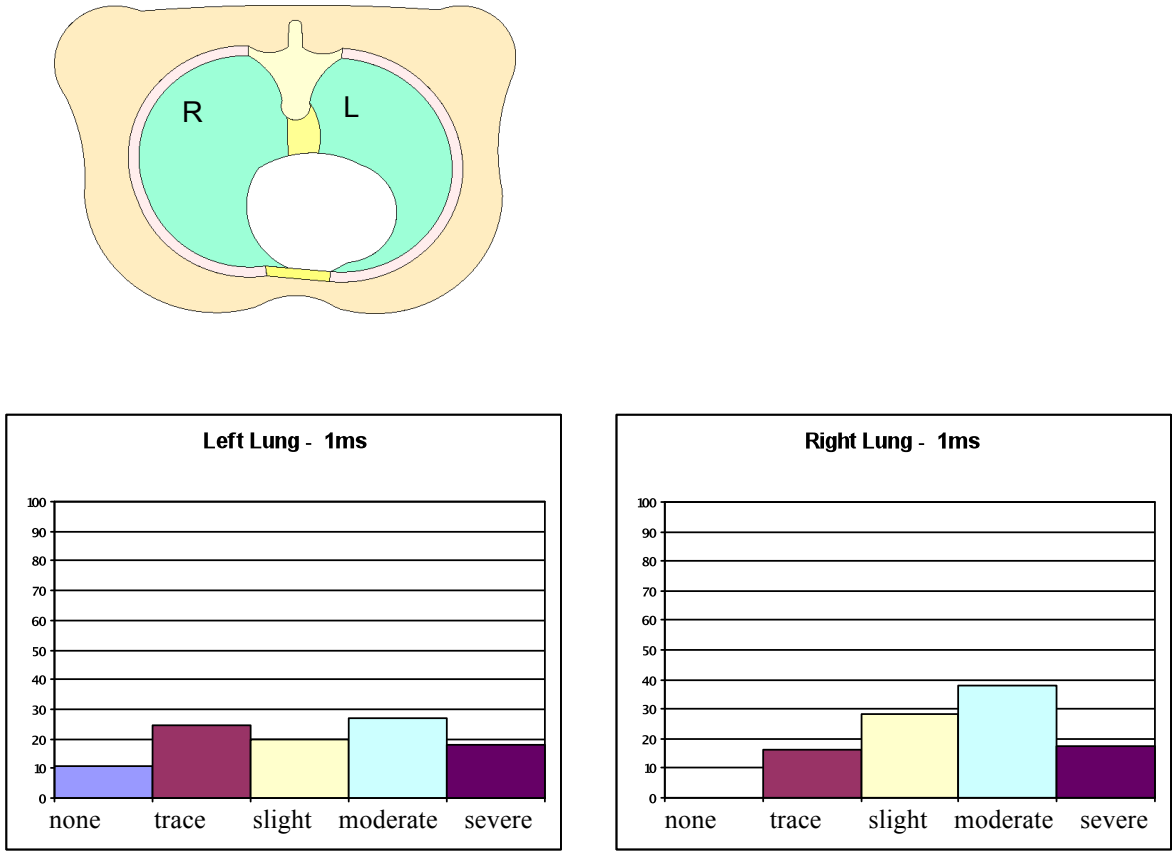

Figure 98: Torso 0 degree rotation– LD 50, 1 ms Blast Duration (Individual Lungs)

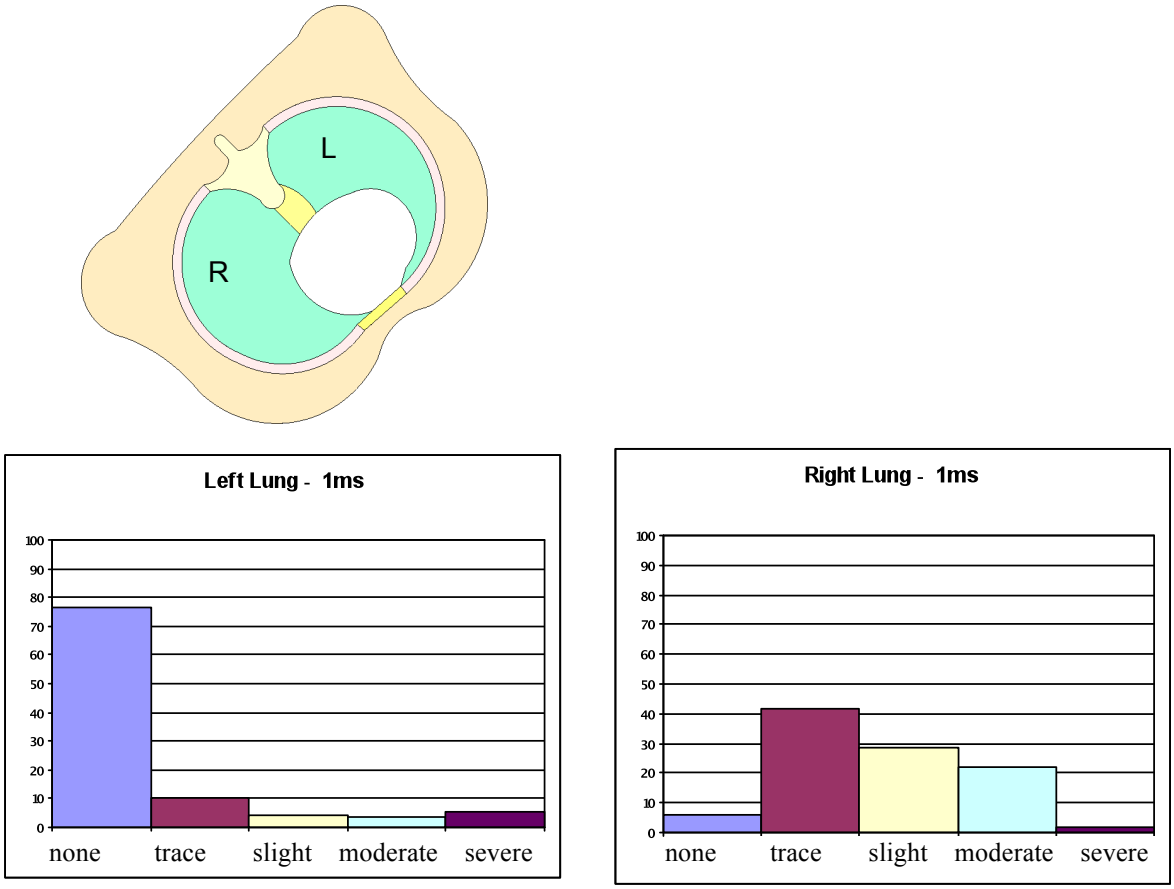

Figure 99: Torso 45 degree rotation– LD 50, 1 ms Blast Duration (Individual Lungs)

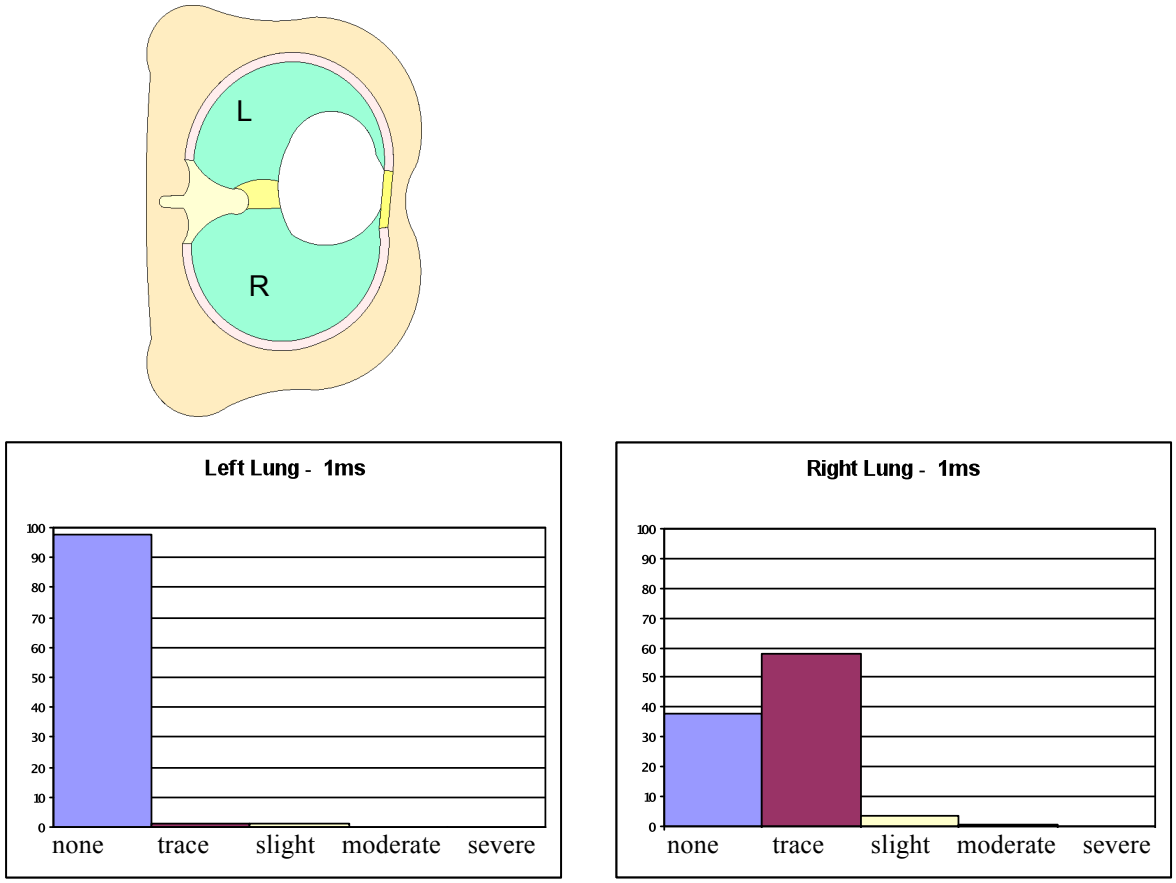

Figure 100: Torso 90 degree rotation – LD 50, 1 ms Blast Duration (Individual Lungs)

At the 0 degree position both lungs experienced generally the same amount of injury. The left lung had a greater curvature and in particular the front lobe has significant curvature near the sternum and heart. The increase in curvature resulted in the magnification of reflecting stress waves, causing increased injury to this lung. These findings are consistent with those by Grimal; the amount of energy transmitted to the lung is increased by a focusing effect due to the curvature of the organs. [Grimal, 2005] There was also significant deformation and crushing of this portion of the lobe as the rib was pushed into the heart and this area of the lung was sandwiched between these two portions.

The results from the 45 degree simulation showed that the one lung experienced more injury than the other, although each lung experiences some amount of severe injury, resulting in damage to portions of the lung tissue. When the blast wave contacted the torso, stress waves traveled through the soft tissue and ribs and then into both the right and left lung. Locating the majority of the left lung tissue farther from the blast source resulted in lower injury in this lung as compared to the right lung. In this orientation, the majority of tissue in the right lung was placed closer to the blast wave as compared to the 0 degree case, however a lower level of injury was predicted. This was a result of the increased stiffness of the torso in relation to the blast wave and a result of a more favorable orientation of the lung in relation to the internal stress waves. The increased torso stiffness, in this orientation resulted in lower chest compression. The lung was also oriented in a more favorable position as there was less of a sharp radius near the back of the torso where the travelling internal stress waves impacted and reflected, resulting in the highest areas of internal pressures.

At the 90 degree orientation only one lung was injured. This is a result of the left lung being placed farthest from the blast wave and the stress waves that originate inside of the right lung were not easily transferred into the left lung. The stress waves from the right lung were required to pass through the vertebrae, heart and cartilage before being transmitted to the left lung. In this orientation the torso was very stiff and did not easily compress in this orientation. Instead of the torso compressing and deflecting it has a tendency to be pushed back as a result of the blast wave. The right lung experienced a reduced amount of injury as compared to the 0 degree case since there was an increased amount of soft tissue directly in front of the lung that absorbs more of the blast energy. The orientation of the lung is also favorable as the location where the internal stress waves coalesce and reflect was also reduced, in this orientation.

Chapter 6
Comparison Between BTD, Sheep and Human Thorax

6.1 Introduction

Sheep have been used in many blast experiments to predict the injury on humans from blast waves [Bowen, 1968; Axelsson, 1996]. In order to better understand the results and evaluate sheep injury relative to humans, numerical results were compared. The numerical results were obtained by exposing these thoraxes to blast waves at different body orientations.

6.2 Injury Prediction Based on Both Lungs

Although the anatomy is different between the sheep and human thorax the injury predicted, based on both lungs is comparable between the two species. The BTD model is also capable of predicting injury levels, which are comparable to those, computed using the numerical model, however the BTD model does not exhibit the same injury trend with respect to body orientation. These results showed that care should be taken when using the BTD model, and that the BTD should be oriented appropriately when using the model for injury predictions.

The anatomy and shape of the sheep and human torso is different however the sheep has been used as a surrogate for the human despite these differences. The most significant difference is the shape of the torso cross-section and placement of the lungs. Examining the sheep torso revealed that when the body is placed in such a way where both lungs are parallel to the blast wave and placed at equal distances to the blast wave, the long portion of the body is perpendicular to the blast wave. This is contrary to that of the human torso. When the human torso is placed such that both the lungs are an equal distance from the blast source, the

long portion of the body is parallel to the blast wave. The torso size of the sheep is similar to that of the human, however the size of the lungs at the cross section used in the calculations shows that the lungs of the sheep are smaller than those of the human. A comparison between the sizes of the human and sheep torso is shown in Figure 101 and a comparison between the sizes of the lungs between these two species is shown in Figure 102.

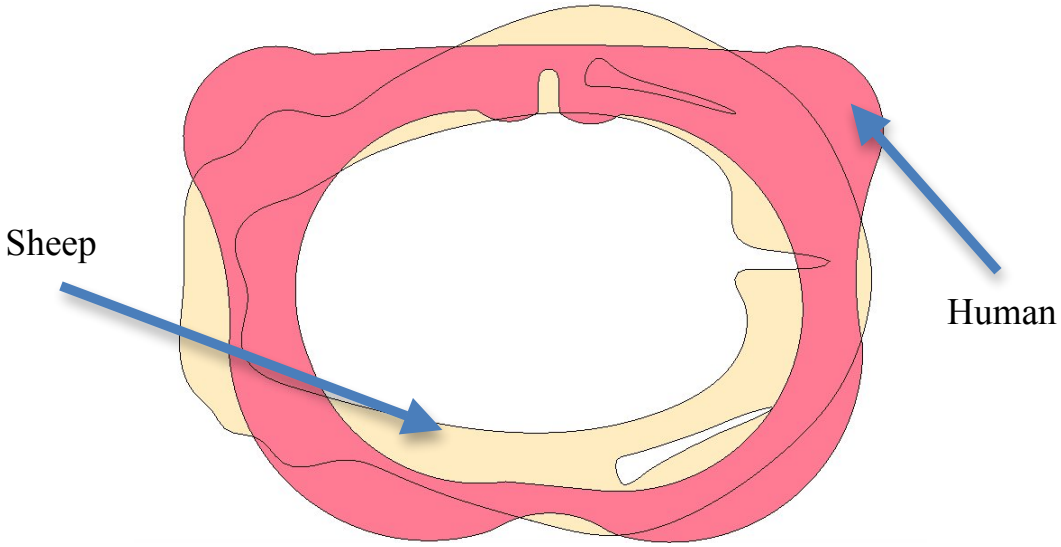

Figure 101: Comparison between human and sheep thorax size (same scale)

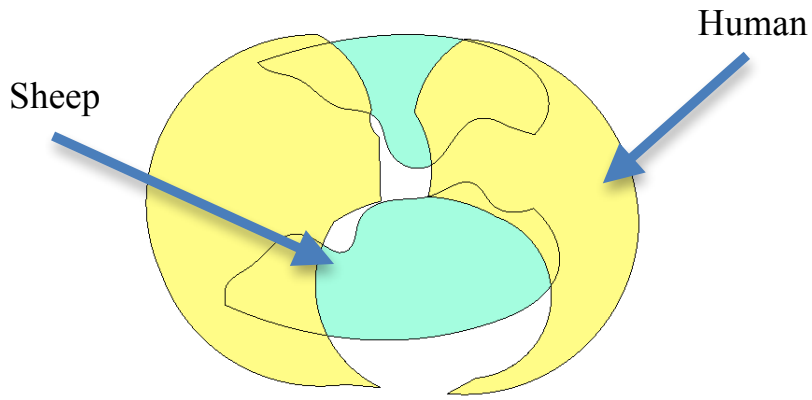

Figure 102: Comparison between human and sheep lung size

In the case of the human torso, as the body is rotated from the 0 degree point (where the long portion of the body is parallel to the blast wave) to the 90 degree point (where the long portion of the body is perpendicular to the blast wave), the injury was reduced as the body was rotated. The highest injury was recorded at the 0 degree position, then injury was diminished when the body is located at an angle of 45 degrees to the blast wave and the lowest injury is predicted at the 90 degree position.

As the sheep and human torso were rotated, overall injury (both lungs) gradually decreased, this is contrary to the injury prediction of the BTD. In the case of the BTD, and injury level, LD50 was observed at the 0 degree position, the predicted injury then reduced dramatically at 45 degrees and then increased at a rotation of 90 degrees. The BTD only used four pressure gauges along the circumference of the cylinder and it is because of these limited points of measurement that they injury predicted using the BTD does not gradually diminish as the BTD is rotated from front to side.

The overall injury results obtained from the human torso were similar to those obtained using the sheep model. This indicates the model is behaving similarly to the observations

noted by the original Bowen study despite the differences in anatomy. The study suggested that the humans be placed in the "high tolerance" group of animals. Animals were grouped by their tolerance or survivability to blast waves and the "high tolerance" group was the group that the humans and sheep were classified. The sheep was one of the tested mammals that were the most representative of the human in response to blast. [Bowen, 1968] The orientation study results showed that overall the injury obtained by the sheep thorax and human thorax is similar, suggesting that it was a valid assumption to group the sheep and human in the same species-tolerance group.

6.3 Injury Prediction Based on Individual Lungs

Although the overall injury prediction results between the sheep and the human torso models agreed quite well for assessing blast lung injury, the injury predicted in each of the lungs was significantly different. This has to do with the orientation of the lungs with respect to the thorax size. Figure 103 shows the comparison between the position of the lungs between the sheep and human when the long portion of the body is parallel with the horizontal plane and blast load.

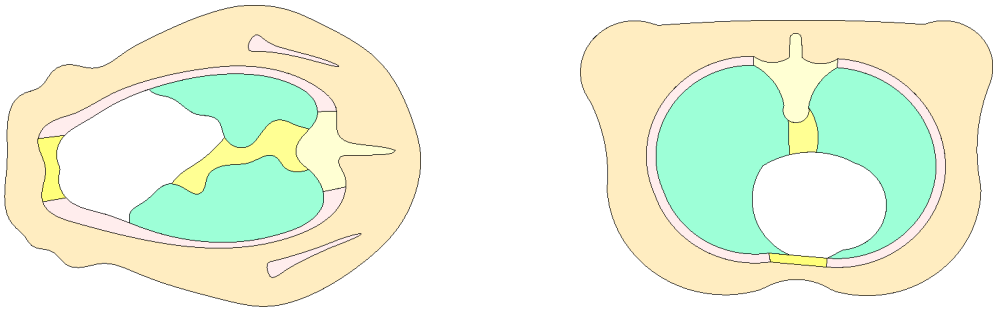

a.) Sheep b.) Human

Figure 103: Comparison between sheep and human in 0 degree position

In the 0 degree case, comparing the results from this orientation indicated that the sheep torso model experienced one lung of greater injury whereas in the human torso model the injury predicted between both lungs was practically the same. This has to do with the left lung of the sheep being placed farther back in the thoracic cage at this orientation and having significant tissue to absorb the blast wave before the stress waves pass into the left lung.

Rotating the human torso at an angle of 90 degrees to the blast wave resulted in the layout of the lungs being similar to that of the 0 degree case for the sheep; looking at the cross section the left lung is on top of the right lung. The results from theses calculations on the human torso showed a similar trend as observed in the sheep torso, the right lung experienced significant injury as compared to the left lung. However in this orientation the overall predicted injury for the torso was significantly reduced.

Similarly at an angle of 90 degrees to the blast wave, the long portion of the body was perpendicular to the blast wave for both the sheep and human models. Figure 104 shows the comparison between the position of the lungs between the sheep and human at this orientation. In this scenario the lungs of the sheep were oriented left to right and were the same distance from the blast source, whereas the lungs of the torso are oriented top to bottom. In this position the injury predicted on the individual lungs of the sheep were practically the same, whereas the injury predicted on the torso showed that the left lung experience practically no injury and the right lung was injured. These results are explained similarly by those recorded at the 0 degree position. In the 90 degree position both the sheep and the torso experienced an overall injury less than that recorded at the 0 degree position, indicating that the area of the torso exposed to the blast wave plays a significant role in predicting injury.

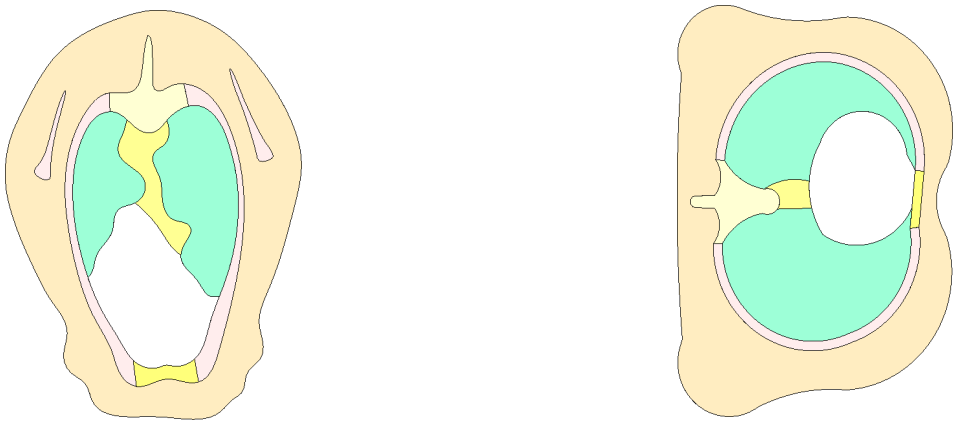

a.) Sheep b.) Human

Figure 104: Comparison between Sheep and Human in 90 degree position

In the 45 degree rotation position, the sheep model experienced no damage to the left lung from the LD50 blast load. For the same orientation the human torso experienced injury to

both lungs. Examining the position of the lungs in these species torso showed that in the sheep torso, one lung is shielded from direct impact with the blast, and at several rotational angles one of the lungs will be shielded from a direct blast wave loading. In the case of the right lung, it was exposed directly to the blast wave; the blast wave struck the torso and the stress waves transmitted directly through the soft tissue, ribs and into the lungs. The left lung was somewhat shielded and did not see the direct loading of the blast. In order to transmit stress waves to the lung, the blast wave first contacted the front and opposite side of the thorax, then the blast wave wrapped around the torso and by this time the blast wave strength was significantly reduced. The reduced blast wave pressures then transmitted stress waves through the soft tissue and bone, which further reduced the strength before being transmitted into the lungs. This did not occur and is not possible with the internal anatomy of the human, as the lungs are positioned differently with respect to the long portion of the body. In the human torso case, at a 45 degree angle from the blast wave, both lungs were subjected to a direct impact with the blast. Figure 105 shows how the position of the sheep lung protected it when the torso was at an angle to the blast wave.

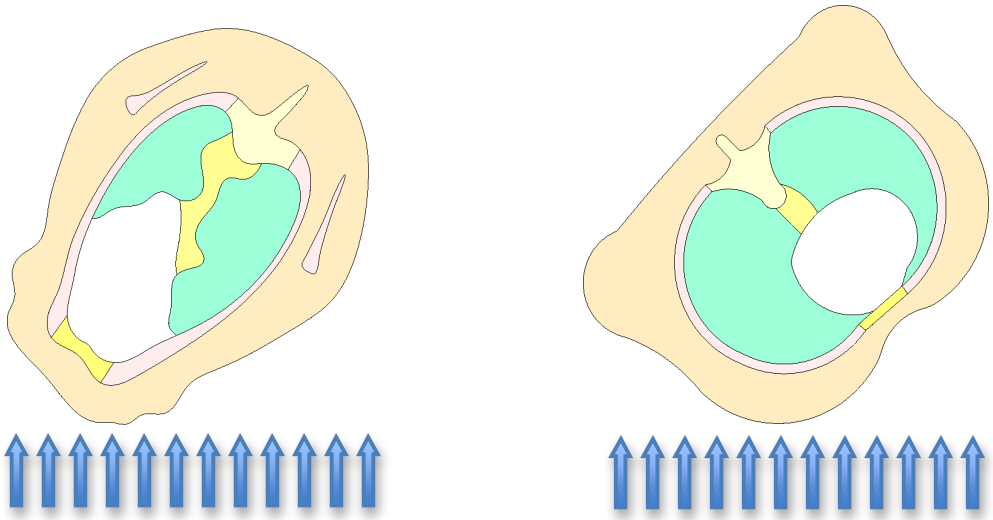

a.) Sheep **b.) Human**

Figure 105: Comparison between sheep and human thorax showing shielding of left lung on sheep

Although the shape and position of the lungs is different between the sheep and the human the overall injury was similar as long as the injury was based on both lungs. Examining individual lungs was not directly comparable, however the ability to examine the injury to each lung is useful in understanding the effect the orientation of the body has on damage to the lungs.

Chapter 7
Conclusions

7.1 Conclusions

The majority of human primary blast lung injury is based on existing test data using animals and predominantly considers free field or simply shaped blast waves. A numerical thorax model has been developed and the injury prediction, based on dynamic pressure in the lung tissue, has been correlated to this data.

7.2 Blast Injury Parametric Study

This study examined the effect of the peak incident overpressure, positive phase duration, impulse and the shape of the waveform on primary blast injury of the lungs. Using a numerical model and adjusting each of these parameters, some basic fundamentals of lung injury, the torso model and its sensitivity to varying parameters were found. These results are consistent with those found in the literature and correlate well with the UVa curves. The results of this study were also able to identify three blast regimes, based on blast duration, where different parameters were dominant. The three regions were defined as: short duration (durations < 1 ms), medium duration (durations 1 ms < 8 ms), long duration (durations > 8 ms)

7.2.1 Short Durations

For blast durations less than 1ms the blast impulse was dominant in predicting injury. The shape, of the waveform and peak pressure were not important in the injury predicted.

7.2.2 Medium Durations

For durations between 1ms and 8ms both the impulse and pressure played an important role in predicting injury. The shape of the waveform therefore becomes important in this region. For blast loads in this region the wave shape, peak pressure and duration were identified as contributing factors to blast lung injury. Importantly, this is the most commonly encountered blast condition.

7.2.3 Long Durations

For durations greater than 8ms, pressure is dominant in predicting injury. For blasts with long durations the duration and shape of the loading wave does not have a significant effect on the injury predict. These results correlate well with those obtained using the Bowen curves. For long durations, the Bowen curves approach a horizontal line, where predicted injury is no longer a function of pressure and duration, but as pressure only.

7.3 Body Orientation Effects

To investigate how the orientation of the torso in the flow field affects the predicted injury a series of simulations were performed. Torso models of the sheep and human were simulated along with a BTD. The bodies were rotated from front to side in 45° increments. For the sheep and human torso models the predicted injury for the right and left lungs along with the overall predicted injury was reported.

7.3.1 Evaluation of the Blast Test Device

For the 0°, 45° and 90° degree cases tested the predicted injury using the BTD was greatest for the 0° (front) case. The predicted injury was slightly reduced for the 90° degree (side-on) case, corresponding to the blast being perpendicular to the body. However the results for the 45° case showed that the predicted injury was further reduced as compared to the front and side blast cases. The results from the 45° case show that the injury was substantially reduced by turning the body slightly off-center, the drastic decrease in predicted injury was attributed to the discrete pressure measurements made by the transducers on the BTD, and indicates that the BTD and Injury 8.1 model should only be used when the front gauge is perpendicular to the flow field.

When using BTD in the flow filed it is important to properly orient the device to predict blast injury. If the location of the front gauge is not perpendicular to the blast wave the injury predicted can be much lower. This is impractical in many experimental situations, especially in complex blast wave environments where it may not be possible to know ahead of time the way in which the blast wave travels. The injury predicted with this tool is dependent on injury and a series of trials would need to be performed in order to determine the worse case injury scenario.

7.3.2 Sheep

For the sheep torso model, the overall predicted injury was the most severe when the torso was orientated in the 0° position. Predicted injury gradually reduced as the body was rotated through 45° and 90°. As the body was rotated, the effective reflecting surface of the body was diminished and reduced the peak reflected pressure. Similarly as the body was rotated

from 0° to 90° the relative stiffness of the torso in response to the wave was increased. The same blast wave compressed the torso more at 0° compared to 90°.

In the 0° case, the right lung was located closest to the blast wave and the left lung was located farther away. In the 0° case the right lung experienced severe injury and the left lung primarily experienced trace injury; the lung closest to the blast wave is severely damaged while the other lung experienced minimal damage. In the 90° case, both the right and left lung were placed at roughly the same distance from the blast wave. The predicted injury was generally the same in each of these lungs for this orientation, as expected.

7.3.3 Human

The human torso was evaluated in the 0°, 45° and 90° orientations. In the 0° position the effective reflecting surface of the torso was greatest and both lungs were placed generally the same distance from the blast wave. In the 90° position the effective reflecting surface was at a minimum and the right lung was located closest to the blast wave. The torso was at maximum stiffness in the 90° case. This increased stiffness and position of the lungs in the torso accounted for the reduction in predicted injury in the 90° case.

The predicted injury was at a maximum in the 0° case and the injury was gradually reduced as the body was rotated to a side-on blast position. The predicted injury in both lungs was similar for the 0° case. In the 90° case the left lung was located farthest from the blast wave and there was primarily no injury predicted in this lung. The right lung was however located closest to the blast wave and suffered increased injury.

7.4 BTD vs. Sheep vs. Human

When comparing the results between the sheep and torso models it was appropriate to compare the overall predicted injury between the two species as long as this injury was predicted based on the lung as a whole. It is invalid to compare the results between the individual, left and right lungs between these two species, due to the differences in anatomy.

Chapter 8
Recommendations

The numerical finite element model of the human and sheep thorax was designed in 2005 and designed for the practical limits of computer hardware at that point in time. The resolution of the finite elements was chosen to ensure that the wave speeds of the tissue and air could be accurately captured. Small timesteps are required to resolve shock waves and reducing the size of the finite elements will reduce the timestep and allow for a higher degree of accuracy in calculating the pressures. With more recent advancements in computer processing speeds and memory it is now possible to run more detailed calculations. It is suggested that the finite element mesh be further refined.

The finite element model is a quai-3D representation of the torso. With this representation the changing geometry of the sternum (from bottom to top) is not modeled. As computer processing power advances it is suggested that a large full 3D model of the torso be developed to model the full interaction of stress waves inside the lung (rather than only looking at a cross sectional slice).

The LS-Dyna software has over 100 material models and many equations of state to model material properties and behaviors. The material model database is being constantly updated and improved. A key requirement to obtaining meaningful injury predictions from the torso models lies on using appropriate material models that are able to replicate high strain rate tissue response. As new, improved and applicable material models become available the model should be updated to utilize these new material models.

The numerical torso model predicts injury by correlating peak pressure in the lung element to an injury level. In the future, if the model becomes further refined and improvements are made to the geometry, the pressure and injury correlation should be investigated to verify that the injury ranges that correlate in this model are still appropriate for injury prediction in a future model.

8.1 Further investigations

The orientation study performed only investigated the following body orientations: front (0°), front-side (45°) and side (90°). Blast from the back-side or back (180°) were not considered. In the case of the blast from the back, the spine is closest to the blast and it is foreseeable that this large mass and geometry will provide additional stiffness to the torso. The stress waves will need to pass through more bone and tissue before entering the lungs (as compared to the 0° case), diminishing as they pass. As the stress waves pass from the back to the front of the lungs, they will follow along the edge of the lung, where they will coalesce at the front of the lungs. The front of the lungs consists of geometry with sharp radii and the reflection of these waves will in turn case injury to front of lungs. The severity of the injury will require additional simulations to evaluate the effect from blasts to the back and back sides.

Complex blast waves are developed in areas where the blast is located close to structures or reflecting surfaces. The wave profile generated by a complex blast will change the load applied to the torso. It is recommended that studies and simulations be performed using complex blast loading on the torso to investigate how multiple pressure peaks and durations affect the blast lung injury predicted by the model.

Bibliography

[Adler, 1988] Adler OB, Rosenberger A., "Blast injuries.", Acta Radiologica, 1988 January - February, 29(1), 1-5.

[Ahnfeldt, 1965] Ahnfeldt, A.L., Thoracic Surgery, Surgery In World War II, Office Of The Surgeon General, Department Of The Army, Washington, D.C., 1965

[Almogy, 2006] Almogy G, Mintz Y, Zamir G, et al., "Suicide bombing attacks: can external signs predict internal injuries?", Annals of Surgery, 2006, 243:541–546..

[Anctil 2004] Anctil, B., Keown, M., Williams, K., Manseau, J., Dionne, J.P., Jetté, F.X., Makris, A., Development of a Mannequin for Assessment of Blast Incapacitation and Lethality, Personal Armour Systems Symposium, p.332-344, The Netherlands, 2004.

[Argyros, 1997] Argyros GJ., "Management of primary blast injury", Toxicology, 1997 Jul 25, 121(1):105-15.

[Axelsson, 1996] Axelsson H, Yelverton JT., "Chest wall velocity as a predictor of nonauditory blast injury in a complex wave environment", The Journal of Trauma, 1996 Mar, 40(3 Suppl):S31-7.

[Baker, 1973] Baker, W.E., Explosions in Air, University of Texas Press, Austin, 1973.

[Bass, 2006] Bass, C., et al., “Pulmonary Injury Risk Assessment for Short Duration Blasts”, PASS 2006,

[Belanger, 2005] Belanger HG, Scott SG, Scholten J, Curtiss G, Vanderploeg RD., "Utility of mechanism-of-injury-based assessment and treatment: Blast Injury Program case illustration.", Journal of Rehabilitation Research & Development, 2005 Jul-Aug, 42(4):403-12.

[Bellamy, 1991] Bellamy R.F., Zajtchuk R., "Conventional Warfare: Ballistic, Blast, and Burn Injuries." In: Bellamy RF, Zajtchuk R, eds. Textbook of Military Medicine, Part 1, Volume 5. Washington, DC: Office of the Surgeon General of the US Army; 1991; pp. 1-51.

[Bouamoul 2007] Bouamoul, A, Williams K and Lévesque H, "Experimental And Numerical Modelling Of A Mannequin For The Assessment Of Blast Incapacitation And Lethality Under Blast Loading", 23rd International Symposium On Ballistics, Tarragona, Spain 16-20 April 2007

[Bowen, 1968] Bowen, I.G., Fletcher, E.R., Richmond, D.R., "Estimate of man's tolerance to the direct effects of air blast," Technical progress report no. DASA-2113, Department of Defense, Defense Atomic Support Agency, Washington, D.C., 1968.

[CDC, 2006] CDC Injury Prevention, "Explosions and Blast Injuries: A Primer for Clinicians", Department of Health and Human Services USA, 2006.

[Cernak, 1999] Cernak I, Savic J, Ignjatovic D, Jevtic M., "Blast injury from explosive munitions", The Journal of Trauma, 1999 Jul, 47(1):96-103; discussion 103-4.

[Chaloner, 2005] Chaloner E., "Blast injury in enclosed spaces.", BMJ, 2005 Jul 16, 331(7509):119-20. Epub 2005 Jul 11.

[CHPPM, 2005] CHPPM, "Program Guidance for Blast Overpressure Analysis", U.S. Army Center for Health Promotion and Preventive Medicine , December 2005.

[CIJ, 2009] Cancer Information Japan: cancerinfo.tri-kobe.org, 2009.

[Cohn, 1997] Cohn SM., "Pulmonary contusion: review of the clinical entity.", The Journal of Trauma, 1997 May, 42(5):973-9.

[Cooper, 1991] Cooper GJ, Townend DJ, Cater SR, Pearce BP., "The role of stress waves in thoracic visceral injury from blast loading: modification of stress transmission by foams and high-density materials.", Journal of Biomechanics, 1991, 24(5):273-85.

[Cooper, 1996a] Cooper GJ, Pearce BP, Sedman AJ, Bush IS, Oakley CW., "Experimental evaluation of a rig to simulate the response of the thorax to blast loading.", The Journal of Trauma, 1996 Mar, 40(3 Suppl):S38-41.

[Cooper, 1996b] Cooper GJ., "Protection of the lung from blast overpressure by thoracic stress wave decouplers", The Journal of Trauma, 1996 Mar, 40(3 Suppl):S105-10.

[Cooper, 1996c]Cooper, PW, *Explosives Engineering*, New York: Wiley-VCH, 1996.

[Cronin, 2004] Cronin, D., Salisbury, C., Greer, A., "Numerical Modeling of Blast Injuries: Phase 1 – Final Report," Contract report for Defence R&D Canada – Valcartier, March 2004.

[D'yachenko, 2005] D'yachenko AI, Manyuhina OV., "Modeling of weak blast wave propagation in the lung.", Journal of Biomechanics, 2005 Oct 6.

[Damon, 1968] Damon EG, Gaylord CS, Yelverton JT, Richmond DR, Bowen IG, Jones RK, White CS., "Effects of ambient pressure on tolerance of mammals to air blast.", Aerospace Medicine, 1968 Oct, 39(10):1039-47.

[Davies, 1987] [Davies et al. 1987] Davies, A.S., Garden, K.L., Young, M.J., Reid, C.S.W., An atlas of X-ray tomographical anatomy of the sheep, Science Information Publishing Centre, Wellington, New Zealand, 1987.

[DePalma, 2005] DePalma RG, Burris DG, Champion HR, Hodgson MJ., "Blast injuries.", New England Journal of Medicine, 2005 Mar 31, 352(13):1335-42.

[Dionne, 2008] Dionne JP, Levine J, Makris A, "Numerical Investigation of Blast Propagation in Confined Environments: Personal Vulnerability", PASS 2008.

[Dorn, 1999] Dorn MR, Cooper GJ, "Prediction of the severity of primary blast injury to the lung from complex blast loads", Journal of Defence Science 1999, Vol 4, #3, pp.317-319.

[Elsayed, 1997] Elsayed NM., "Toxicology of blast overpressure.", Toxicology, 1997 Jul 25, 121(1):1-15.

[Frykberg, 1988] Fyykberg E.R., et al., "Terrorist Bombings: Lessons Learned from Belfast to Beirut", Annals of Surgery, 1988, 208 (5), 569-576.

[Foster, 1977] Foster J, Kortge J, Wolanin M, , "Hybrid III--A Biomechanically-Based Crash Test Dummy", SAE, 1977.

[Godfrey, 1994] Godfrey, E.A, et al., “Human Injury Information System Concept Exploration”, Armstrong Laboratory (US Air Force), 1994.

[Greer, 2006] Greer, A., “Numerical Modeling for the Prediction of Primary Blast Injury to the Lung”, University of Waterloo, 2006.

[Grimal, 2002] Grimal Quentin, Watzky Alexandre, Naili Salah , "A one-dimensional model for the propagation of transient pressure waves through the lung", Journal of Biomechanics, 2002, 35, 1081-1089.

[Grimal, 2005] Grimal, Q., et al, “A high-Frequency lung injury mechanism in blunt thoracic impact”, Journal of Biomechanics, 2005, 38, 1247-1254.

[Gruss, 2006] Gruss, Eyal , "A Correction for Primary Blast Injury Criteria.", Journal of Trauma-Injury Infection & Critical Care, 2006 June, 60(6):1284-1289.

[Guy, 1998a] Guy RJ, Glover MA, Cripps NP., "The pathophysiology of primary blast injury and its implications for treatment. Part I: The thorax.", Journal of Royal Navak Medical Service, 1998, 84(2):79-86.

[Guy, 1998b] Guy RJ, Kirkman E, Watkins PE, Cooper GJ., "Physiologic responses to primary blast.", The Journal of Trauma, 1998 Dec, 45(6):983-7.

[Guzzi, 1996] Guzzi LM, Argyros G., "The management of blast injury", European Journal of Emergency Medicine, 1996 Dec, 3(4):252-5.

[Halquist, 2003] Livermore Software Technology Corporation, “LS-DYNA Keyword User’s Manual – Version 970,” Livermore Software Technology Corporation, April 2003.

[Hayda, 2004] Hayda Roman, Harris Robert M, Bass Cameron Dale , "Blast Injury Research: Modeling Injury Effects of Landmines, Bullets, and Bombs", Clinical Orthopaedics and Related Research, 2004, Number 422, pp. 97–108.

[Ho, 2002] Ho AM., "A simple conceptual model of primary pulmonary blast injury", Medical Hypotheses, 2002 Nov, 59(5):611-3.

[Hunter, 1941] Hunter, J. B., "Sections of Surgery and Pathology", Proceedings of the Royal Society of Medicine, 1941 January, 31-52.

[Hyde, 1988] Hyde, D.W., “Users Guide for Microcomputer Programs CONWEP and FUNPRO”, US Army Corps of Engineers, 1988, SL-08-1.

[Irwin, 1998] Irwin RJ, Lerner MR, Bealer JF, Lightfoot SA, Brackett DJ, Tuggle DW., "Global primary blast injury: a rat model.", Journal of Oklahoma State Med Assoc., 1998 Oct, 91(7):387-92.

[Jonsson, 1988] Jonsson A, Arvebo E, Schantz B., "Intrathoracic pressure variations in an anthropomorphic dummy exposed to air blast, blunt impact, and missiles.", The Journal of Trauma, 1988 Jan, 28(1 Suppl):S125-31.

[Josephson, 1988] Josephson LH, Tomlinson P., "Predicted thoraco-abdominal response to complex blast waves", The Journal of Trauma, 1988 Jan, 28(1 Suppl):S116-24.

[Josey, 2006] T. Josey, .B. Sharman, “Quadtree Space Partitioning for Mapping Two-Dimensional Results on Three-Dimensional Domains”, Computational Fluid Dynamics Journal, International Society of CFD, vol.15, no. 1, pp 94-100, April 2006, Tokyo, Japan.

[Katz, 1989] Katz E, Ofek B, Adler J, Abramowitz HB, Krausz MM., "Primary blast injury after a bomb explosion in a civilian bus", Annals of Surgery, 1989 April, 209(4):484-8.

[Kessler, 2004] Kessler C., Dionne J.P., Jetté F., Makris A, Josey T., Whitehouse D., “Computationl Analysis of Explosions Near a Rigid Wall – Effect of Injury Potential”, MABS 18, Germany, 2004.

[Kinney, 1962] Kinney, G.F., Explosive Shocks in Air, The Macmillan Company, New York, 1962.

[Liu, 2005] Liu, G.R., Smoothed Particle Hydrodynamics: A Meshfree Particle Method, World Scientific Publishing; Oct 2003

[Martec, 2006] Martec Limited, "Chinook Input Manual", Martec Limited, 2006.

[Mayo, 2006a] Mayo, A. and Yoram Kluger, Y., "Blast Induced injury to air containing organs", ADF Health, 2006, 7:40-44.

[Mayo, 2006b] Mayo, A. and Yoram Kluger, Y., "Terrorist bombing", World Journal of Emergency Surgery, Published online 2006 November 13, 1:33.

[Mayorga, 1997] Mayorga MA., "The pathology of primary blast overpressure injury.", Toxicology, 1997 Jul 25, 121(1):17-28.

[Mellor, 1992] Mellor, S., et al., “The relationship of blast loading to death and injury from explosion”, World Journal of Surgery, 1992, 16, 893-898.

[Meyers, 1994] Meyers, M.A., Dynamic Behavior of Materials, John Wiley & Sons, Inc., Toronto, 1994.

[Mitchell, 1864] Mitchell, S.W., Morehouse, G.R., and Keen, Jr., W.W., “Reflex Paralysis, Circular #6, Surgeon General’s Office”, Washington, DC, March 10, 1864.

[NATO, 2007] NATO, North Atlantic Treaty Organization, RTO, Research and Technology Organisation, “Test Methodology for Protection of Vehicle Occupants against Anti-Vehicular Landmine Effects ”, TR_HFM-090, April 2007

[Nelson, 2006] Nelson TJ, Wall DB, Stedje-Larsen ET, Clark RT, Chambers LW, Bohman HR., "Predictors of mortality in close proximity blast injuries during Operation Iraqi Freedom.", Journal of the American College of Surgeons, 2006 Mar, 202(3):418-22.

[Ouellet, 2008] Ouellet S, Williams K, “Characterisation of Defence Research and Development Canada’s Mannequin for the Assessment of Blast Incapacitation and Lethality (DRDC MABIL)”, PASS 2008.

[NLM, 2004] National Library of Medicine (NLM), The Visible Human Project, National Institutes of Health, www.nlm.nih.gov/research/visible/visible_human.html.

[Phillips, 1986] Phillips YY., "Primary blast injuries", Annals of Emergency Medicine, 1986 Dec, 15(12):1446-50.

[Phillips, 1988] Phillips YY, Mundie TG, Yelverton JT, Richmond DR., "Cloth ballistic vest alters response to blast.", The Journal of Trauma, 1988 Jan, 28(1 Suppl):S149-52.

[Pizov 1999] Pizov, R., Oppenheim-Eden, A., Matot, I., Weiss, Y.G., Eidelman, L.A., Rivkind, A.I., and Sprung, C.L., "Blast Lung Injury From an Explosion on a Civilian Bus", Chest, 1999, 115:165-172.

[Rafaels 2008] Rafaels K, Bass C, Salzar R, "Pulmonary Injury Risk Assessment for Long-Duration Blasts", PASS 2008.

[Salisbury, 2004] Salisbury, C., "Investigation of the Arbitrary Lagrangian Eulerian Formulation to Simulate Shock Tube Problems", 8th International LS-DYNA User's Conference, 2004 May 2-4.

[Sasser, 2006] Sasser SM, Sattin RW, Hunt RC, Krohmer J., "Blast lung injury.", Prehospital Emergency Care, 2006 Apr-Jun, 10(2):165-72.

[Stuhmiller, 1988] Stuhmiller JH, Chuong CJ, Phillips YY, Dodd KT., "Computer modeling of thoracic response to blast", The Journal of Trauma, 1988 Jan, 28(1 Suppl):S132-9.

[Stuhmiller, 1996] Stuhmiller JH, Ho KH, Vander Vorst MJ, Dodd KT, Fitzpatrick T, Mayorga M., "A model of blast overpressure injury to the lung.", Journal of Biomechanics, 1996 Feb, 29(2):227-34.

[Stuhmiller, 1997] Stuhmiller JH., "Biological response to blast overpressure: a summary of modeling.", Toxicology., 1997 Jul 25, 121(1):91-103.

[Stuhmiller, 1991] Stuhmiller JH, Phillips YY, Richmond DR, “The Physics and mechanisms of primary blast injury”, Textbook of Military Medicine, Cnventional Warfare: Ballistic, Blast and Burn Injuries, (edited by Bellamy, RF and Zajtchuk, R) Office of the Surgeon General, Dept. of the Army, Washington, DC, 1991.

[Stuhmiller, 2006] Stuhmiller, J.,et al, “Mathematical Modeling of Physical and Cognitive Performance Decrement from Mechanical and Inhalation Insults”, US Army Medical Research, 2006, Award Number: W81XWH-06-C-0051.

[Trudeau, 1998] Trudeau DL, Anderson J, Hansen LM, Shagalov DN, Schmoller J, Nugent S, Barton S., "Findings of mild traumatic brain injury in combat veterans with PTSD and a history of blast concussion.", Journal of Neuropsychiatry, 1998 Summer, 10(3):308-13.

[Tsokos, 2003] Tsokos, M., et al, “Histologic, Immunohistochemical, and ultrastructural findings in human blast lung injury”, 2003, American Journal of Respiratory and Critical Care Medicine , 168, 549-555.

[Viano, 1985] Viano, D.C. and Lau, I.V., “Thoracic impact: A viscous tolerance criterion”, 10th International Conference on Experimental Safety Vehicles. Oxford, England, 1985.

[Viano 1988] Viano, D., et al, “A viscous Tolerance Criterion for Soft Tissue Injury Assessment”, Journal of Biomechanics, 1988, 21 (5), 387-399.

[Viano, 1989] Viano DC, King AI, Melvin JW, Weber K., "Injury biomechanics research: an essential element in the prevention of trauma", Journal of Biomechanics, 1989, 22(5):403-17.

[Weiler-Ravell, 1975] Weiler-Ravell D, Adatto R, Borman JB., "Blast injury of the chest. A review of the problem and its treatment", Israel Journal of Medical Sciences, 1975 Feb-Mar, 11(2-3):268-74.

[Wharton, 2000] Wharton, R.K. et al., "Airblast TNT Equivalence for a Range of Commercial Blasting Explosives", Journal of Hazardous Materials, 2000, A79, 31-39.

[Wightman, 2001] Wightman JM, Gladish SL., "Explosions and blast injuries.", Annals of Emergency Medicine, 2001 Jun, 37(6):664-78.